AD 360 14

med Services Technical Information Agency

Reproduced by

DOCUMENT SERVICE CENTER
KNOTT BUILDING, DAYTON, 2, OHIO

UNCLASSIFIED

NAVAER 50-1P-521
FORMERLY
NAVAER 50-1R-249

THE JET STREAM

PUBLISHED BY DIRECTION OF
THE CHIEF OF THE BUREAU OF AERONAUTICS

The Jet Stream

PUBLISHED BY DIRECTION OF
THE CHIEF OF THE BUREAU OF AERONAUTICS

1 June 1953

FOREWORD

It is true in many fields of science that the requisite data for the revision of an antiquated hypothesis or the development of a new theory are available long before the actual formulation of a neoteric concept. Such has been the case of the Jet Stream in the science of Meteorology.

As early as 1933, a cross-section depicting a relatively narrow, high-speed stream of air in the upper westerlies was published in the text, Physikalische Hydrodynamik. The implications of this cross-section were disregarded by the authors themselves, possibly in view of the inadequacy of the observational material upon which it was based. Eleven years later, in 1944, Dr. Hurd C. Willett published mean cross-sections pertaining to the North American continent which also substantiated the existence of a meandering, high-velocity stream of air particles in the upper tropospheric regions. It wasn't until the year 1946, however, that this latest meteorological phenomenon became the object of rather intensive research at a Navy-sponsored research project at the University of Chicago and that its numerous potentialities were gradually being recognized.

Subsequent to that time, considerable research on the subject has been conducted by various individuals and institutions at different geographical locations, with the result that a great deal of uncoordinated and sometimes controversial material has been presented. This material has appeared in divers professional journals, bulletins and periodicals, not readily available to the Naval Aerologist in the field or afloat.

Because of the tremendous import and the numerous potentialities of this newly-discovered phenomenon, it was deemed imperative that an evaluation and summary of existing research and data on the Jet Stream be compiled under a single cover and distributed to the Naval Aerological Service as soon as possible. Accordingly, Task 6 (TED-UNL-MA-501.6), JET STREAM ANALYSIS, was assigned to Project AROWA by Bureau of Aeronautics letter Aer-MA-5 serial 24803 dated 14 March, 1951, for prosecution and/or coordination.

This document is the coordinated effort in the fulfillment of this purpose. Much of the material presented herein is based on lectures by Dr. Herbert Riehl of the Department of Meteorology, University of Chicago, who also edited the manuscript. Intimately associated with the entire project, also, were Messrs. M. A. Alaka, C. L. Jordan, and R. J. Renard of the Department of Meteorology, University of Chicago.

This publication encompasses the synoptic structure of the Jet Stream, as well as its climatology and relation to middle latitude cyclones and extended forecasting. In addition, one chapter is devoted to the techniques and procedures of high-level wind analysis. The dynamic principles relating to Jet Stream formation and maintenance are also incorporated.

Much of the information presented herein has been derived from a great variety of source material, with the result that several different units of wind speed are expressed throughout. It is regretted that time did not permit the conversion of the various units to one system.

<div align="right">
F. A. BERRY
Captain, U.S. Navy
Officer in Charge
Bureau of Aeronautics Project AROWA
</div>

CHAPTER I.   INTRODUCTION

1. Discovery of the Jet Stream

During World War II, American pilots flying high-altitude bombers over Japan with air speeds exceeding 250 mph, at times, encountered head winds so strong that they found themselves in the unenviable predicament of remaining stationary over their target areas.

Such surprisingly strong winds had not been visualized for the upper troposphere by atmospheric models then in vogue. These models were based on the concept of air masses of broad horizontal extent, with properties depending on their source and their history, and separated by a surface of discontinuity or a finite transition zone — a front (fig. 1.1). Within the individual air masses, the isotherms are level or have a uniform slope. The wind speed is uniform at any level but increases upward when the isotherms slope vertically. The currents move with constant speed at all heights when the isotherms are level. A wind discontinuity marks the front where the temperature gradient is concentrated.

The essential features of this model enjoyed acceptance in most meteorological circles during the interval between the two world wars. Observations verified them to a satisfactory extent up to 10,000 feet beyond which the atmosphere was not systematically explored. In the low levels, it is an observed fact that wind speed varies little with latitude. To the extent that the classical models discuss the currents in the upper troposphere, they largely extrapolate from the lower levels. They do not visualize a concentration of high velocities in narrow regions. Thus, the very strong winds encountered by the bombers introduced a feature of the circulation in the westerlies that was not allowed for by existing models.

The earliest intimation of the existence of a narrow, high velocity region in the upper westerlies appeared in a cross-section published in *Physikalische Hydrodynamik* [12] (fig. 1.2). It revealed that the kinetic energy of the westerlies in the upper troposphere was not evenly distributed with latitude, in marked contrast with the lower layers. This initial indication of the modification which our concepts of atmospheric structure were to sustain later on, did not attract much attention at the time of its publication.

In 1944, Willett [108] published mean cross-sections over North America (fig. 1.3) which again featured a localized high velocity stream in the upper westerlies. Together with the analyses of upper-air data compiled during the war, these sections made it clear that a revision of the concepts regarding the structure of the upper westerlies was in order.

Simultaneously with these synoptic developments, and to a great extent stimulated by them, theoretical investigations [82, 102] sought to discover the dynamic principles responsible for these high winds the importance of which, at least from the point of view of
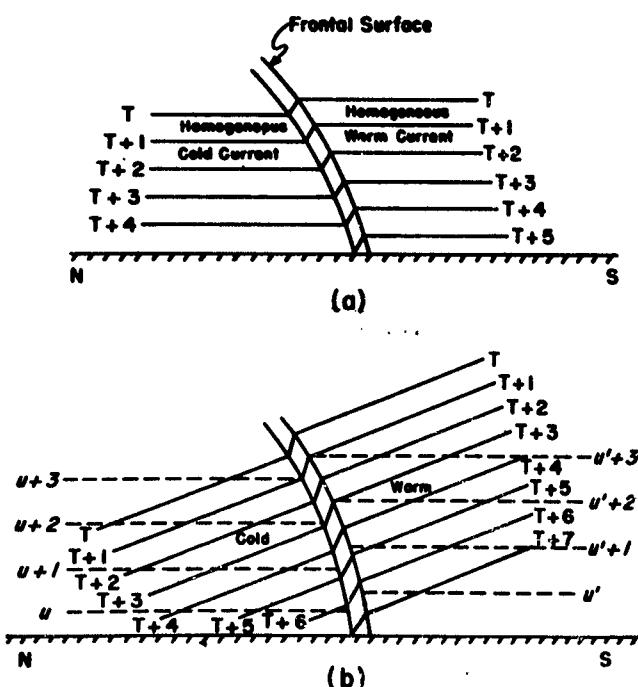
Fig. 1.1: Schematic representation of the wind and temperature fields in the vicinity of a frontal surface according to classical concepts: (*a*) level isotherms and a uniform current in each air mass; (*b*) sloping isotherms and currents (*u*, *u'*) increasing uniformly with height.
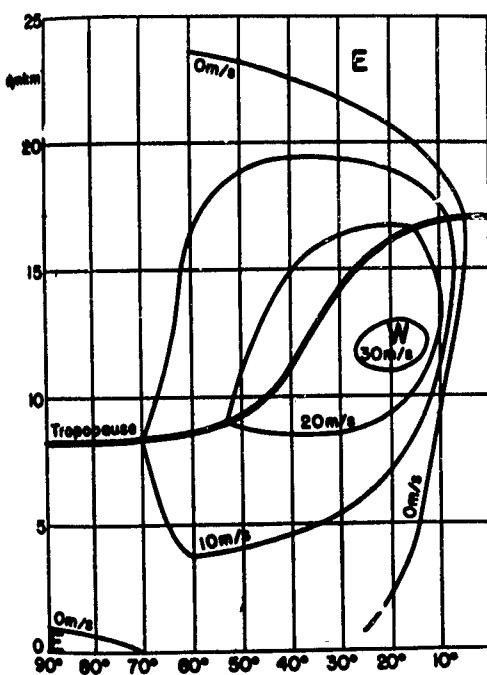
FIG. 1.2: Mean vertical distribution of zonal component of geostrophic wind in northern hemisphere for February [12].

air navigation, was easy to appreciate. Rossby [82] suggested that thermally driven lateral mixing associated with a tendency toward equalization of the vertical component of the absolute vorticity with latitude brought about, from time to time, an/ accumulation of the kinetic energy of the westerlies at the tropopause level equatorward of lat. 50°. His theory (cf. chap. VII) required that these maxima should increase in intensity as they were displaced equatorward toward lat. 30°. A paper published in the same year by Staff Members of the Department of Meterorology, University of Chicago [102], showed that the zonal winds observed at the tropopause during periods of straight west wind circulations appeared to agree fairly well with profiles computed on the basis of equalization of the vertical component of the absolute vorticity. The same paper also furnished synoptic evidence corroborating Rossby's statement that the flow configuration aloft in middle latitudes is suggestive of *a broad stream meandering eastward around the hemisphere in wavelike patterns. The kinetic energy of this stream is concentrated in a narrow band of high wind speed embedded in a relatively quiescent surrounding atmosphere.* This narrow band was named the JET STREAM.
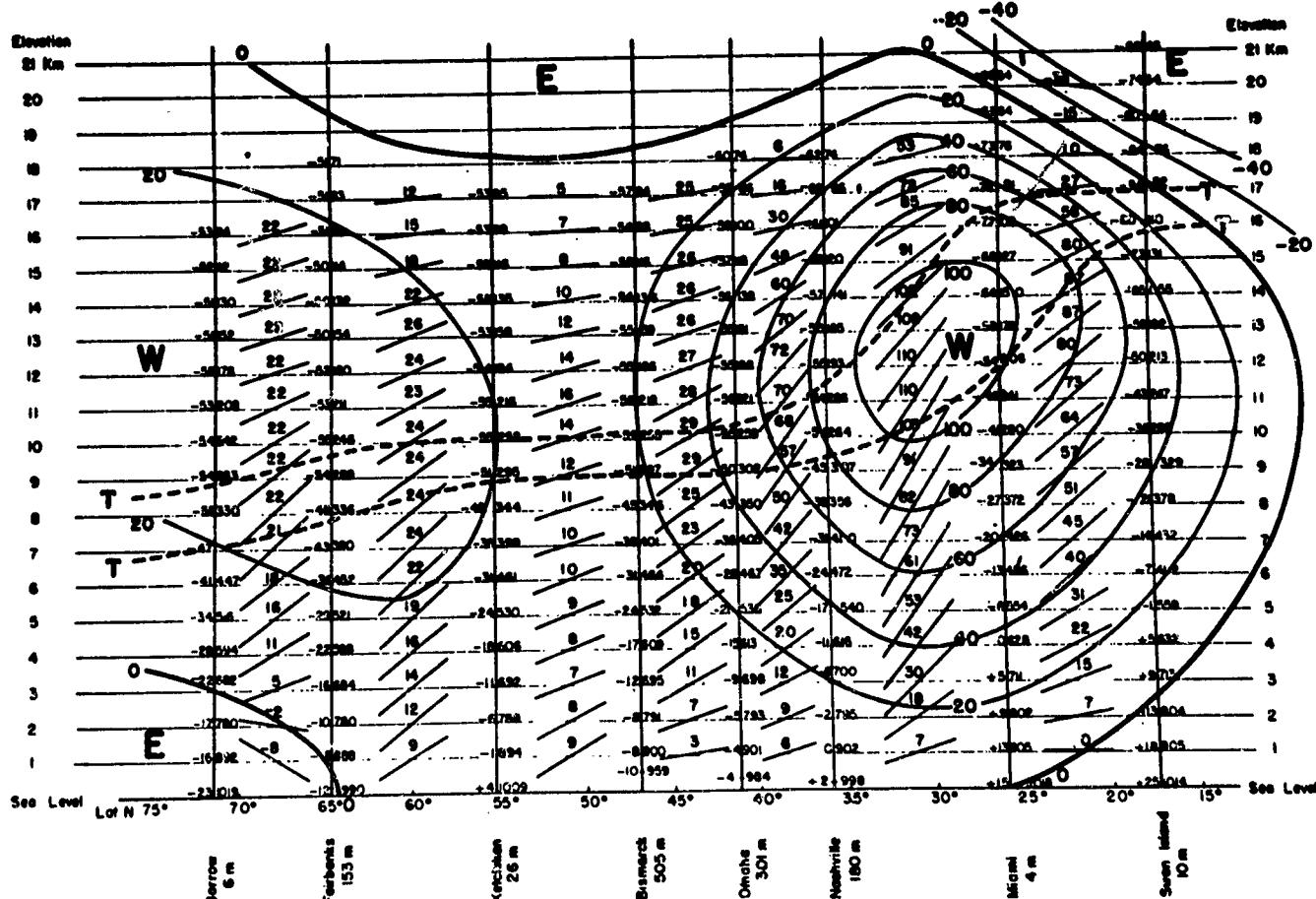

FIG. 1.3: Vertical cross-section of pressure (mb), temperature (°C) and wind (knots) for North America during winter [108].

2. Some Consequences of the Discovery of the Jet Stream

The discovery of the jet stream was destined to have far-reaching consequences. It revealed, for instance, a striking similarity between the structure of the atmosphere and that of major oceanic currents like the Gulf Stream. The establishment of this similarity is of much importance, since features known to exist in one fluid give a clue as to what to look for in the other. This leads to a better understanding of both. Further, in the few years since the jet stream came into promi-

nence as an important feature of the general atmospheric circulation, it has become known as a significant factor in diverse weather phenomena ranging from cyclogenesis in middle latitudes [68] to the "burst of the monsoon" over India [115] and rainfall over the Hawaiian Islands [114]. Of particular importance is the role it plays in the problems of short- and long-range forecasting (chaps. IV and V), and in understanding the climate of middle latitudes (chap. III).

CHAPTER II.   SYNOPTIC STRUCTURE OF THE JET STREAM

I. The Wind Field

A GENERAL VIEW

The jet stream may be visualized as a tube containing high wind velocities meandering around the hemisphere. A complete representation of its instantaneous structure must take into account its variations in all three dimensions.

a. Cross-sections constructed normal to the direction of flow. — Figs. 2.1 and 2.2 give two typical views of the structure of the westerlies as it appears on cross-sections drawn normal to the current. We are enabled to draw such sections because we observe that the wind direction within the band of strongest westerlies changes only slightly with altitude from the lower troposphere to the substratosphere.

The jet stream is depicted by the narrow and somewhat elongated core of closed isotachs[1] about 5°-10° lat. in width. Its axis slopes poleward with height below 500 mb. Higher up, it remains almost vertical to the level of strongest winds (about 250-200 mb) beyond which it reverses its slope and shifts equatorward with elevation. This equatorward elongation of the jet core sometimes appears as a separate maximum.

In fig. 2.1, the jet center is located at 47°N, and the strongest winds occur at 260 mb. In fig. 2.2, which shows the jet stream at a more southerly latitude (39°N), the strongest winds occur at a somewhat higher level (220 mb). This rise of the level of strongest winds with the shift of the jet stream from high to low latitudes is typical of most cases.[2]
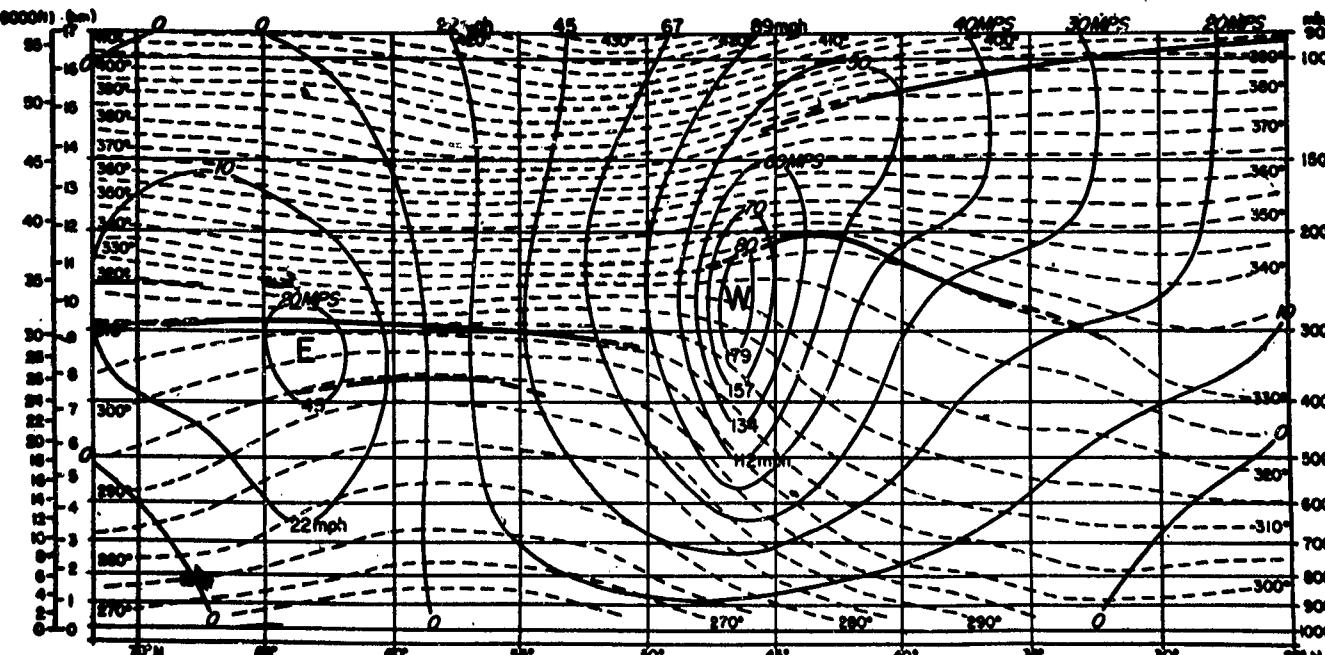

Fig. 2.1: A mean cross-section for 0300 GCT, November 30, 1946, showing the average distribution of geostrophic westerly wind and temperature over North America from lat. 25°N to 75°N, in a case of approximately straight westerly flow. Heavy lines indicate tropopause surfaces. Thin solid lines indicate the velocity of the westerly component of the geostrophic wind (mps and mph). Dashed lines indicate the potential temperature in °A [59].

[1]Lines of equal wind speed.

[2]An exception is a wind maximum found along the rim of the arctic in midwinter at extremely high altitudes.
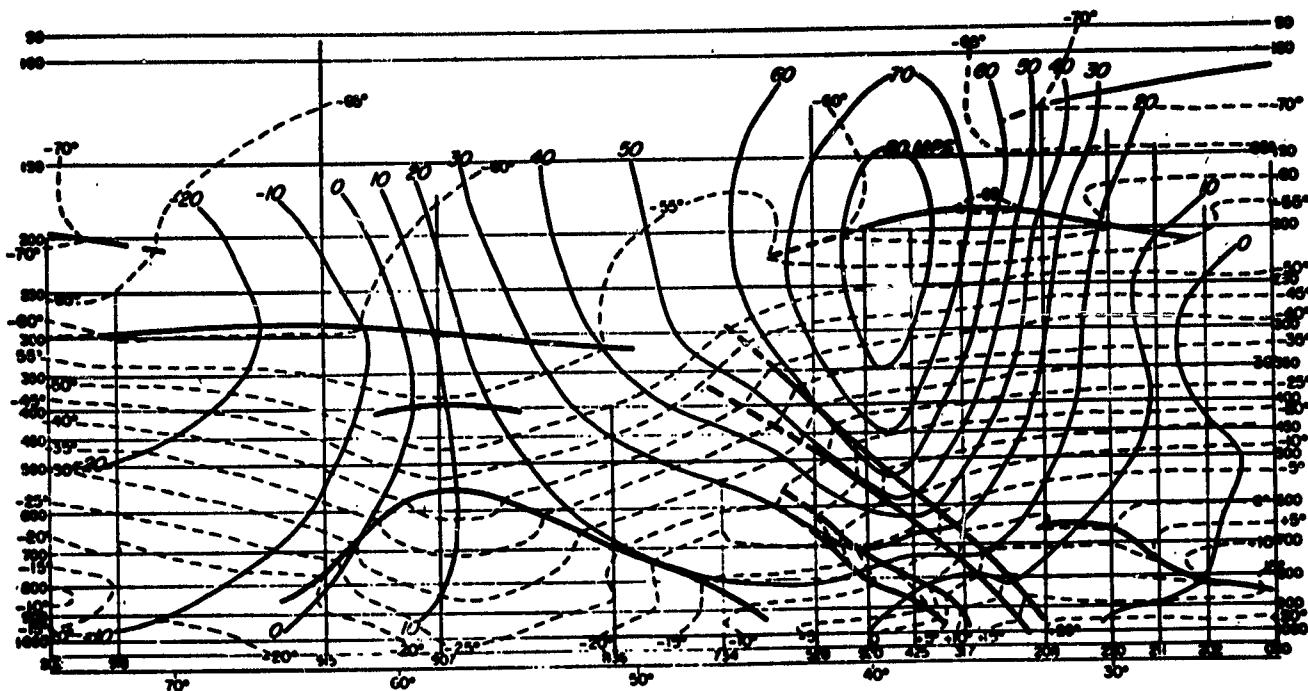
FIG. 2.2: Vertical cross-section approximately along the meridian 80°W from Havana in the south to Thule (Greenland) in the north. Vertical lines indicate the soundings used in the diagram with the international station numbers below. Frontal boundaries, inversions or tropopause surfaces are indicated by thick, solid lines when they are distinct, and by thick, dashed lines when not distinct. Thin solid lines indicate geostrophic wind velocity (mps) perpendicular to the cross-section, dashed lines isotherms (°C) [55].
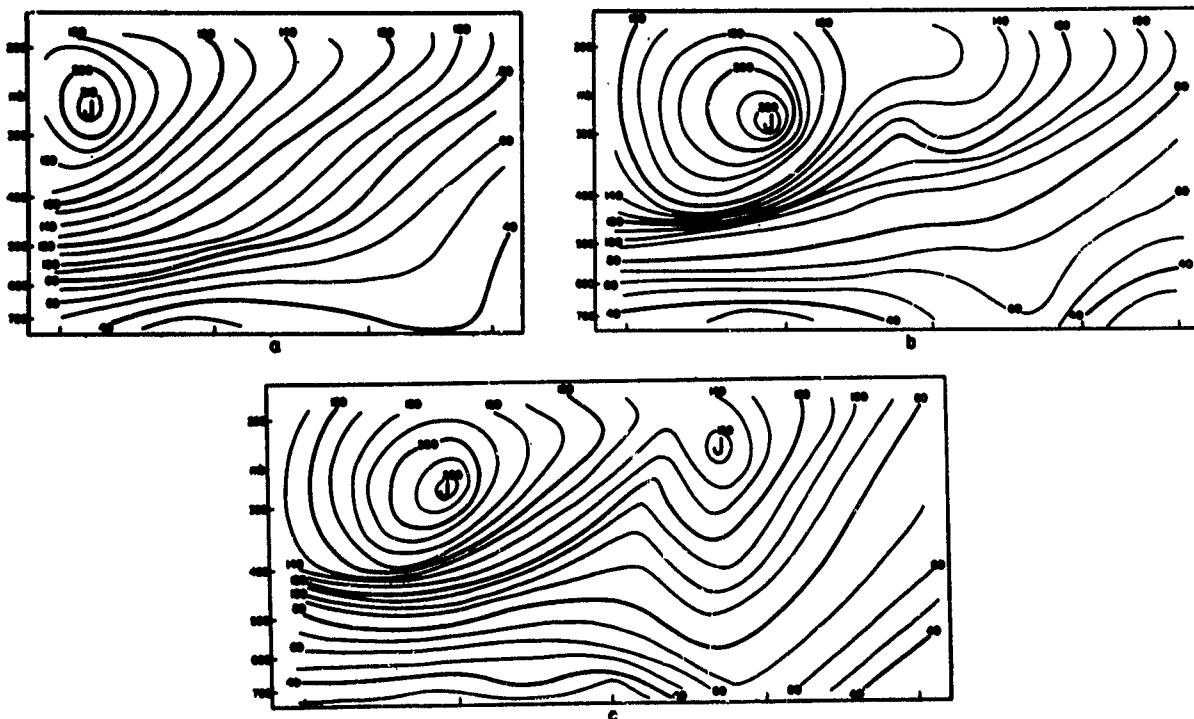
FIG. 2.3: Cross-sections showing isotach patterns (in knots) along the current through jet stream core: (a) November 12, 1951, 1500Z, (b) November 13, 1951, 0300Z, (c) November 13, 1951, 1500Z. J denotes jet stream center. Sections are constructed from isotach analyses at 700, 500, 300, and 200 mb. Lines connecting points of highest speed on each surface are projected on the 300-mb axis. Marks at bottom of sections correspond to tick marks along axis of jet in figs. 4.3, ac [75].

b. Cross-sections constructed along the direction of flow. — Fig. 2.3 gives a side-view of a jet stream seen on a cross-section constructed along the direction of flow. The wind is far from uniform in this direction. Fig. 2.3a shows that the strongest winds are confined within a region of small longitudinal extent, depicted by the closed isotachs. Downstream from this region, the wind speed decreases steadily. The isotachs form elongated patterns. The surface of strongest winds which runs along this elongation appears to slope upward downstream from the maximum.

Jet streams undergo a distinct life cycle consisting of a period of organization and one of disorganization; their horizontal structure as it appears on high-level maps depends on the phase of this life cycle. Periods when the jet is organized are illustrated by fig. 2.4a which shows a well-developed jet as it appears on a 300-mb map. The jet reveals itself as a narrow band of high wind velocity meandering over North America. The thick black line joining the points of highest wind speed at different meridians within this band describes the axis of the jet. This axis follows the pattern of the
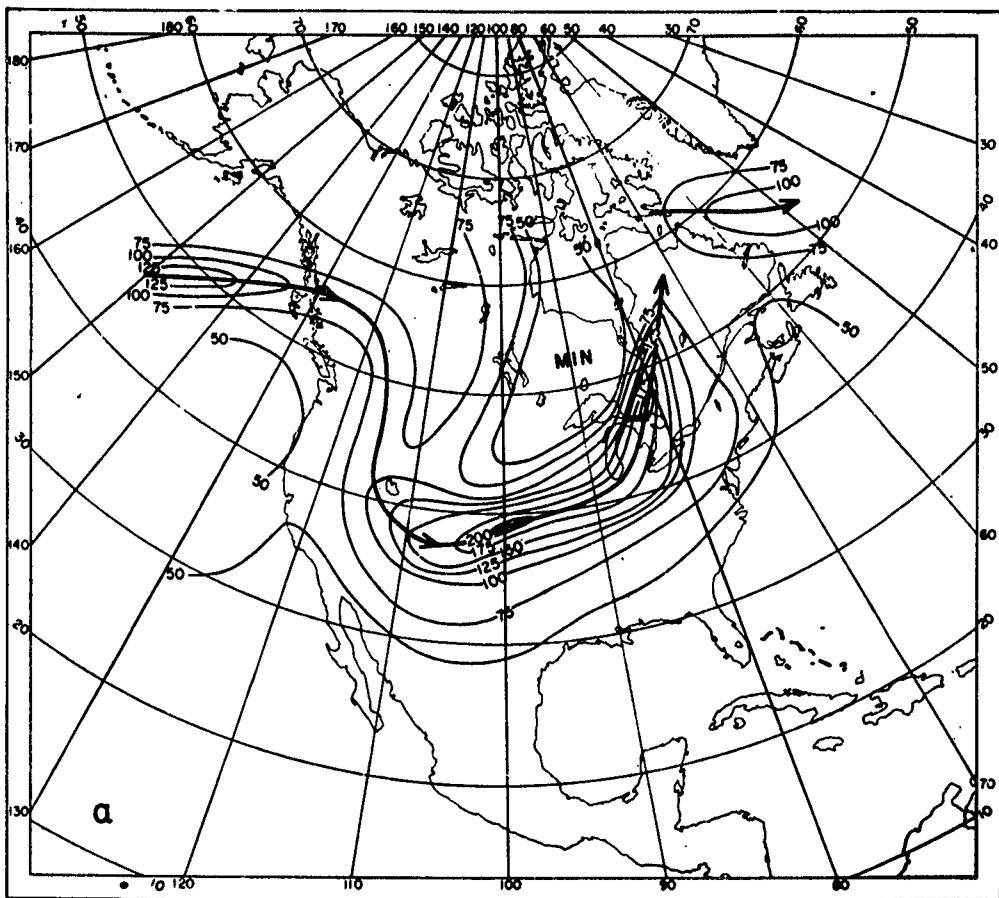

Fig. 2.4a: Isotachs (Knots) at 300 mb, November 10, 1950, 0400 Z. [72].

Occasionally, the downstream elongation of the speed patterns develops into a separate center. Fig. 2.3b-c shows successive stages in such a development.

c. Constant pressure maps. — The horizontal structure of the jet stream is closely portrayed on constant pressure maps of the middle and upper troposphere. In view of the variation of the level of the jet center with latitude, just described, and its known tendency to shift to higher elevations with the advent of the warmer season of the year, the 300-mb map is considered most suitable for furnishing a horizontal view at high latitudes and in winter, and the 200-mb map for low latitudes and in summer.

long waves and its amplitude is comparable to that of the 300-mb contours (fig. 2.4b). The lack of uniformity in wind speed along the axis, revealed by fig. 2.3, is very much in evidence on these maps. A succession of velocity maxima alternate with intervals where the winds are comparatively weak. The wind gradient along the axis is sharp, and the difference between the wind speeds at the maximum and minimum points may amount to over 100 knots.

During disorganized periods, the clear-cut concentration of velocities is missing. The westerlies either break up into vortical circulations or show fairly uniform velocities throughout the middle latitudes. Nu-
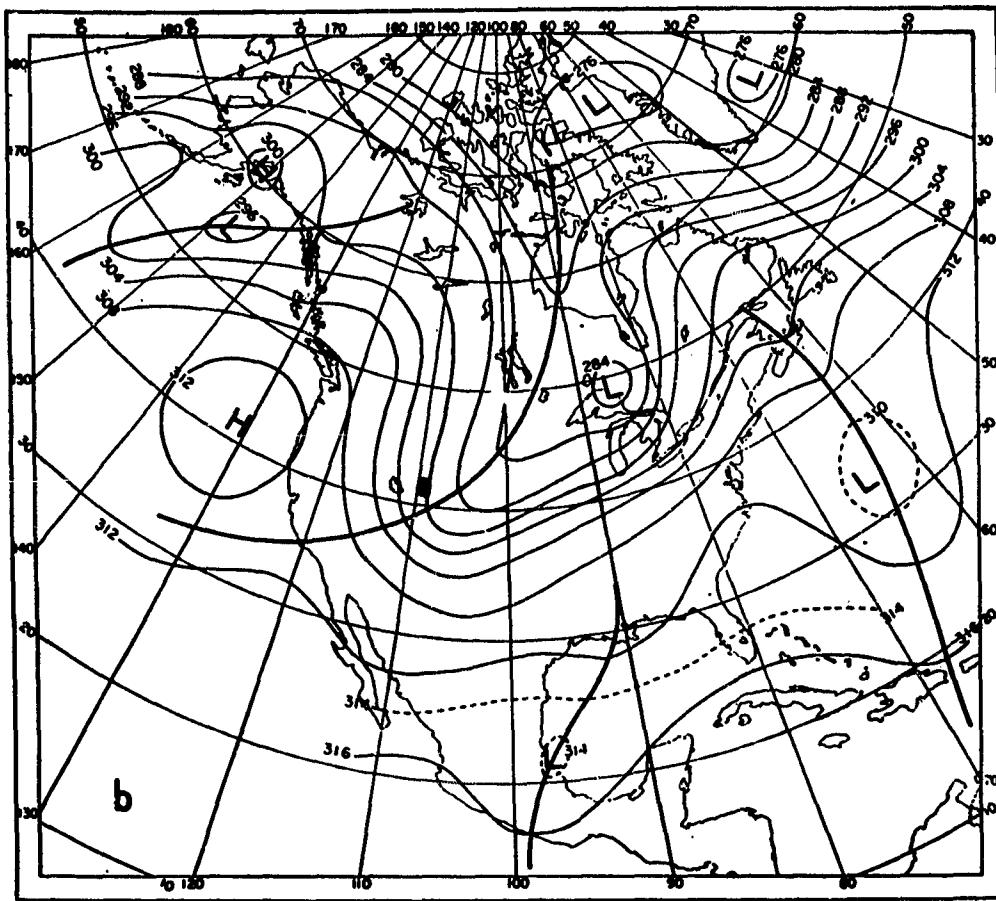
FIG. 2.4b: Contours at 300 mb, November 10, 1950, 0400Z [72].

merous "jet fingers" (fig. 2.5), all comparatively weak and sometimes separated by as little as 5° lat., characterize the wind speed pattern. The velocity difference between the fingers and the intervening slow areas may not amount to more than 25 knots — in marked contrast with the strong velocity differences observed during organized periods.

VELOCITY MAXIMA AND MINIMA ALONG THE JET AXIS

The velocity maxima and minima which alternate along the axis of a well-developed jet are connected with the short waves in the westerlies and usually move downstream with a speed geared to that of these waves. The distance between successive maxima is not constant but varies from about 10°-25° long.

The magnitude of the velocities which occur in the central regions of jet maxima is a matter of conjecture since little direct evidence concerning them is available. For one thing, the network of upper-air observations is not close enough. Moreover, balloon observations which constitute the major source of upper-wind data are least accurate for high winds. Thus, the best

available estimate of the wind speeds in these central regions is based on geostrophic computations according to which they may reach 150 mps. But no such speeds have been directly observed.

The regions of wind concentration along the jet axis retain their identity and to a certain extent their con-
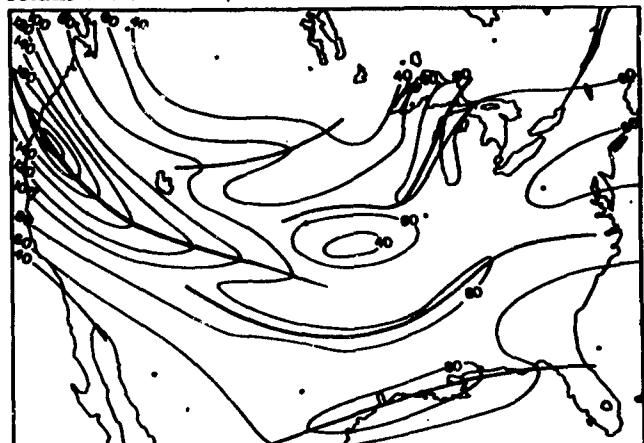

FIG. 2.5: 300-mb isotachs (knots) on November 12, 1951, 1500Z, showing a disorganized jet with several jet "fingers" over central and eastern United States, and an organized jet approaching from the west [75].

figuration for short periods of time. But they have a definite life history during which they undergo a continual evolution which can be followed on maps or cross-sections. Formation and decay of these regional jets conform to a cycle which is regular enough to allow description by means of a model [73]. Fig. 2.6 illustrates this model:

Starting with a symmetrical distribution of isotachs along the axis (fig. 2.6a), the isotachs downstream from the center move faster than those to the rear (fig. 2.6b). Furthermore, high-speed isotachs move faster than the slower ones, with the result that the area enclosing the highest winds increases and, at the same time, the isotachs ahead of the center become crowded in a very narrow leading edge (fig. 2.6c). Subsequent to this stage, a rapid adjustment takes place in the wind field. The low-speed area ahead of the maximum disappears as the latter merges with the maximum further downstream. The resulting pattern shown in fig. 2.6d leads back to the starting stage (fig. 2.6a) and the cycle may be repeated. However, this is not invariably the case. As mentioned above, the jet stream as a whole has a definite life cycle which

spans a week or more and which consists of a period of organization and another one of decay. Fig. 2.6a-d describes the evolution of the wind pattern during periods when the jet stream is fully organized. Eventually, when the jet stream is on the decline, the situation
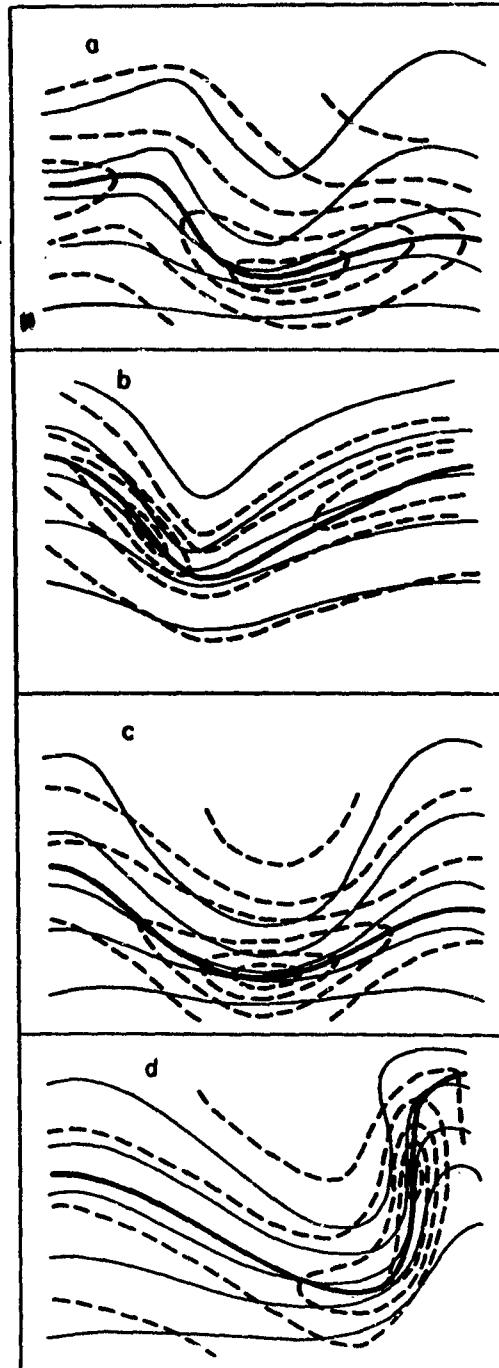
Fig. 2.7: Model of velocity distribution in the high troposphere in middle latitudes during the passage of a short-wave trough through a long-wave trough when speed of westerlies is above average in the lower middle latitudes. Solid lines are isobaric contours, dashed lines are isotachs. Heavy line marks jet axis. Time interval between successive stages is about one day [72].

Fig. 2.6: Five stages during eastward progression of velocity maximum along jet stream axis. Isotachs are in knots [73].

shown in fig. 2.6c is followed by that in fig. 2.6e rather than 2.6d. The various maxima combine and the wind speed along the current becomes uniform. This stage is a precursor of the disintegration of the current and its breakdown into "jet fingers."

The behavior and configuration of the travelling jet maxima and minima vary with broadscale conditions in the westerlies. We shall now consider two model
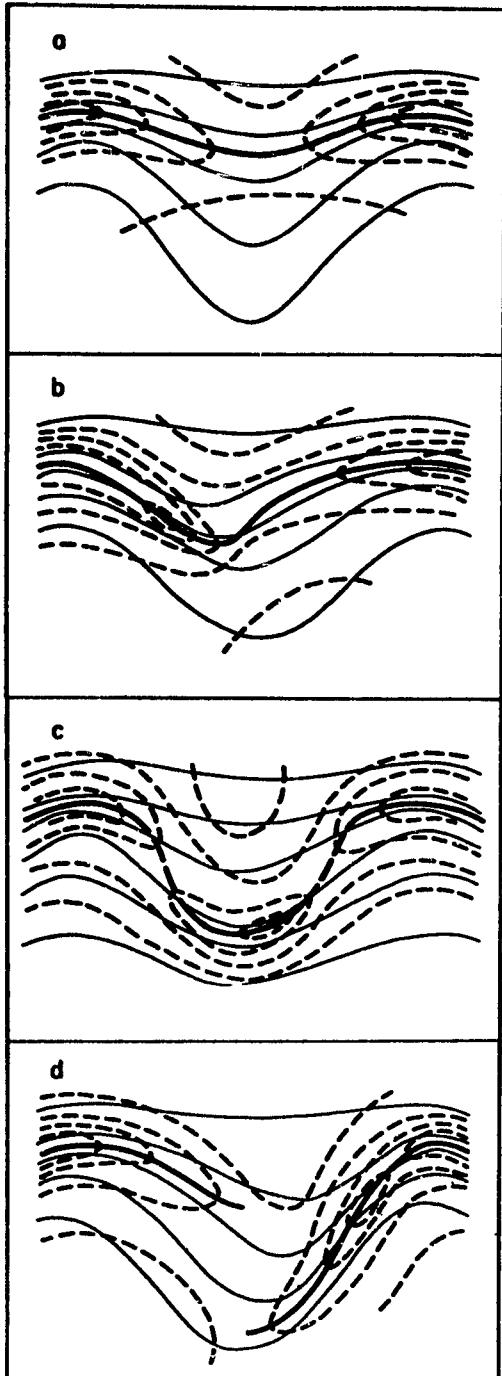
FIG. 2.8: Same as fig. 2.7 when westerlies are above average in upper middle latitudes [72].

sequences describing the upper tropospheric flow pattern when a travelling maximum passes through a long-wave trough during periods when the jet stream is well organized and the energy of the westerlies is concentrated in a well-defined narrow belt. These sequences are schematically represented in figs. 2.7 and 2.8.

The first sequence occurs when the hemispheric westerlies have above-average strength in the lower middle latitudes. During such periods, velocity maxima along the jet stream in middle latitudes occur with preference in long-wave troughs and velocity minima in long-wave ridges [72].

In fig. 2.7a, we find a maximum reflecting the broadscale conditions in the westerlies, centered in the long-wave trough, and another maximum associated with a short-wave trough arriving on the long-wave ridge to the west. As the short-wave trough reaches the inflection point downstream from the ridge (fig. 2.7b), the two maxima begin to merge, and the composite maximum — which appears as if it had suffered a westward shift — drives into the long-wave trough with a well-defined leading edge.

Next (fig. 2.7c) we see a complete superposition of the two maxima in the long-wave trough. The composite maximum is well-defined and shows a sharp decrease of wind speed both upstream and downstream from it.

Fig. 2.7d represents a likely, though not a unique development ensuing from the stage represented by fig. 2.7c. This latter stage is very favorable for cyclonic intensification (see chap. IV), and the stage illustrated by fig. 2.7d assumes that such intensification has occurred. In this case the ridge downstream from the trough builds up and the jet maximum intensifies further. In fact, some of the strongest tropospheric winds have been reported during this stage.

The second sequence (fig. 2.8) occurs during periods when the hemispheric westerlies have above average strength in the upper middle latitudes. At such times, velocity maxima tend to occur with preference in long-wave ridges.

The initial stage (fig. 2.8a) shows two velocity maxima, one in each of the ridges. As a short-wave trough advances (fig. 2.8b), the maximum upstream from the ridge is elongated. At the time of superposition of the short- and long-wave troughs (fig. 2.8c), three distinct maxima are in evidence, one in the long-wave trough and one in each of the ridges.

Fig. 2.8d depicts the ensuing pattern on the assumption that a cyclone has formed or intensified (see chap. IV). The central maximum leaves the trough and increases in intensity as it moves toward the ridge.

The above models for the upper-flow patterns and their variations do not exhaust the possible isotach patterns occurring in the long-wave train with the described broadscale conditions. Often, the jet stream

structure and the flow patterns associated with it are too complicated to allow portrayal in model form.

THE VERTICAL WIND SHEAR IN THE JET STREAM REGION

The narrow jet stream band concentrates within its boundaries the strongest vertical wind shears observed in the belt of the westerlies. In the meridional cross-sections presented in figs. 2.1 and 2.2, the isotachs north and south of the core of strongest wind run close to the vertical indicating little variation of wind speed with height. Large values of the vertical wind shear are restricted to a narrow zone along the vertical axis of the jet, where it reaches an order of magnitude of 10 mps/km. Even here, however, the vertical shear is not uniform throughout the troposphere. In general, we encounter the highest values above the 500-mb surface. It is here that the wind increases most rapidly with height up to the tropopause level. Indeed in summer, and occasionally even in winter, the strongest wind shears may be situated above 300 mb, and dwindle downward to negligible proportions near 500 mb. *And while some jets seem to be tied with the surface temperature gradient and so extend — with greatly diminished intensity — clear down, others, particularly in lower latitudes and in summer often exist only at high levels, and conditions at 500 mb give no indication of those higher up.* A case in point is illustrated in fig. 2.9, which clearly shows the vertical wind shear to be concentrated above 15,000 feet.

Palmén and Newton [60] bring out the vertical distribution of wind shear graphically by drawing pressure profiles in a diagram with latitude and wind speed as coordinates (fig. 2.11) for the mean cross-section shown in fig. 2.10. The vertical shear is given by the vertical distance between the pressure surfaces at any latitude. At lat. 55°, for instance, these surfaces are very close together indicating nearly uniform wind speed at all heights up to 300 mb. In contrast, the wind increases very strongly upward to 300 mb in a narrow belt centered on lat. 46°. In fig. 2.11, the vertical shear is strongest within the polar front zone which is marked by the dotted lines. The wind speed changes by as much as 20 mps from the lower to the upper boundary of the front at lat. 46°. The surface wind is about nine mps; it is 27 mps at the lower boundary of the front, 47 mps at the upper boundary, and 68 mps at 300 mb. Thus, the total shear is 17 mps in the cold air mass, 20 mps in the frontal zone, and 21 mps in the upper warm air mass. In spite of the strong concentration of shear in the frontal layer, the latter contributes only one third of the total increase of wind in the troposphere.

THE HORIZONTAL WIND SHEAR

Fig. 2.11 also demonstrates the lateral concentration of strong winds and the rapid drop of speed on either side of the jet stream core. Fig. 2.12 gives values for the horizontal wind shear normal to the jet axis, computed from fig. 2.10. The greatest cyclonic and anticyclonic shears are located at the level of strongest winds, about 200 km respectively to the north and south of the axis of the jet stream. To the right of the jet, at about lat. 43°N, the anticyclonic shear reaches a value of 10^{-4} sec^{-1} — slightly less than the Coriolis parameter for that latitude. This amounts to about 50
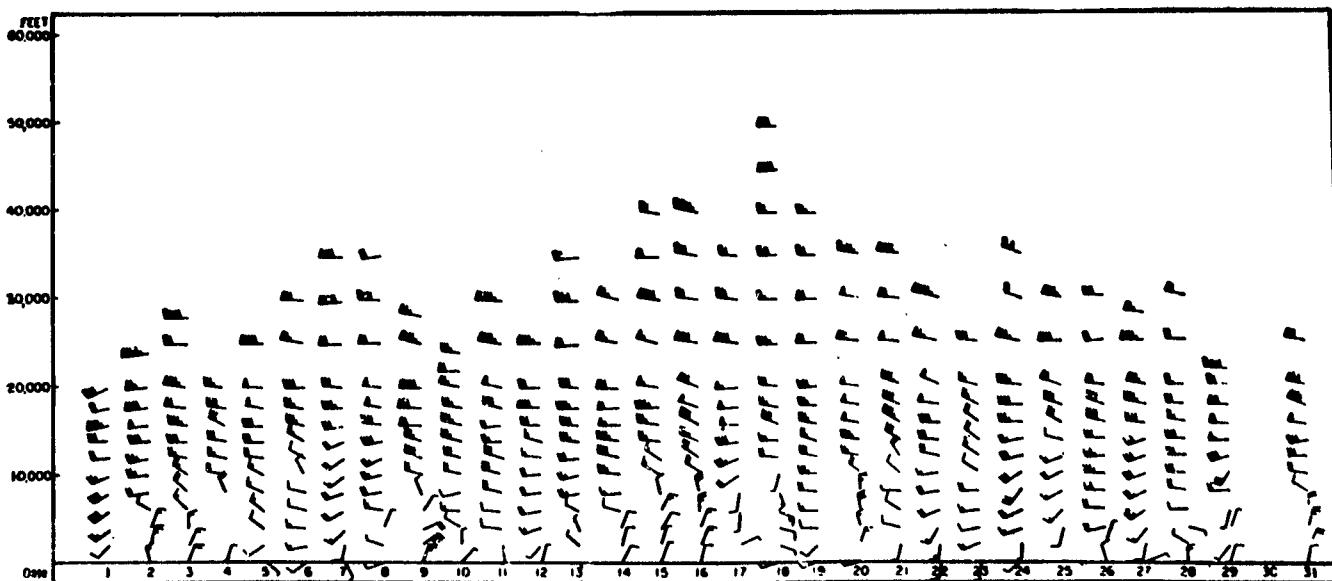

Fig. 2.9: Vertical time section of the winds at Hankow, China, for January 1946. One barb is 10 mph; one triangular barb, 50 mph; and one block, 100 mph [112].
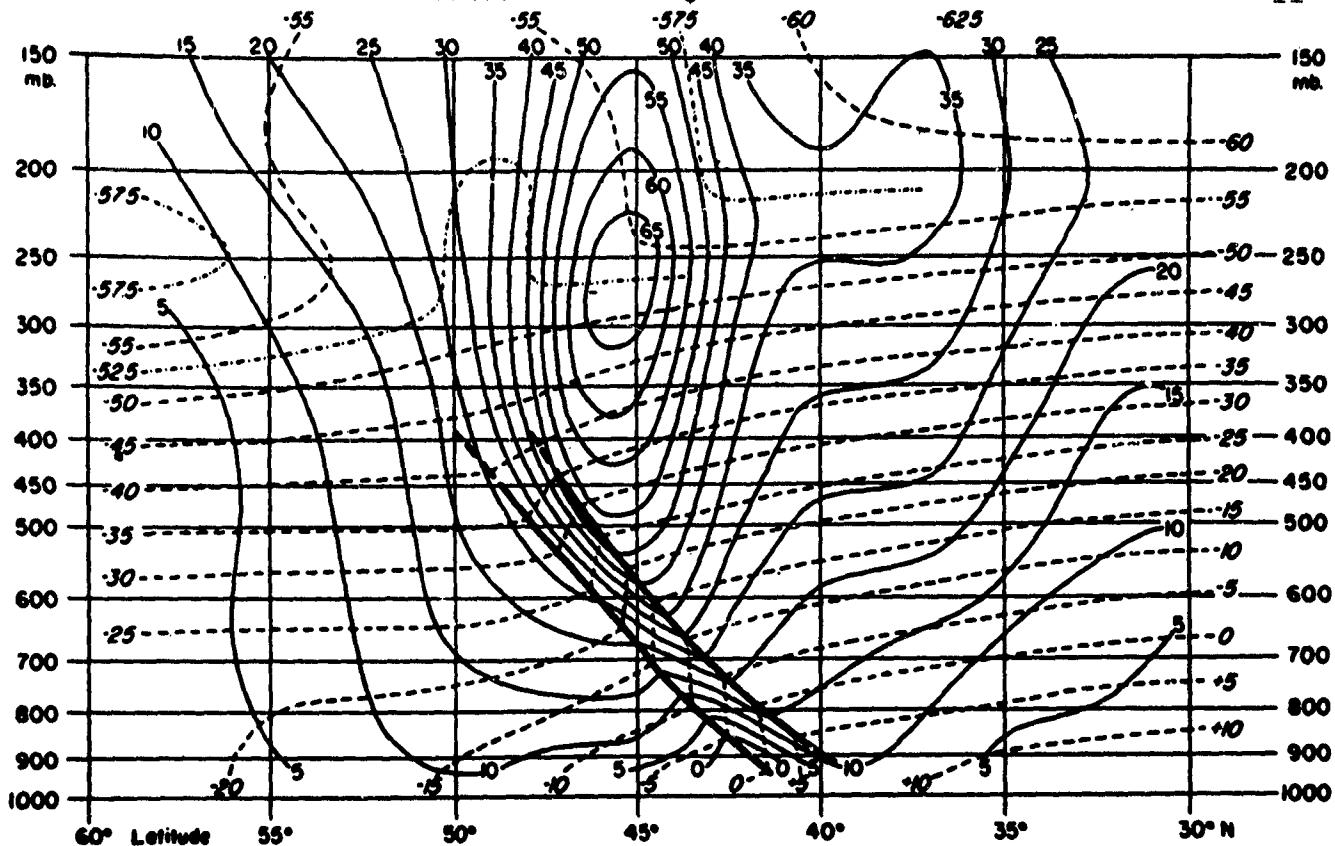
FIG. 2.10: Mean temperature and zonal component of geostrophic wind, computed from 12 cases in December 1946. The cross-section lies along the meridian 80°W. Heavy lines indicate mean positions of frontal boundaries. Thin dashed lines are isotherms (°C, slanting numbers) and solid lines are isolines of westerly component of wind (mps, upright numbers). Means were computed with respect to the polar front [60].
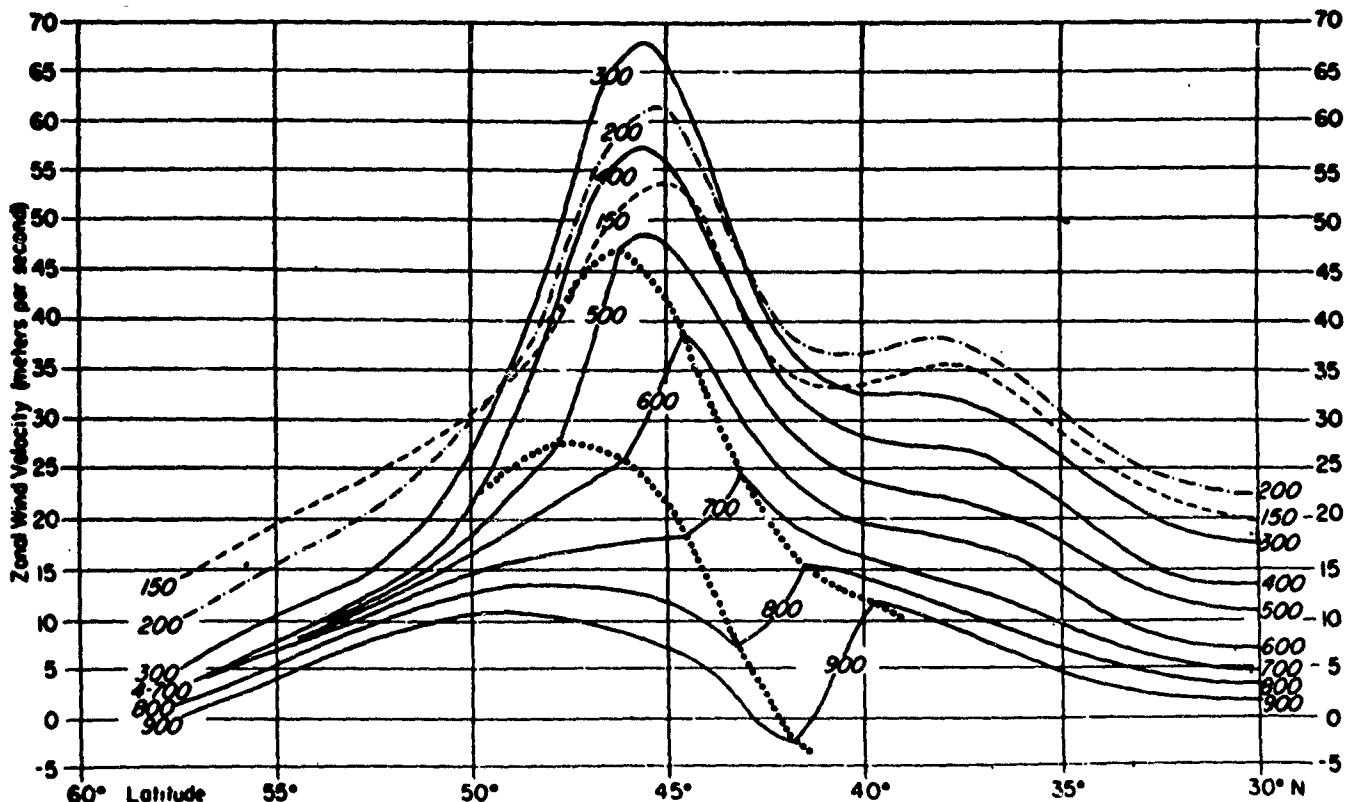
FIG. 2.11: Mean geostrophic wind profiles at isobaric surfaces from fig. 2.10. Heavy dotted line connects intersections of frontal surface with wind profiles at different levels [60].
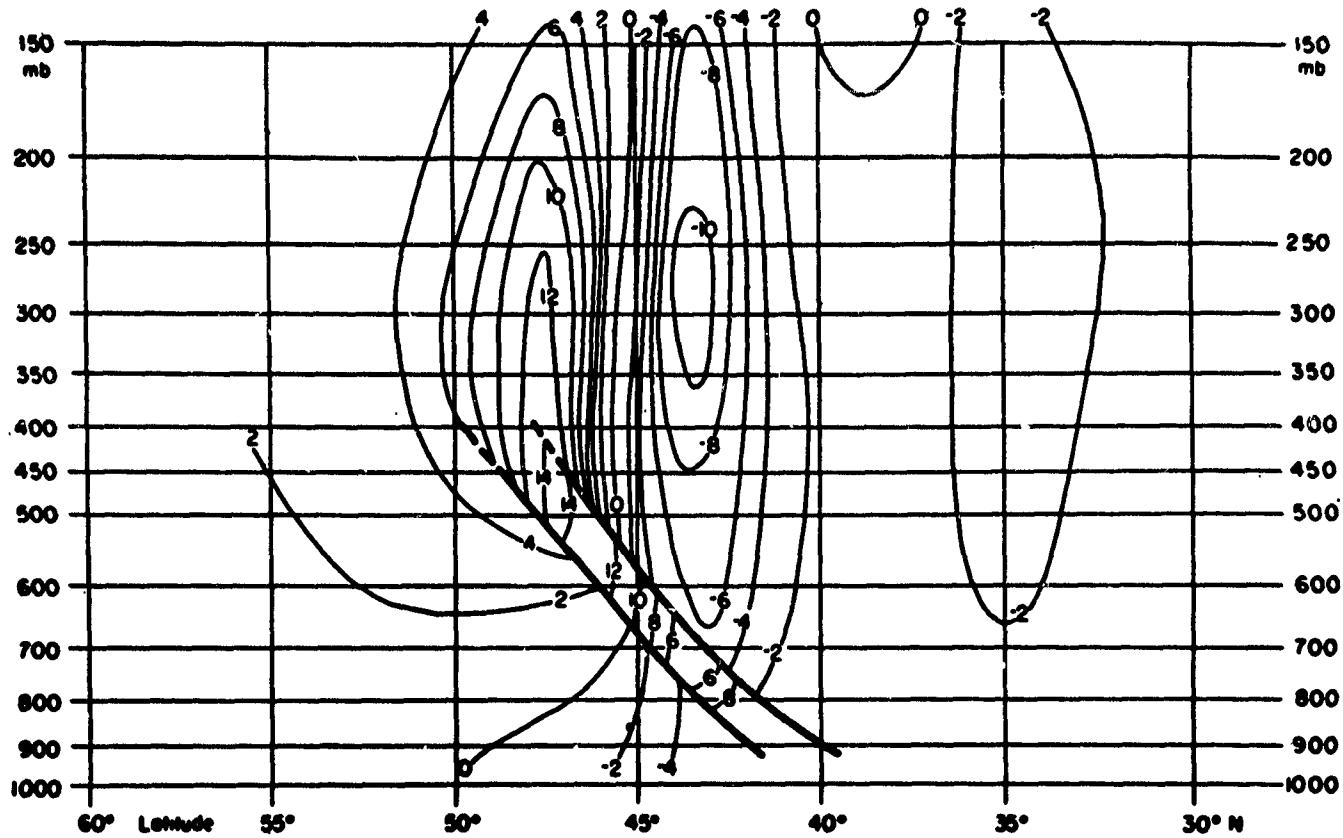
Fig. 2.12: Mean horizontal wind shear from fig. 2.10. Units are m/sec/(100 km), or 10^{-5} sec^{-1}. Positive numbers indicate cyclonic shear; negative numbers, anticyclonic shear [60].
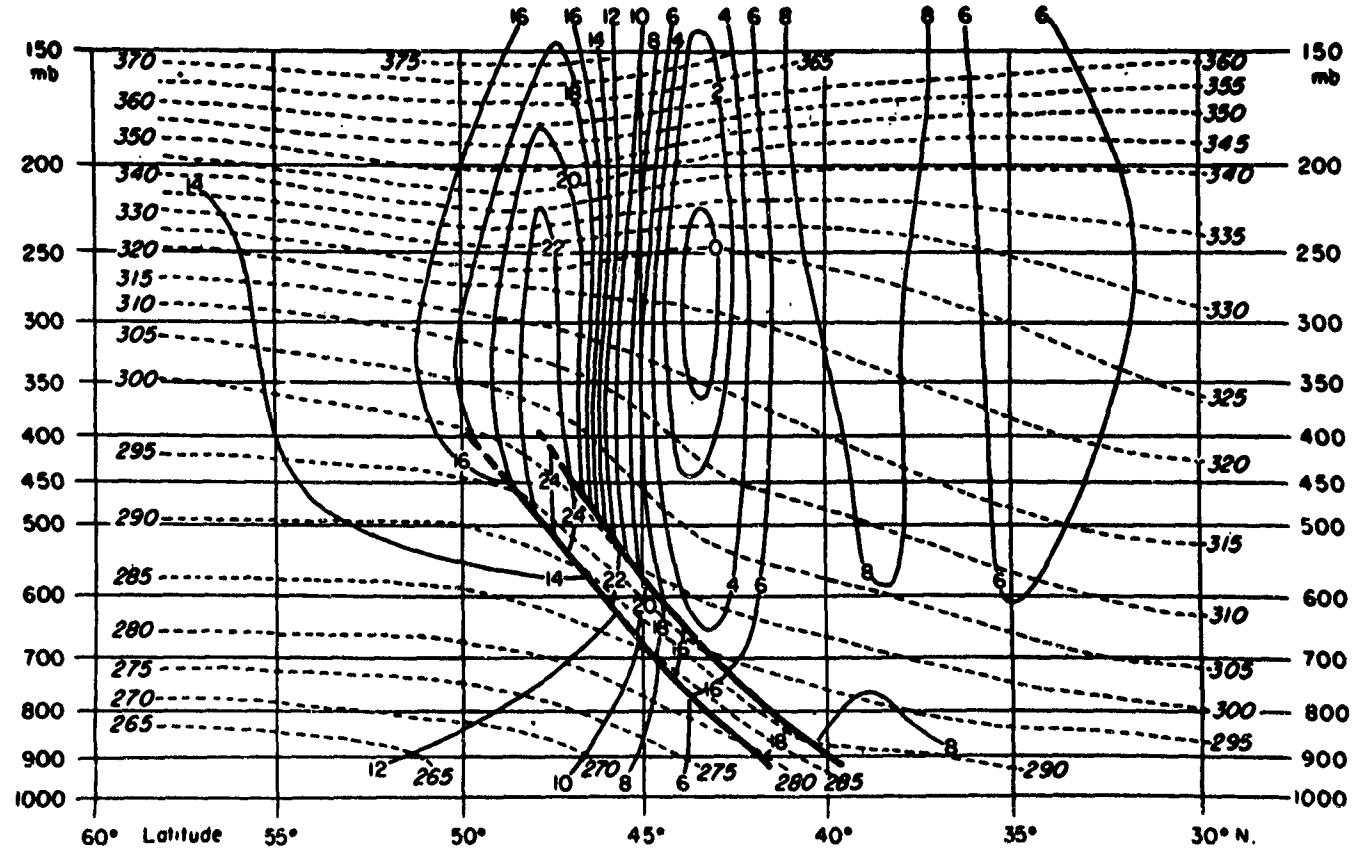
Fig. 2.13: Mean absolute vorticity (solid lines, upright numbers, units 10^{-5} sec^{-1}) and potential temperature (dashed lines, slanting numbers, °A) from fig. 2.10. Axis of jet stream corresponds to line 10×10^{-5} sec^{-1} vorticity above frontal layer [60].

mps within a distance of 5° lat. Although the values of the shear given in this figure are admittedly inexact owing to the assumption of geostrophic flow, there is strong evidence that values of the shear equal to the Coriolis parameter are often reached just south of the jet stream core. The cyclonic shear to the left of the axis is even more spectacular than the anticyclonic shear to the right of it, and often amounts to several times the Coriolis parameter.

THE DISTRIBUTION OF ABSOLUTE VORTICITY

The vertical component of the absolute vorticity is intimately connected with the wind shear and is given by

$$\zeta_a = \frac{\partial u}{\partial r} + \frac{u}{r} + f$$

where ζ_a denotes the absolute vorticity, r the radius of curvature of the streamlines taken positive for cyclonic circulations, f the Coriolis parameter, and u the wind speed. Palmén and Newton [60] have computed the vorticity distribution for the cross-section of fig. 2.10. Their results are presented in fig. 2.13. The assumption that the curvature may be neglected, plus the fact that the Coriolis parameter changes only gradually with latitude, makes the absolute vorticity pattern almost identical with that of the horizontal wind shear (fig. 2.12). The axis of the jet corresponds to the isoline of absolute vorticity with the value 10^{-4} sec^{-1}. To the north of this axis, the vorticity increases very rapidly and reaches a maximum of 22×10^{-5} sec^{-1} about 200 km away. This value greatly exceeds the Coriolis parameter at the pole (14.6×10^{-5} sec^{-1}). South of the jet axis the vorticity decreases very sharply, and perhaps is even discontinuous in some cases. At a distance of 200 km from the core, Palmén and Newton found that the absolute vorticity is nearly zero.

Although the assumption of geostrophic flow tends to exaggerate the extremes, there seems to be little doubt about the existence of zones of absolute vorticity far exceeding that of the polar region to the north of the jet, and of vorticity very near zero to the south of it. We should note, however, that we lack reliable evidence for the existence of negative absolute vorticity over extended areas although zero vorticity is frequent. It appears that zero vorticity represents the limit which the atmosphere attains, apart from a possible microstructure within the jet stream region. This fact can be used as an aid in high-level wind analysis over regions with sparse data (cf. also chap. VI).

THE JET STREAM ON A HEMISPHERIC SCALE

a. Multiple jets. — So far, our attention has been confined to the structural features of the wind field in belts where the energy of the westerlies is concentrated. Maps of the middle and upper troposphere which cover an extensive latitudinal belt show that the concentration does not usually occur along a single axis. On almost any day, these maps reveal the presence of at least two bands of velocity concentration (fig. 2.14). Occasionally three or four distinct bands are in evidence for short periods.

The multiple structure of the jet has been investigated by several writers [6, 19, 65]. Their results permit the following statements:

(1) The individual jet bands tend to lie parallel to the upper contours, but appreciable departures from this alignment are often observed, especially to the east of long-wave troughs (fig. 2.14).

(2) The different jets are not equally intense. The most intense among them constitutes the principal jet, generally situated in middle latitudes and connected with the zone of greatest temperature gradient in the low and middle troposphere.

(3) The individual jet axes often show a general net equatorward shift of the order of one-half degree of latitude per day. New maxima form in high latitudes as older maxima move into the tropics. This is illustrated in fig. 2.15 which also shows that the general equatorward trend is interspersed with periods during which the maxima remain stationary or even show a poleward drift. The latitudinal drift of the jet axes is much too irregular to be used as a forecasting tool.

(4) Jets show a tendency to attain their maximum strength in middle latitudes.

(5) Their equatorward migration is usually accompanied by a rise of the core to a higher elevation. A notable exception to this is the wind maximum found in midwinter along the rim of the arctic which is located at an extremely high elevation — probably exceeding 100 mb.

(6) Although separate jet bands usually retain their identity on a hemispheric scale, they occasionally appear to coalesce in one or more regions (fig. 2.16). Phillips [64] has observed that in such cases, both tributaries upstream from the point of confluence can be as fully developed in the high troposphere as in the "confluence" zone.

(7) Conversely, a single well-defined jet is often observed to split into two or more branches. In this case the northern branch often shows a temporary northward trend.
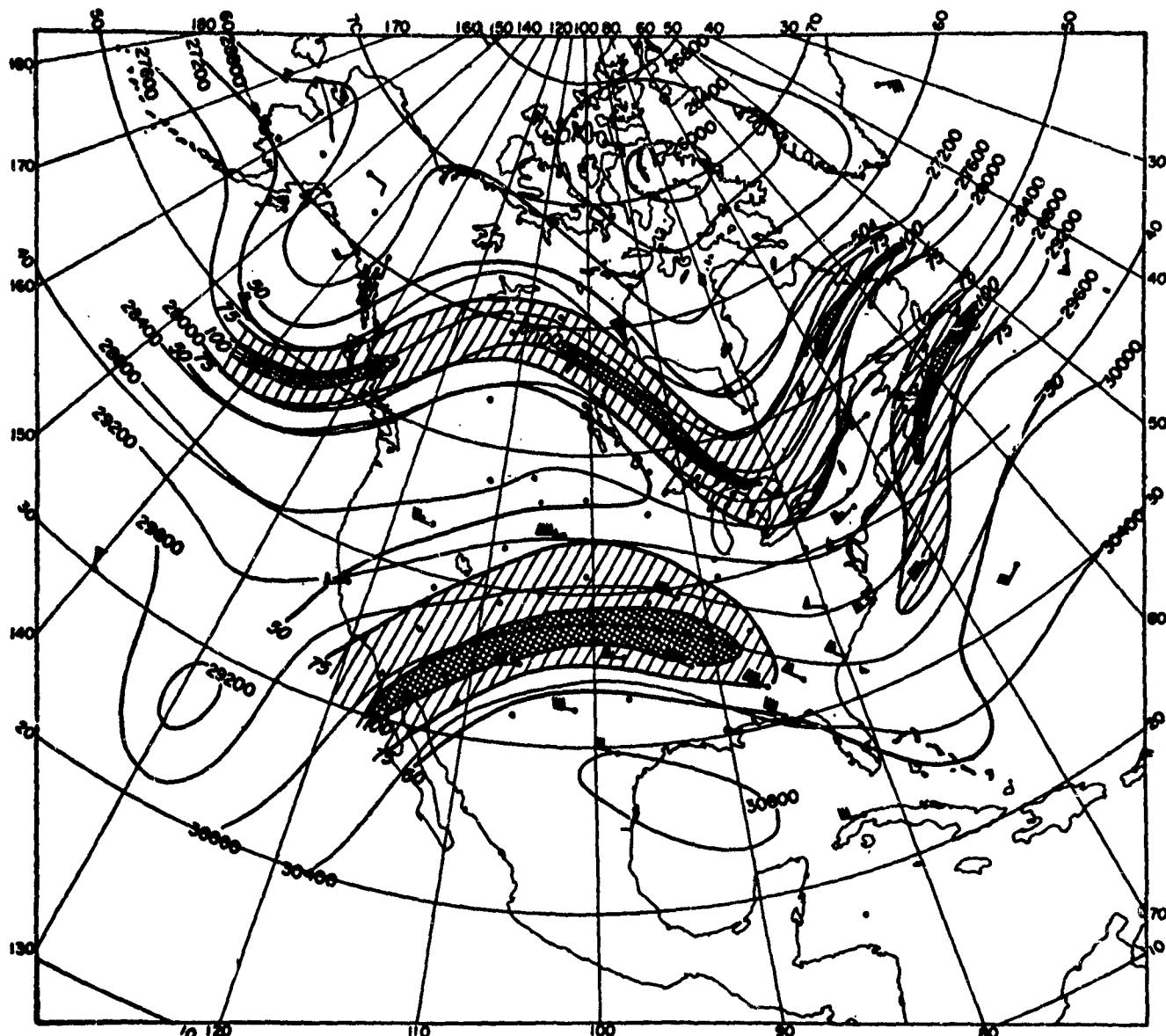
Fig. 2.14: A synoptic example of the wind field at 300 mb on October 25, 1950, 0300 GCT, showing the mutiple structure of the jet stream. Hatched areas denote regions with wind speed exceeding 75 knots, cross-hatched areas have wind speeds exceeding 100 knots [86].

b. Blocks. — A distinctive and important type of split in the westerly flow, which is known as "block," is of frequent occurrence. According to some authors [9, 66], blocks have the following characteristics:

(1) The basic westerlies split rather abruptly into two branches at a well-defined longitude. Upstream from the split the flow is essentially zonal for some distance and forms a narrow jet. Downstream it is wavy or cellular, but the two branches still have intense velocity concentration. In well-developed blocks, such as is fig. 2.17, a dynamic high lies just south of the northern branch and a dynamic low just north

of the southern branch with easterly flow between them.

(2) The split must be symmetrical in the sense that about half the contours of an upper pressure surface constitute the northern branch and half the southern branch.

(3) The blocking pattern, when established, must persist at least 10 days.

(4) Blocks form with preference over the eastern parts of the oceans, and particularly over Great Britain and Scandinavia. Once developed, they have a tendency for westward motion during intensification and for eastward motion during dissipation.
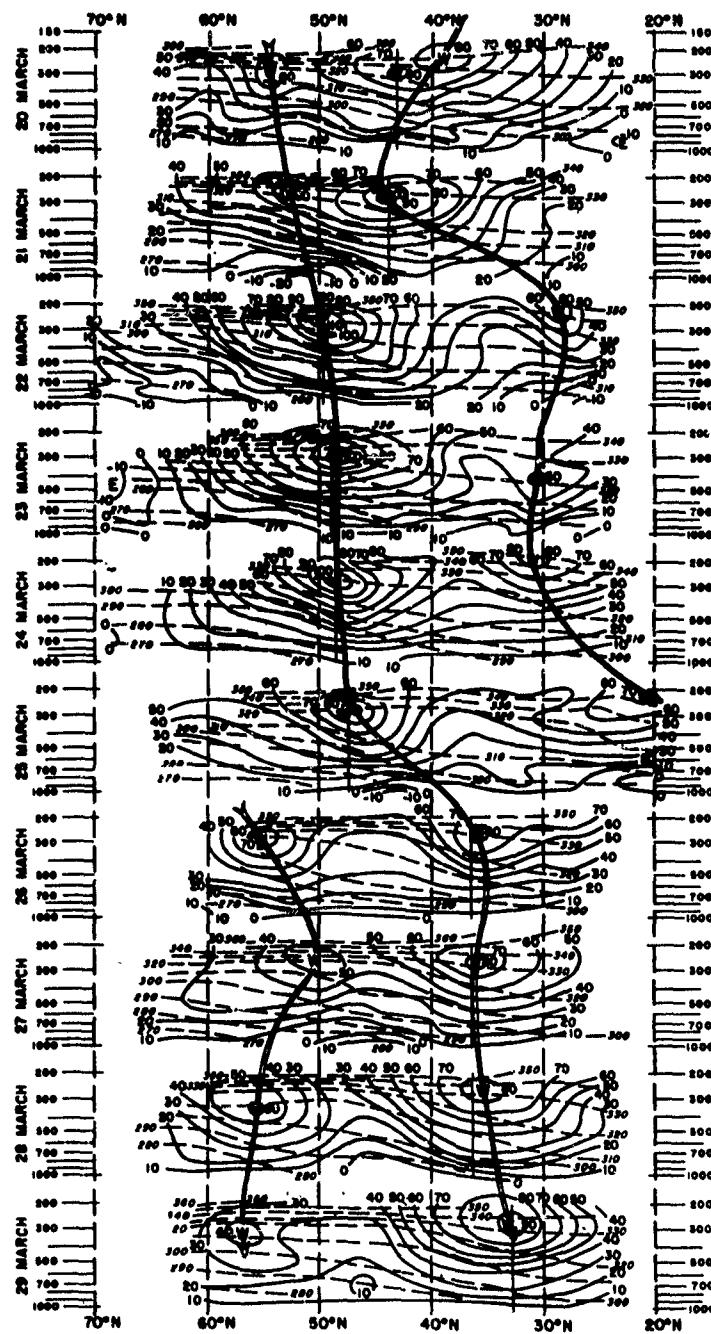
Fig. 2.15: Mean cross-sections for the period between March 20-29, 1948, representing the geostrophic wind (solid curves) and potential temperature (broken curves) over North America from 60°W to 130°W, and from about 25°N to about 65°N. Each mean cross-section is the average of eight individual north-south cross-sections prepared at 10° longitudinal intervals. The center of averages for each mean section is the line following the strongest continuous wind maximum at 300 mb and is indicated by a solid vertical line [19].

CLEAR-AIR TURBULENCE

Until recent years, the following principal sources of atmospheric turbulence were known to produce eddies of sufficient vigor and appropriate linear scale to cause irregular accelerations in aircraft, known as bumps: (a) The flow of air over irregular country and mountains; (b) large cumulus or cumulonimbus clouds; (c) unstable cold air masses and some cloudless frontal zones, and (d) temperature inversions.

Fig. 2.16: 500-mb charts at 0300 GCT for February 22, 1949 (upper left), February 27, 1949 (upper right), March 4, 1949 (lower left), and March 9, 1949 (lower right). Solid bands indicate approximate location of zones of maximum wind [19].

Fig. 2.17: Contours and isotherms on the 500-mb surface, 0300Z, February 20, 1948, showing a well-developed block [9].

With the recent increased trend toward high-level flying, both meteorologists and aircraft pilots have become aware that turbulence in clear air can occur in the high troposphere as well as in the low levels. Observations to date reveal that the optimum level for its occurrence is about 30,000 ft—roughly the height of the tropopause in middle latitudes. But numerous cases have been reported at much higher and lower levels. It prevails most frequently in shallow layers less than 500-ft thick; but turbulent layers of more than 6,000 ft in thickness have been observed on several occasions [3]. Its severity is comparable with the turbulence experienced in nonprecipitating cumuliform clouds [3, 40].

The majority of cases of clear-air turbulence observed so far are associated with jet streams. Of 92 severe cases observed over or near Great Britain [4], 67 per cent were encountered near jet streams. In the United States, all cases of moderate or severe clear-air turbulence studied by United Air Lines [30] occurred along or near the periphery of cold lows, or near the edge of jet streams.

The distribution of clear-air turbulence relative to the jet stream axis is interesting. Bannon [4] has analysed 56 cases of severe turbulence occurring in clear weather above 20,000 ft. His results are presented in fig. 2.18 which represents a schematic cross-section at right angles to the general flow of a composite jet stream obtained by taking a mean of three "typical jet stream cross-sections." The unit of measurement on the abscissa is the distance from the center of the jet over which the wind velocity at the level of the jet axis, on the low pressure side, diminishes to half its maximum value. The ordinate represents the pressure on a logarithmic scale relative to that at the jet axis. The dashed lines are isolines of wind speed normal to the section, and expressed as a percentage of the maximum. A concentration of clear-air turbulence on the cold air side of the jet stream axis is evident.

Fig. 2.18: The distribution of observed occurrences of severe clear-air turbulence relative to the jet stream axis. The unit horizontal distance is one through which the wind speed to the left of the jet axis (looking downstream) falls to half its maximum value [4].

2. The Field of Temperature

THE POLAR FRONT AND ITS POSITION RELATIVE TO THE JET

Below the jet stream core, it is often possible to identify a well-defined polar front [102] which intersects the ground south of the jet. While this front frequently is diffuse near the ground and in the upper troposphere, it generally is distinct at the 500-mb level. Maps drawn for this surface often give the impression of a continuous frontal zone around the hemisphere in which the temperature contrast between high and low latitudes is concentrated, and which for the most part coincides with the latitude of the highest winds and migrates with it [55, 56].

THE DISTRIBUTION OF THE LATITUDINAL TEMPERATURE GRADIENT IN THE TROPOSPHERE

In meridional cross-sections, the maximum westerly winds lie between 200 and 300 mb, directly above the strongest meridional temperature gradient at 500 mb, which at this level corresponds to the frontal zone between the subtropical and polar air masses in cases where a distinct front exists [55]. This concentration of the temperature contrast between high and low latitudes in the west wind belt is clearly brought out in fig. 2.19 which shows a striking parallelism between the profiles of the zonal components of geostrophic and thermal winds computed for different longitudes. The question arises as to whether the horizontal temperature gradient is concentrated in the frontal zone throughout the troposphere. This question can best be answered by a study of vertical cross-sections. Owing to the temperature errors inherent in individual radiosonde ascents, which might give false indications of the temperature field, it is preferable to study the problem on some mean section. But the jet stream and the polar front fluctuate strongly north and south with both time and longitude. Therefore, ordinary statistical averaging of soundings with reference to a fixed geographical location will necessarily damp out the sharpness of the very features which are to be studied.

In order to obviate this damping, and at the same time to eliminate as much as possible the temperature errors of individual soundings, Palmén and Newton [60] used the migrating polar front at 500 mb as a reference surface and computed a mean section with respect to it. Fig. 2.10 represents this section along the meridian 80°W, obtained from 12 daily maps in December 1946. It is noteworthy that the jet stream shows up as distinctly in this mean section, computed with reference to the moving polar front, as in daily sections. This indicates the very small positional deviation of the jet with respect to the polar front.

Fig. 2.10 clearly shows that the latitudinal temperature gradient is by no means confined to the frontal layer. This is true especially in the polar air beneath the frontal layer where secondary fronts often form between arctic air and modified polar air. Above 700-800 mb the temperature gradient almost vanishes north of lat. 50°N. In the warm air, on the other hand, the southward decrease of lateral temperature contrast is more gradual.

The foregoing is brought out clearly if we plot pressure profiles in grid of temperature against latitude (fig. 2.20). The slope of these profiles provides a relative measure of the strength of the temperature gradient in different parts of fig. 2.10. Within the frontal zone, the strongest gradients (about 5.5°C/100 km) appear near the 800-mb surface. At 500 mb, we still encounter comparable gradients within the same zone in many situations. Above this level, the maximum concentration of isotherms remains almost vertical while the


FIG. 2.19: Profiles of zonal and thermal wind components in different longitudes for the 500-mb lev l on October 12, 1945, at 0400Z. Note that strongest zonal motions occur in latitudes of maximum isotherm concentration [102].

FIG. 2.20: Profiles of temperatures of isobaric surfaces (labelled in slanting numbers) taken from fig. 2.10. The latitudinal temperature gradient at any isobaric level may be judged by the slope of the profile [60].

frontal surface slopes northward.

As seen from fig. 2.20, the total temperature difference between pole and equator is strongest at the ground and decreases with altitude. This decrease is slow in the lower levels but becomes rapid above 500 mb. Temperatures become nearly uniform at the level of strongest winds. Above this level, we encounter the complicated temperature field of the lower stratosphere.

THE TEMPERATURE DISTRIBUTION IN THE LOWER STRATOSPHERE

Beyond the level of the maximum winds, which in middle latitudes usually coincides with the tropopause, the temperature gradient reverses. But this reversal is confined to the middle latitudes and does not extend to polar and equatorial regions in winter. At 200 mb, for instance, the isotherms frequently describe a closed center just south of the jet in meridional sections (fig. 2.2). This will reveal itself on synoptic maps at that level as a narrow band of cold air south of the axis of the jet stream (fig. 2.21) [68]. To the south of this band, the temperature again increases. North of the jet, there is a broad warm area above a low-lying tropopause. But this warm band may be shallow. At higher

levels, the temperature may again decrease with height before the deep isothermal stratum and the region of increasing temperature with height of the ozone layer are reached. In addition, the temperature again decreases toward the polar regions north of the warm band.

Palmén and Nagler [59] (fig. 2.22) bring out the latitudinal distribution of temperature and wind at different isobaric levels in profile form. Here we can see clearly the transition from the concentrated temperature gradient at 500 mb to the much more indifferent field at 300 mb, and then to the complicated structure at 200 mb with alternating warm and cold bands. Similar to fig. 2.21 we observe a band of cold air near lat. 43° just south of the jet and a warm band to the north centered around lats. 55°-60°N. These cold and warm bands migrate with the jet stream. This indeed is necessary if along the vertical the winds reach a peak value somewhere and then decrease upward as is true near the jet stream core in all analyses shown in this chapter, and if the actual wind speed does not deviate too widely from the geostrophic. Then, in the layers in which the wind increases upward, the slope of the isobaric surfaces also must increase upward; and in the layers in which the wind decreases with height, the slope of

the isobaric surface also must decrease with height. From static considerations, the vertical distance between two isobaric surfaces increases with increasing temperature. We can, thus, provide the requisite variation of the slope of the isobaric surfaces along the vertical by introducing a poleward directed temperature gradient below the level of strongest winds, and the reverse gradient above, in accord with the observed temperature fields.

It is one of the most remarkable facts of the upper atmospheric temperature field that the warm band of the subarctic zone in figs. 2.20 and 2.21 does not extend to the pole, nor does the cold band of middle latitudes reach to the equator. These figures *furnish indisputable proof that the 200-mb temperature field in middle latitudes cannot be explained as due to horizontal advection of a warm arctic "stratosphere" from the polar zone and a "cold tropical substratosphere" from the equatorial belt. High-level air masses of the type found at 200 mb in middle latitudes simply do not exist at this level near pole or equator. It follows that the classical hypothesis on stratosphere temperature fields in middle latitudes is not tenable, and that the temperature distribution above the jet stream core is a consequence of dynamic processes.* This will be explored further in chap. VII.

POTENTIAL TEMPERATURE DISTRIBUTION AND TROPOPAUSE STRUCTURE

The location of the jet stream core coincides with a break in the tropopause. Immediately to its north, there is a low tropopause which, on the average, lies at about seven km but occasionally can be as low as five km. Another tropopause, lying immediately to the south, is located near the 200-mb surface. Fig 2.1 shows this multiple tropopause structure well. We distinguish three tropopauses:

(1) A tropopause with characteristic potential temperature of 330°-335°A lies between lats. 35° and 47°N at pressures varying from 300 to 200 mb. This tropopause is situated to the south of the jet and slopes upward sharply toward the south on the equatorward margin of the maximum winds. Farther tropicward, its height again decreases; its intensity weakens, and finally it disappears. In the steeply sloping part of the tropopause, the isentropic surfaces reach their highest elevation—the cold band of figs. 2.21-22.

(2) A real tropical tropopause is found south of lat. 40°N near the 100-mb level with a temperature below —70°C and a potential temperature
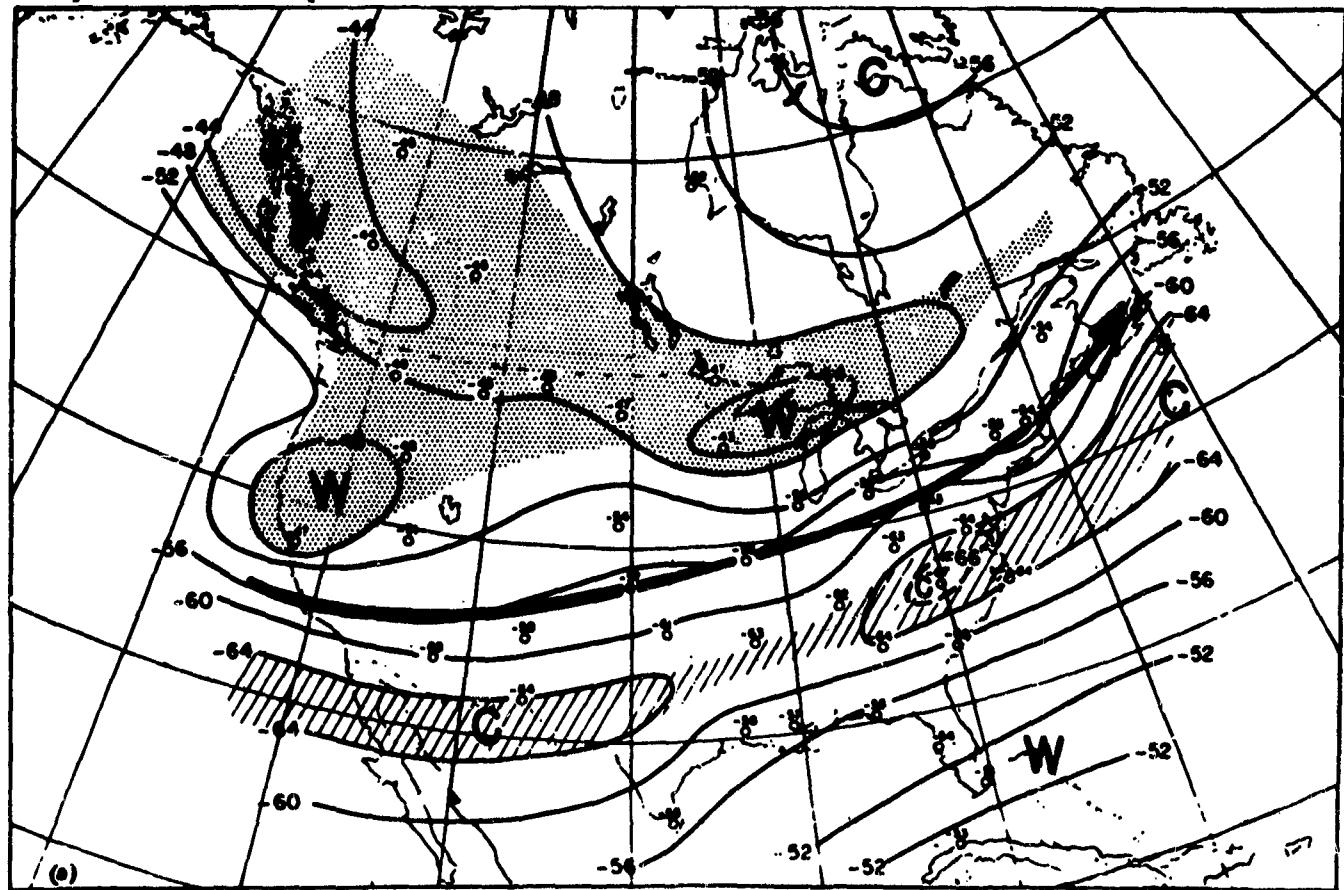
Fig. 2.21: Isotherms (°C) at 200 mb, January 28, 1947, 0300Z. Heavy arrow indicates center of jet [68].

Fic. 2.22: Meridional distribution of wind (solid curves) and temperature (dashed curve) for 0300 GCT, November 30, 1946, at: (a) 500 mb, (b) 300 mb, and (c) 200 mb [59].
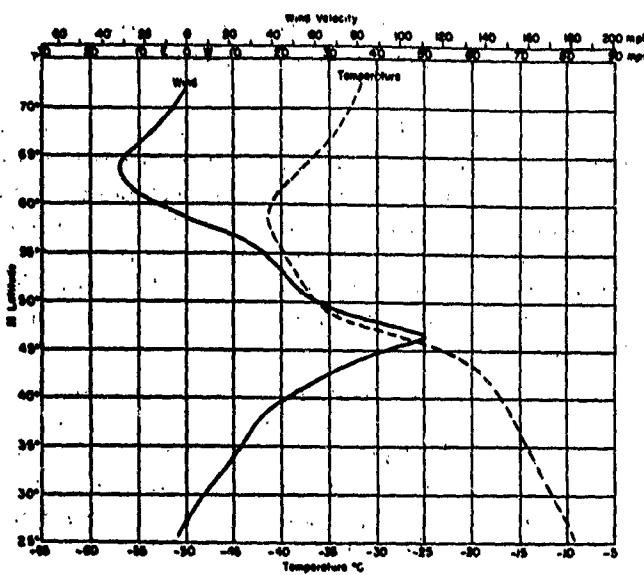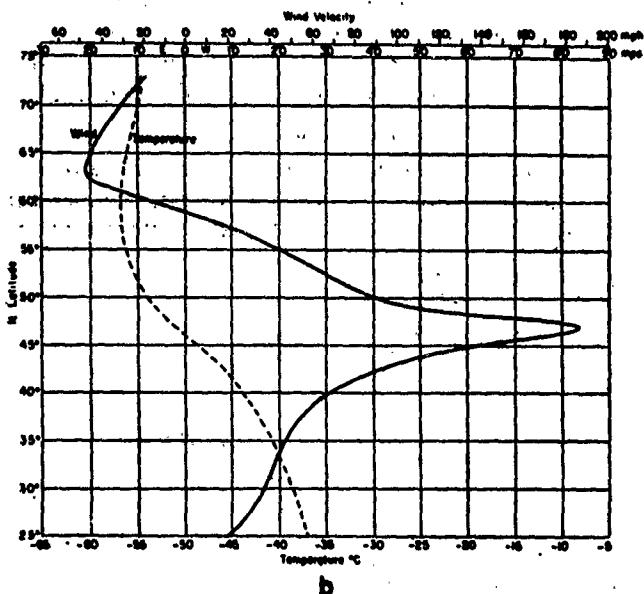
around 390°A. In the gap between the two tropopauses described, commonly located over the northern margin of the trade wind belt in winter, there is frequently a second jet which, in general, is less intense than the first.

The tropical tropopause sometimes extends surprisingly far northward and has been ob-

served not far from the northern jet stream maximum. A typical sounding for the southern United States would show some break in the lapse rate at or a little above 200 mb, followed by a thin isothermal layer. Above this, the temperature decreases again and reaches a minimum at about 100 mb—the height of the tropical tropopause. The general isothermal layer or. temperature increase with height starts above this tropopause.

(3) A tropopause with a characteristic potential temperature of 310°A extends poleward from the jet stream and is situated at about 300 mb. This tropopause usually has its minimum elevation just north of the jet stream, and slopes upward toward the north. Frequently, it does not extend all the way to the pole, but disappears at some intermediate latitude. While another tropopause, at a much higher elevation is in evidence in polar latitudes in winter. The southern part of the latter tropopause can be seen near the left margin of fig. 2.1.

CHAPTER III. CLIMATOLOGY OF THE JET STREAM

1. Seasonal Variations

MEAN SEASONAL ISOTACHS

The jet stream features described in the preceding chapter and the latitude and altitude at which we observe the core not only vary rapidly with the synoptic situation but, in addition, change gradually with the season. As is evident from fig. 3.1, the accumulative effect of this seasonal change is large. This figure contains isotachs of the mean monthly geostrophic west wind distribution for January and July at the level of strongest wind, obtained from cross-sections constructed with the aid of normal monthly pressure maps for the northern hemisphere [52].

The level of strongest wind, as given by these mean sections, was located between 11 and 14 km. Although the data available for the construction of the normal monthly pressure charts was sparse over large parts of the hemisphere, especially the Pacific Ocean and the Far East, fig. 3.1 nevertheless is the only attempt to date at hemispheric representation of the seasonal

FIG. 3.1b: Same as 3.1a for July.

FIG. 3.1a: Average position and strength of the jet stream for January. Solid lines indicate geostrophic wind speed (mph) at the level of maximum speed [52].

zonal flow distribution in the high troposphere. In presenting this figure, we wish to stress that future charts of this kind will show large changes in some areas.

The average latitude of the hemispheric jet as given by fig. 3.1 is 25°N in winter and 42°N in summer. Thus, the jet axis and all climatological and synoptic features associated with it migrate seasonally over a range of nearly 20 degrees of latitude, which is a considerable distance though only half of the sun's movement. In the core, the mean jet intensity is more than 40 mps in winter but drops to about 15 mps in summer. This seasonal decrease of the strength of the upper-air circulation from winter to summer—amounting to 65 per cent in the jet core—is a typical feature also of the southern hemisphere.

In addition to the average intensity and latitude of the mean jet stream, fig. 3.1 clearly shows that the intensity varies greatly with longitude. This is especially true in winter when we find the highest wind concentrations near the east coasts of the continents and the

weakest winds near the west coasts. Thus, in the mean picture, *the upper westerlies during this season strengthen as they move over the anticyclonic surface circulations of the continents and weaken as they pass over the oceans.* To some extent, at least, this mean picture is deceptive as far as application to daily situations is concerned. The mean latitude of the jet stream fluctuates more from day to day on the west coasts than on the east coasts. Quite generally, the variability of the upper winds increases from the western edge toward the eastern edge of the oceans.

Another aspect of the mean high-level flow pattern of winter, not very evident in fig. 3.1, should be mentioned here. In winter the whole belt of westerlies does not always circulate symmetrically around the North Pole, but around a "circulation pole" which is displaced from the geographic pole toward the western Pacific Ocean. On daily charts this tendency toward eccentricity manifests itself by the fact that the jet stream center in the Pacific Ocean lies at an appreciably lower latitude than in the Atlantic Ocean and Europe, often by 20° or more. Fig. 3.1 fails to bring this out, probably on account of the lack of reliable data and also because of the existence of a second mean jet stream center over the low latitudes near the northern rim of the trades. We suggest that a different picture would result if we would tabulate the latitude of the jet stream center as a function of longitude from daily or five-day mean charts, and then determine the mean latitude of the jet as the mean of these tabulations.

It is worth re-emphasizing that the climatological jet is a result of averaging. This has been emphasized by Palmén [57] who states: "In order to avoid misunderstanding it should be pointed out that this upper jet computed from mean meridional cross-sections for seasons or longer periods is not identical with the "meandering" jet stream associated closely with polar front disturbances. This latter phenomenon can hardly be studied by the aid of climatological data, as Palmén and Newton [60] have shown, because of the strong irregular displacements of the polar front and the principal air masses."

Petterssen [63] has summarized the charts forming the basis for fig. 3.1 into hemispheric cross-sections of the zonal wind component for the different seasons (fig. 3.2). These sections of necessity corroborate what we have just said. They also show that in the seasonal mean the average altitude of the jet stream center is nearly unchanged. The average increase of west wind with height is more than twice as strong in winter as in summer, and the altitude of the upper limit of the westerlies lowers considerably in summer. Perhaps the most surprising feature of figs. 3.1-2 is that in spite of the method of averaging and the synoptic variability of the
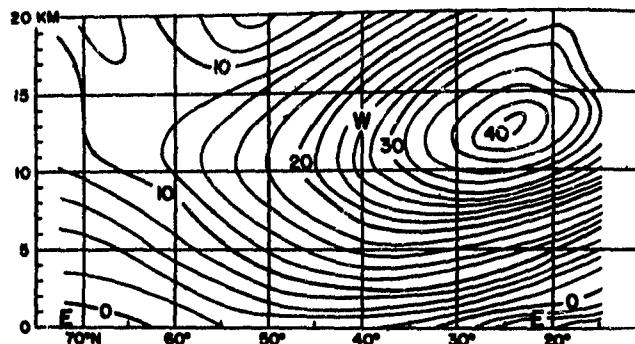
FIG. 3.2a: Mean zonal component of the geostrophic wind (mps) in winter averaged over the northern hemisphere [63].
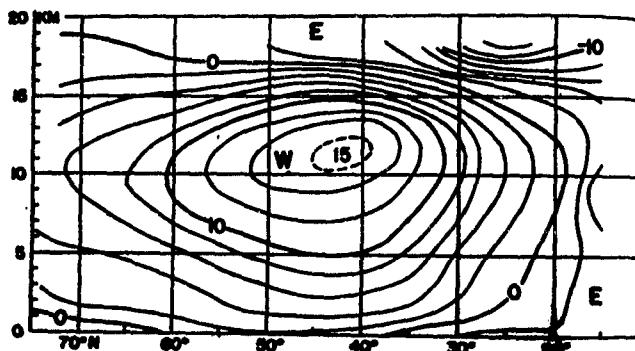
FIG. 3.2b: Same as 3.2a for summer.

jet position, a definite core nevertheless is observed both in the horizontal and in the vertical view.

As a final point of interest of fig. 3.2, we should point out that the latitude of the strongest westerlies was above or a little south of the dividing line between the easterlies and westerlies at the surface, i.e., the subtropical ridge line. This is true especially in winter. We shall come back to this surprising fact in chap. VII in connection with the problem of jet stream formation and maintenance.

MEAN CROSS-SECTIONS FOR VARIOUS LONGITUDES

North America.—The first mean cross-sections constructed after aerological data became more abundant in the early 1940's were those of Willett [108] (fig. 1.3). Unfortunately, the stations available to him were spread over a large longitudinal range (76°) and the sections thus were not located everywhere normal to the mean upper air flow. Subsequently, Hess [31] prepared mean winter and summer sections along 80°W (fig. 3.3). This is a longitude where a mean upper trough is located in winter and the flow is, therefore, essentially from the west.

Thus Hess's sections are normal to the average flow aloft and bring out the mean west wind distribution

with latitude. But the reader should remember that the structure of the westerlies as portrayed is representative of mean trough conditions.

On the whole figs. 3.2 and 3.3 are similar as they show a well-defined jet stream core in summer and winter. This core moves poleward in summer and its strength weakens. We see, however, that the jet center over North America lies at a higher latitude throughout the year — approximately by 10° — and that its strength averages about 10 mps more than that of fig. 3.2. The secondary jet shown in the far north in winter is associated with the cold upper troposphere of the arctic night.

Central Asia and China. — A cross-section, prepared by Chaudhury [17] from data for January and February in 1946 for stations roughly along 76°E (fig. 3.4), reveals a different structure of the westerlies over central Asia. A maximum of 70 mps and more lies at about 30°N and a weaker one, whose existence is not considered to be proved beyond doubt, is indicated near 15°N. From the slope of the low-level isotherms and on the basis of data from other winter periods, it is certain that a third jet center exists north of the Himalayas. This northern current does appear in a section prepared by Yeh [112] from wind observations taken roughly along 120°E during December 1945

and January 1946 (fig. 3.5). Yeh also verifies the presence of the principal jet further south which skirts the equatorward rim of the Himalayas and then crosses eastern China between 25°-30°N with a speed of over 120 mph. Apparently, it is this current which is featured on the isotach chart of winter for the Far East (fig. 3.1) drawn by Namias and Clapp [52]. We see from the more recent data that the mean latitude of the current should appear more than 10° further north.

As brought out later in this chapter large mountain barriers of the type of the Himalayas tend to channel the upper air currents around their periphery and therewith produce a much more steady wind regime aloft than is found elsewhere. Yeh [112] has demonstrated clearly that the latitude of the main jet center varies very little from day to day over eastern Asia after the winter regime of the atmosphere has established itself during October or November. If we plot wind speed as a function of time and latitude, as done by Yeh at 115°E (fig. 3.6), we see this rather invariant jet position. Thus, over the Far East in winter, a vertical section fixed with respect to the earth would also be fixed with respect to the jet axis. Mean sections averaged over a fixed geographical interval would retain the sharp features of synoptic situations (fig. 3.7) to the same extent as the section computed relative to

Fig. 3.3a: Meridional cross-section along 80°W showing the distribution of potential temperature in °A (thin solid lines), geostrophic west wind in mps (dashed lines), and the tropopause (heavy lines) in winter [31].

Fig. 3.3b: Same as fig. 3.3a for summer.

Fig. 3.4: Mean meridional cross-section for January and February 1946 along 76°E. Thin solid lines are isolines of the geostrophic zonal wind (mps) and dashed lines are isotherms in °C [17].

the 500-mb polar front over the U. S. by Palmén and Newton [60] (fig. 2.10). When the vorticity distribution is computed from fig. 3.7, the resulting profile (fig. 3.8) somewhat resembles that of fig. 2.13. North of the jet center the absolute vorticity almost attains the Coriolis parameter at the pole and, speaking generally, is fairly constant from the arctic to the latitude of

strongest westerlies. South of this latitude, we encounter a broad band in which the absolute vorticity is zero, a most remarkable result (cf. chap. VII).

It is noteworthy that the jet stream crossing Siberia fluctuates greatly compared to the southern jet (fig. 3.6). This northern jet is not constrained in its motion by the great high plateau of central Asia.

FIG. 3.5: Meridional cross-section of mean zonal wind (mph) for December 1945 and January 1946 computed from rawin data along 120°E [112].
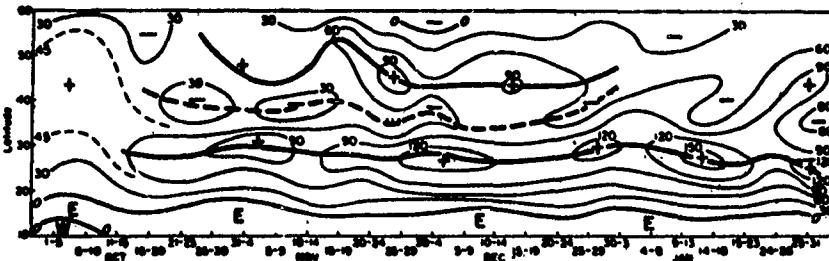
FIG. 3.6: Time section of the 300-mb geostrophic zonal wind (mph) along long. 115°E from October 1945 to January 1946 [112].

Europe.— A mean cross-section for the Greenwich meridian constructed for February 1951 [38] (fig. 3.9) shows a broad jet of 35 mps in the vicinity of 40°N. The broader maxima and lower speed of this section compared to fig. 3.3 at least partly reflect the large latitudinal oscillations of the jet over western Europe.

The structure of the northern hemisphere winter jet shown by the preceding figures is quite different at the four longitudes. Agreement is best at 80°W and 120°E in comparison with 76°E and 0°. This may be accounted for by the fact that both 80°W and 120°E lie along the east coasts of continents where a mean long-wave trough persists during winter. The height of the principal jet, shown by the cross-sections, is near 200 mb over eastern North America and eastern Asia but somewhat lower over western Europe. It is note-

worthy that the magnitude of the wind speeds shown by Yeh's cross-section, which is based on mean winds from rawin stations, compares closely with the computed geostrophic speeds of the other northern hemisphere sections, and also with the geostrophic wind distribution over the Far East.

Southern hemisphere.— Mean winter and summer cross-sections for the southern hemisphere have been computed along 150°E and 170°E [36, 43]. It is very interesting to note how little winter conditions at 170°E in the southern hemisphere (fig. 3.10a) differ from those at 80°W in the northern hemisphere (fig. 3.3a) even though one longitude extends over an ocean and the other crosses the eastern part of a continent. Intensity and mean altitude of the jet core are about equal. The southern jet lies a little closer to the equator at 170°E than the northern jet at 80°W, but its latitude
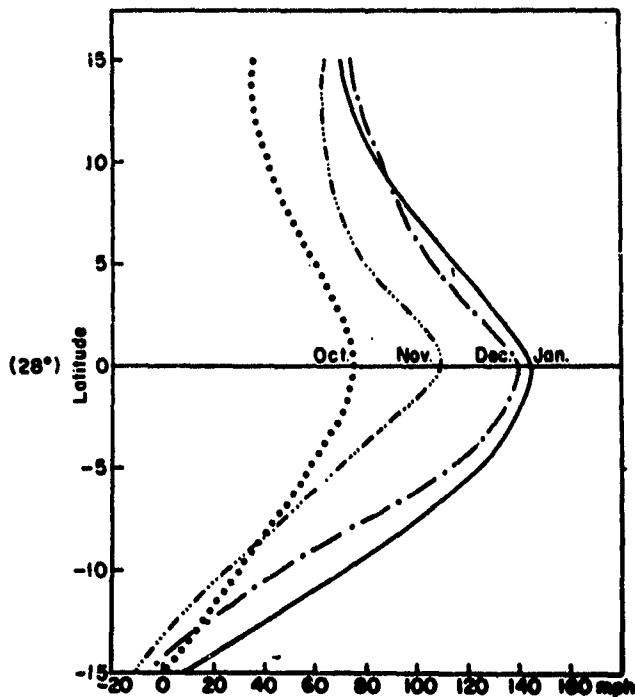
FIG. 3.7: Monthly mean profile of 300-mb zonal wind along 115°E averaged with respect to the center of the southern jet stream computed from fig. 3.6 [112].

is the same as the latter at 120°E (fig. 3.5).

Agreement between the winter sections of the southern hemisphere is quite good, but in summer conditions at 150°E and 170°E differ considerably. At 150°E a single jet of over 50 mph appears at 40°S while at 170°E (fig. 3.10), we note a double structure with slightly stronger jets at 45°-50°S and 30°S. In either case the summer jet is found at a lower latitude than in Hess's summer section (55°N). However, a tendency for a secondary maximum near 40°N is also shown by Hess.

TIME SECTIONS AT 300 MB AND 700 MB

Figs. 3.11-12 give the seasonal variation of west-wind speed at 300 mb and 700 mb from July 1945 to January 1946 averaged over the northern hemisphere exclusive of Asia. As should be expected, the strength
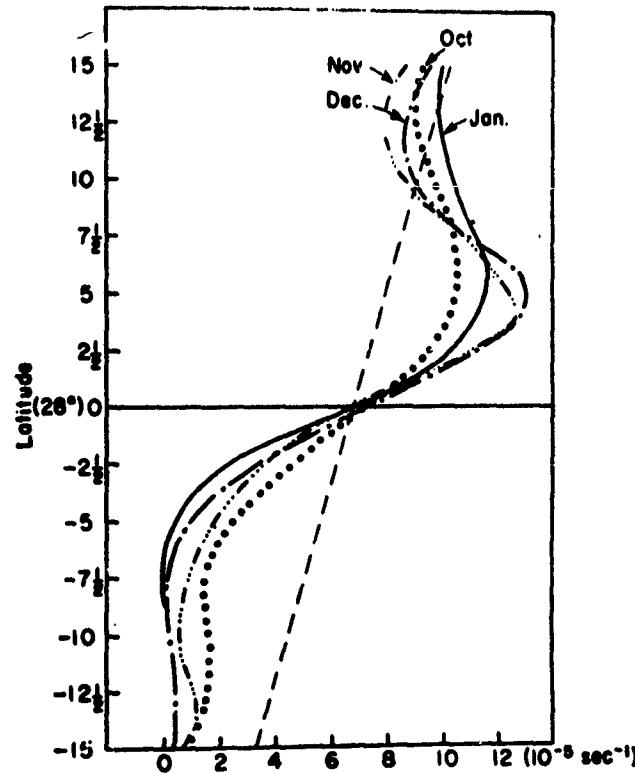
FIG. 3.8: Monthly mean profile of absolute vorticity computed from fig. 3.7 [112].

of the westerlies is greater at 300 mb compared to 700 mb. The slope of the axis of strongest westerlies is nearly vertical in summer, whereas in winter we find
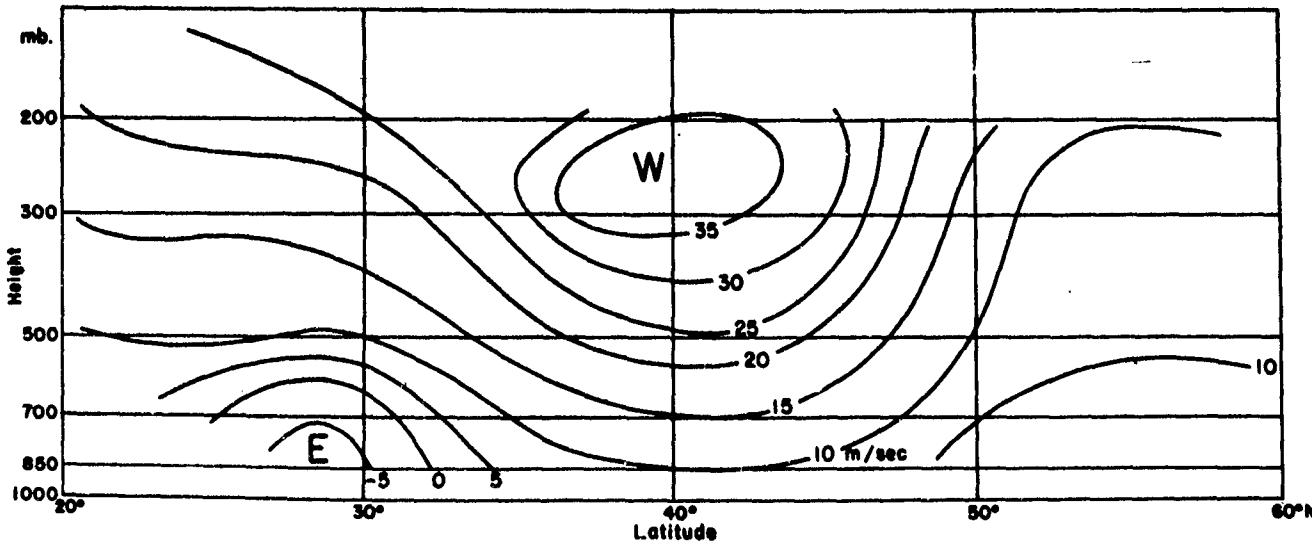
FIG. 3.9: Cross-section of mean zonal geostrophic wind (mps) for February 1951 along Greenwich meridian [38].
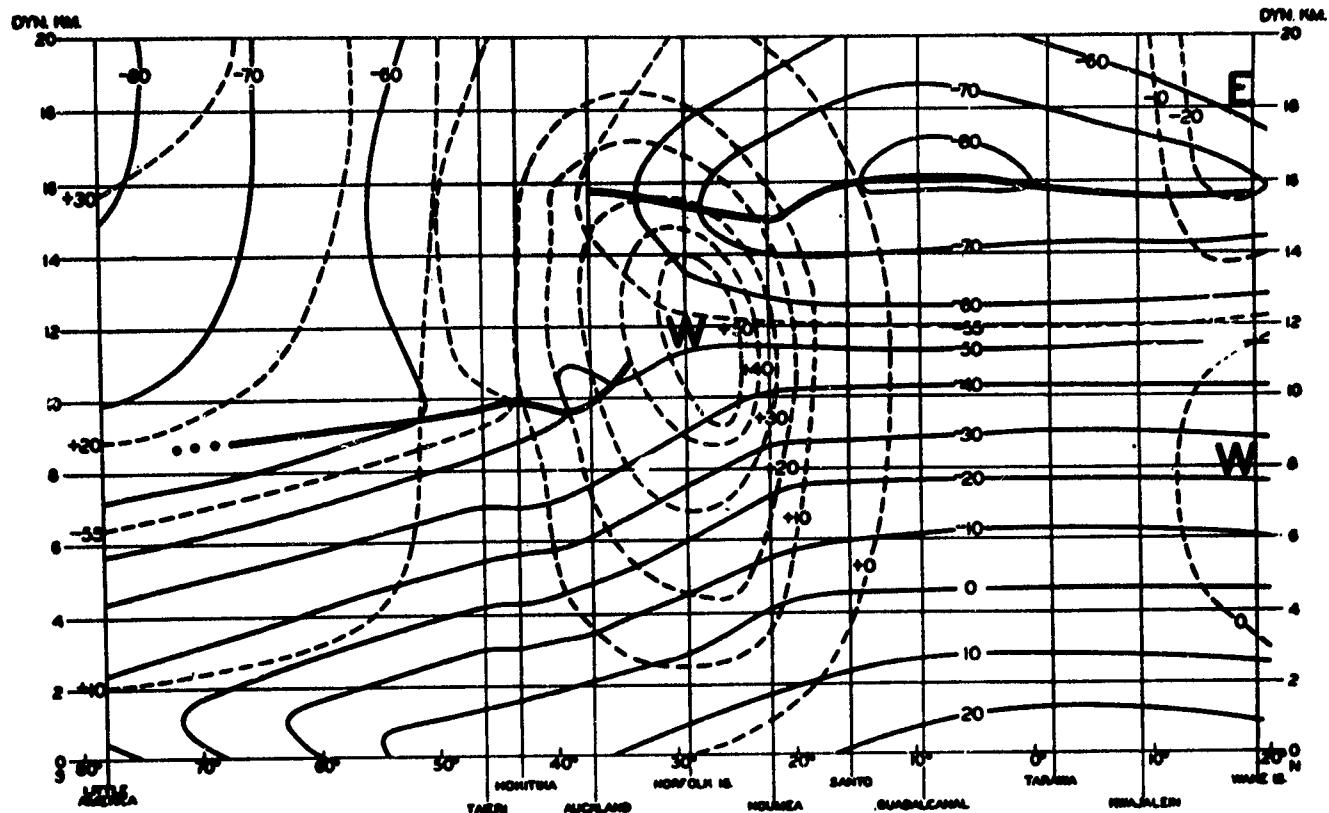
Fic. 3.10a: Meridional cross-section for southern hemisphere winter along 170° E. Thin lines are isotherms (°C) ; dashed lines, geostrophic zonal winds (mps) ; and heavy lines, the tropopause [36].
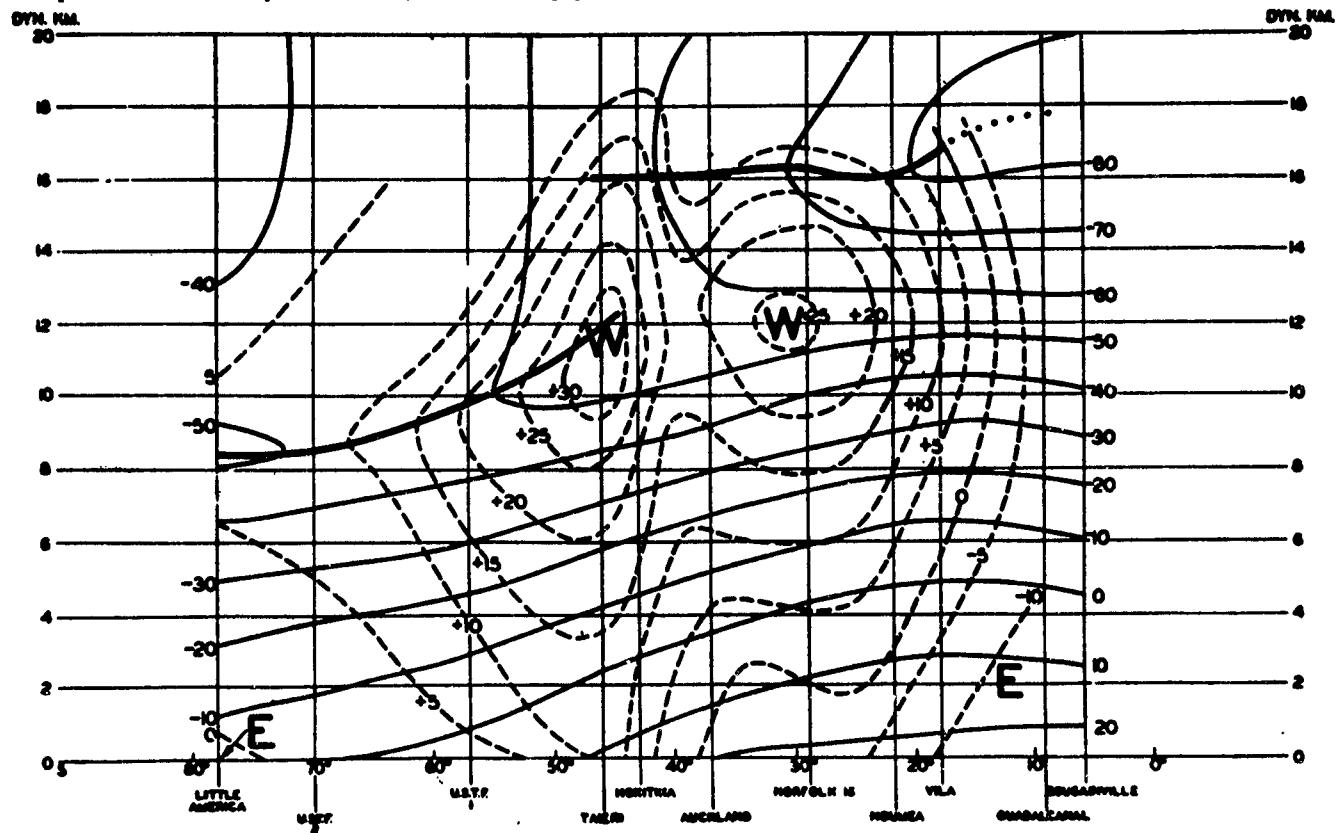
Fic. 3.10b: Same as fig. 3.10a for southern hemisphere summer.
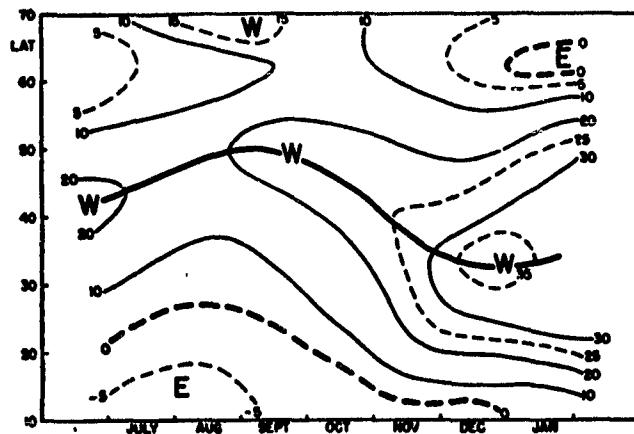
Fic. 3.11: Seasonal distribution of zonal flow (mps) at 300 mb, July 1945-January 1946. Heavy solid line indicates maximum westerlies, and heavy dashed line, boundary between easterlies and westerlies [71].

the strongest 300-mb current well south of that at 700 mb. This is in agreement with mean cross-sections such as fig.3.2 but is the opposite from what we often observe synoptically. This peculiar difference between jet structure on individual days and in the mean must find its explanation in the methods of averaging used to determine mean conditions. It is noteworthy that at 120°E, where daily and seasonal jet positions agree closely (fig. 3.5), this reversed slope does not exist.

The latitude of strongest westerlies as given by figs. 3.2 and 3.11 agree closely in July, and so does their intensity. Subsequently, the mean jet stream continues

to shift further northward and reaches 50°N in September. At the same time the seasonal increase in wind speed aloft has begun. Thus, the time of highest jet latitude and lowest intensity does not coincide but differs by two months.

In the period December 1945-January 1946, the strongest westerlies were located at about 32°N. This is not nearly as far southward as is indicated for mean conditions in fig. 3.2. But we should remember that only the general features of figs. 3.11-12 are representative to any great extent. Variations of detail from year to year are very great. The strongest westerlies, for instance, in some years reach their lowest latitude as early as November, and in other years not until March-April.
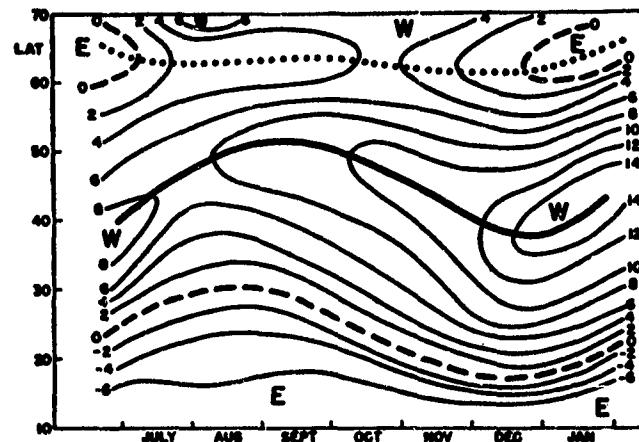
Fic. 3.12: Same as 3.11 for 700 mb.

2. Influence of Large-Scale Thermal and Physical Features

MEAN TEMPERATURE FIELD

It has long been realized that at upper levels, as well as at the surface, the pole to equator temperature difference and consequently the zonal thermal wind is not evenly distributed. Instead, a large proportion of the temperature gradient is concentrated in middle latitudes (cf. fig. 3.10) and this concentration shifts latitudinally with the seasons. In associating the region of strongest mean temperature gradient with the jet, it is not implied that the existence of the jet can be explained by the temperature field, or vice versa. However, the close relation between the fields of temperature and motion is useful in discussing seasonal changes in the structure of the westerlies.

The seasonal variation of the jet shown by the preceding sections is approximately equal to the seasonal variations of the thermal wind given by the pole to equator temperature difference and by the latitudinal shift of the zone of greatest horizontal temperature gradient. For example, the displacement of the jet from 55°N in summer to 35°N in winter in eastern North

America and its increase in speed from 25+ to 50+ mps (fig. 3.3) is closely connected with the southward movement of the mean polar front and increased temperature contrasts between polar and tropical air masses. The greater strength and the more equatorward position of the jet in the southern hemisphere during the southern hemispheric summer compared to that of the northern hemisphere during the northern hemispheric summer are related to the fact that during the hot season the troposphere of the southern hemisphere middle latitudes remains much colder and the zone of maximum temperature gradient remains further equatorward than in the northern hemisphere.

Thus, seasonal variations of the mean westerlies in middle latitudes may be related to changes in the mean latitudinal temperature distribution. However, any longitudinal variations in the upper westerlies must be accounted for by other means. These variations appear to be principally controlled by the land-sea distribution and by the location of large mountain areas.

THE LAND-SEA DISTRIBUTION

In chap. VII, the analogous behavior between the jets of atmosphere and ocean and those produced in model experiments is cited as evidence for the dynamic maintenance of jets. In addition, *the similarity between the structure of the westerlies in northern and southern hemispheres ' renders untenable any jet hypothesis which requires large permanent thermal contrasts such as a snow line or a coast line.* Nevertheless, the differential heating and cooling between the large land and water bodies undoubtedly exerts some influence on the upper westerlies.

In winter the maximum temperature gradients are found over the continents and, as we have seen (fig. 3.1), the mean jet intensifies from the western to the eastern end of a continent. However, marked strengthening of the jet also is indicated over the continents in summer when the temperature gradients are weak. Clearly, reasoning from differential heating and cooling effects of land and sea would not predict in an obvious way the longitudinal variations shown by fig. 3.1.

Comparison of long-wave patterns and areas of wind concentrations in northern and southern hemispheres should conclusively test the importance of the land-sea distribution in shaping the mean flow pattern aloft. Continental influences operating through differential heating should be small in the southern hemisphere. This check must await more complete upper-air data from the southern hemisphere. In the following section, however, we shall be able to make some observations on the upper-air circulation over South America.
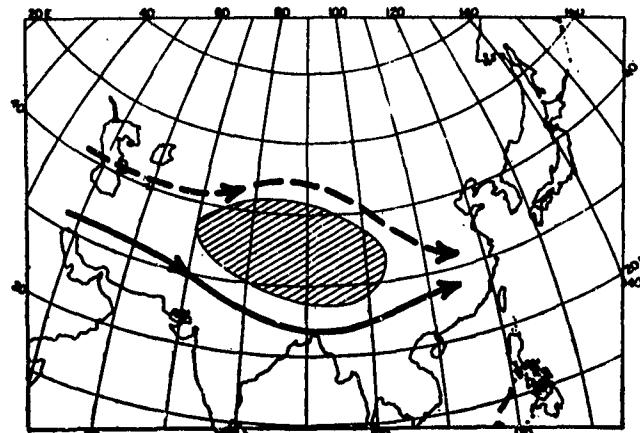

Fic. 3.13: Schematic representation of flow around the Himalayan plateau [115].
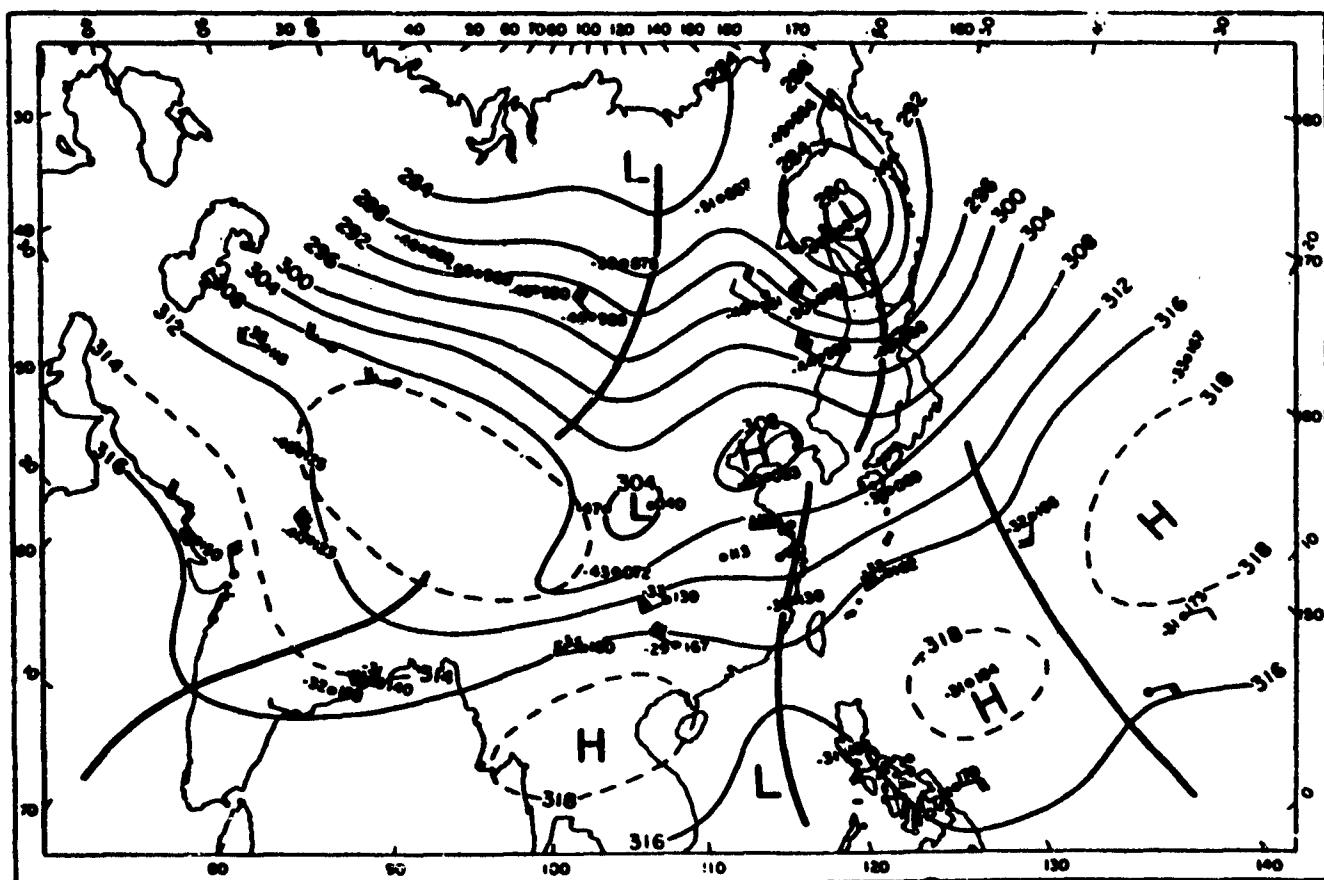

Fic. 3.14: 300-mb chart, November 4, 1945, 0400Z. Contour heights are in 100's of feet [112].

LARGE MOUNTAIN BARRIERS

The large barriers in temperate latitudes are of two types: (a) Those oriented roughly along the current, and (b) those normal to the flow. An obstacle of the first type, for example the Himalayas, largely diverts the westerlies. A long barrier of the second type, such as the Rockies, forces the westerlies to ascend over it.

The Himalayas markedly influence the upper-flow pattern over eastern Asia, particularly during the winter season. This effect is shown schematically by fig. 3.13 in which the westerly current is divided by the mountain barrier. The split of the westerlies over central Asia is demonstrated by the sections presented by Yeh [112] and Chaudhury [17]. In addition to these sections, Yeh presents a synoptic 300-mb chart (fig. 3.14) which indicates the spreading of the contours over central Asia leaving a dead spot over the mountains and producing small vortices in their lee.

During summer, the westerlies are entirely north of the Himalayas. The shift to the north side of the barrier in late spring and early summer produces a marked change in the circulation over India and Burma which, according to Yin [115], is coupled with the "burst of the monsoon" in that region. In the case studied by Yin the collapse of the southern jet at the onset of the monsoon was shown quite clearly by a latitudinal time section at the 500-mb level (fig. 3.15).

The return of a portion of the westerlies to the south of the high plateau marks the beginning of the steady
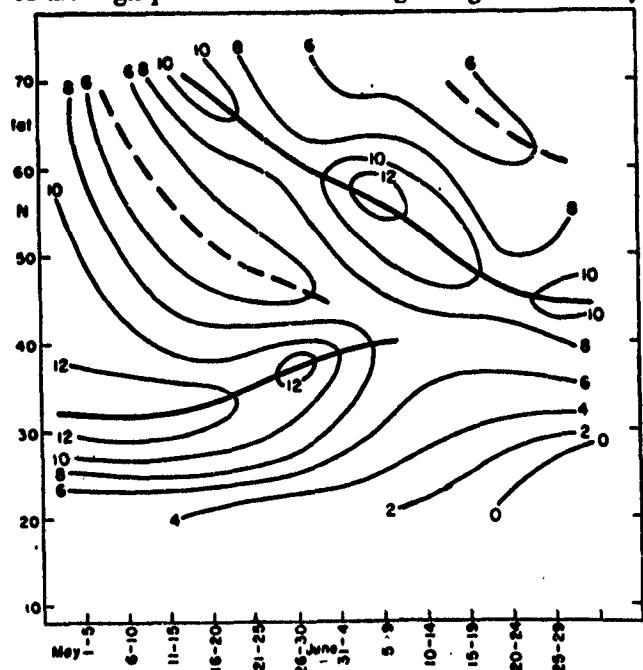
Fig. 3.15: Mean geostrophic west wind at 500 mb between long. 0° and 130°E as a function of time and longitude, computed for five-day periods during May and June 1946. Isotachs are labelled in mps with the position of the maximum (the jet) and minimum being indicated by heavier solid and dashed lines [115].

winter regime of eastern Asia described by Yeh [112]. We have already seen the effectiveness of the mountain barrier in maintaining a steady flow in fig. 3.6 which showed that the latitude of the jet center was nearly invariant during the winter of 1945-46. The constancy of the strong jet near 30°N is corroborated by computations of wind steadiness at a number of stations in China (table 3-I) and by fig. 2.9.

	Canton 23.2°N 113.3°E	Liuchow 24.3°N 109.3°E	Chihkiang 27.4°N 109.6°E	Hankow 30.6°N 114.2°E	Shanghai 31.2°N 121.5°E	Peking 39.9°N 116.4°E
2,000 feet....	22	8	94	32	11	62
10,000 feet....	65	69	47	57	84	84
20,000 feet....	91	95	89	95	97	87
30,000 feet....	85	96	94	97	98	89
40,000 feet....	98	98	92	96	97	99

Table 3-I: Wind steadiness in per cent as a function of height for stations in China computed for the winter of 1945-46. Wind steadiness (S) in per cent is defined by the formula $S = \frac{R}{V} \cdot 100$ where R is the speed of the vector resultant wind and V the average speed regardless of direction [112].

No other mountain barrier of similar shape and orientation relative to the mean flow aloft approaches the size and height of the Himalayan plateau. The Alps, which have a somewhat similar orientation, are not only lower but also have a very much smaller area. Their effect certainly is small in comparison with that of the Himalayas.

The principal barriers situated normal to the westerlies are the Rockies of North America and the Andes of South America. These ranges affect the upper flow quite differently from the Himalayas. Because of the large latitudinal extent of these barriers the westerlies are forced to move over rather than around them. The deformation to which an initially straight flow is subjected while ascending and then descending over a barrier of this type has been discussed from the standpoint of vorticity by Holmboe, Forsythe, and Gustin [32] and by Boffi [13]. The theorem of conservation of potential vorticity states that the ratio of absolute vorticity to the vertical depth of an air column is constant [79]. The following qualitative discussion of this theorem has been given by Boffi:

"As the air currents approach the mountains from the west, their vertical depth decreases, and therefore their absolute vorticity must also decrease. In a broad-scale current such as is considered here, extending over a wide band of latitude, the decrease of absolute vorticity is ac-

complished by turning of the air columns toward lower latitudes, associated with the appearance of anticyclonic-flow curvature over the mountains. This decrease of the relative vorticity and the transport of air toward lower latitudes both contribute to the decrease in the absolute vorticity.

"East of the Continental Divide the absolute vorticity again increases. Since the upper-air current is there flowing from the southwest (in the southern hemisphere, northwest in the northern hemisphere), it is still moving toward regions where the earth's own vorticity becomes smaller. The increase in absolute vorticity, therefore, must be accomplished by an overcompensating increase in the relative vorticity. The anticyclonic-flow curvature must decrease rapidly and give way to cyclonic-flow curvature, turning the current back toward east and eventually to southeast (northeast in the northern hemisphere). The trough east of the mountains must be more sharply defined than the ridge over the mountains, at least in its western portions.

"It is evident that the higher the mountain range which the broadscale air current must cross, the more pronounced will be both the resulting ridge of high pressure over the mountains and the trough to their east. It follows also that the larger the obstacle over which the air has to flow the more permanent a feature of the general circulation must be the deformation in the general flow pattern produced by the mountains, and the smaller the aperiodic variations from average conditions that should be found."

Seasonal upper-air charts over both North and South America (figs. 3.16, 3.17) clearly show that a ridge tends to be established in the mean over the mountains,
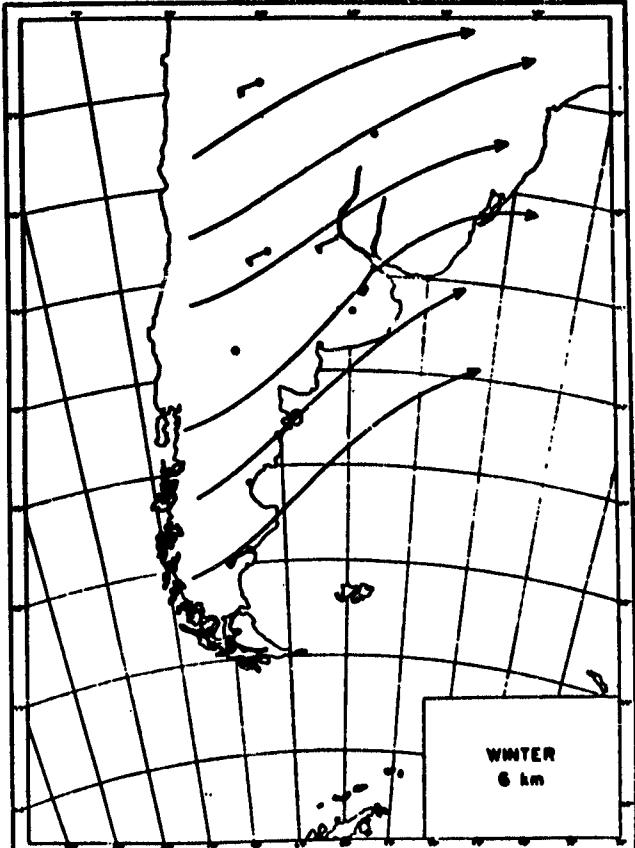
FIG. 3.16: Mean flow at six km in winter over South America [13].

while a trough persists downstream in their lee. This trough over North America lies at about 80°W. In South America, data are not sufficient to accurately place the Andes lee trough. According to the best available information, it is located over the Atlantic at approximately the same distance downstream from the mountain barrier as in North America.
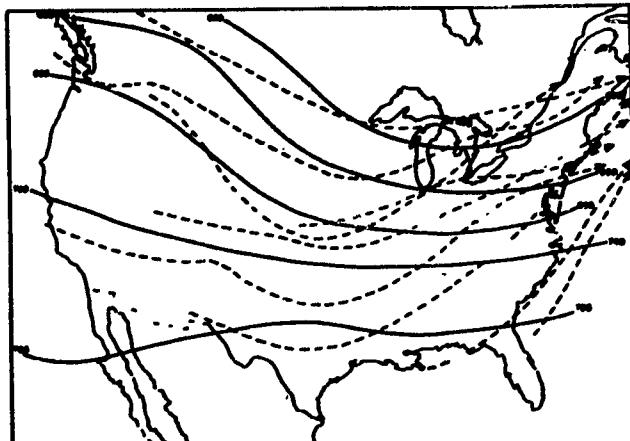
FIG. 3.17: Average January isobars at 10,000 ft. for the United States (solid lines) and storm tracks [13].
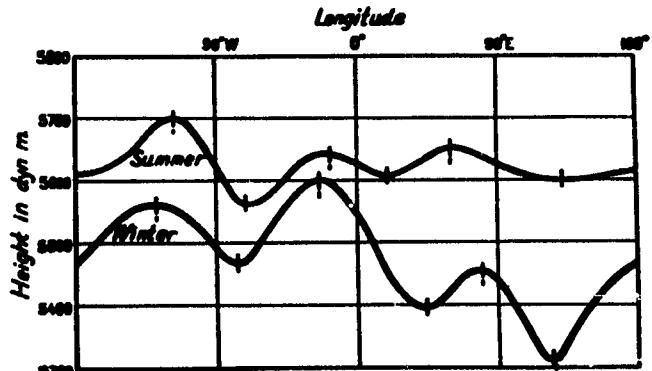
FIG. 3.18: The mean height of the 500-mb surface as a function of longitude. In summer the figure represents conditions in the latitude belt 45°N-50°N, in winter 35°N-40°N [14].

The fact that the trough is located over the ocean can be cited as *strong evidence against a simple thermal explanation of the maintenance of east coast troughs. It is not possible to explain the existence of such a trough on the basis of differential heating when in the same season the North American trough lies on one side of the coastal thermal field and in South America on the other side.* As stated by Boffi [13]:

"It is evident that the position of the mean ridges and troughs aloft is primarily a function of the dynamic effect that the mountains produce on the broadscale air currents crossing the mountains, irrespective of the distance of the eastern coast line from the mountains. Therefore, it is deduced that the local solenoid field produced at east coasts by the temperature contrast between land and water is an effect of an entirely subordinate order of magnitude as compared with the influence of the large mountain barriers. These mountain barriers, moveover, must be considered as the primary anchor of the long wave pattern in the westerlies."

Since both the Rockies and Andes have a large latitudinal extent, seasonal variations in the location of the westerlies could be expected to be of much less importance than in the case of the Himalayas if the mountains exert the primary control on the air flow. Mean 500-mb longitudinal profiles for winter and summer presented by Bolin [14] (fig. 3.18) show clearly that such is the case. As observed by Bolin:

"We know that the continents act as cold sources and the oceans as warm sources in winter while conditions are reversed in summer. In spite of this fact certain basic features of the wave pattern at upper levels do not change essentially from summer to winter. ... Even though the intensity of the waves around the hemisphere is much less in summer than in winter, the position of the troughs and ridges is almost the same."

Bolin herewith deduces from the lack of seasonal variation of trough position what we have noted above in comparing North and South America during the same season. We also can point out that although the intensity of the troughs downstream from both the Rockies and the Himalayas decreases from winter to summer (fig. 3.18), the change over East Asia is much greater. This may be connected with the fact that the westerlies cease to flow around the southern rim of the Himalayas in summer whereas they are still forced to cross the Rocky Mountains in spite of the poleward displacement of the jet stream center.

3. Influence of the Jet on Surface Climates

In this section, we shall attempt to relate some of the elements of surface climate—such as temperature, rainfall, and storm tracks—to structure, motion, and location of the hemispheric jet. A complete discussion of the relation between climatological features at the surface and the upper flow would require consideration of all large-scale features such as mean long-wave trough and ridge positions. Within the limits of this volume, we shall not undertake such a complete treatment. It appears, however, that many climatological features can be fitted into a physical pattern by using the jet as a basis for classification. We shall illustrate these relations with a few selected examples.

INFLUENCE OF JET STRUCTURE

The climate of western Europe is strongly affected by the structure of the upper westerlies. Rex [67] has shown that during certain periods well-defined blocks are established over the Atlantic with the jet splitting into two branches (fig. 3.19). The northern branch usually passes in the vicinity of Iceland and northern Scandinavia, and the southern branch runs near the Azores and then across Spain or North Africa. During blocking periods, a deep, persistent anticyclone is maintained over western Europe. Temperature anomalies are positive over the north Atlantic and over northwest Europe and negative in central and southwest Europe (fig. 3.20). This anomaly pattern can be interpreted partly as a result of the displacement of the normal cyclone track into a more SW-NE orientation over the Atlantic. The warm air masses on the west side of the anticyclone are brought further north than usual and on the east side Siberian air masses extend much further into western Europe. The mean precipitation anomalies (fig. 3.21) show, in general,
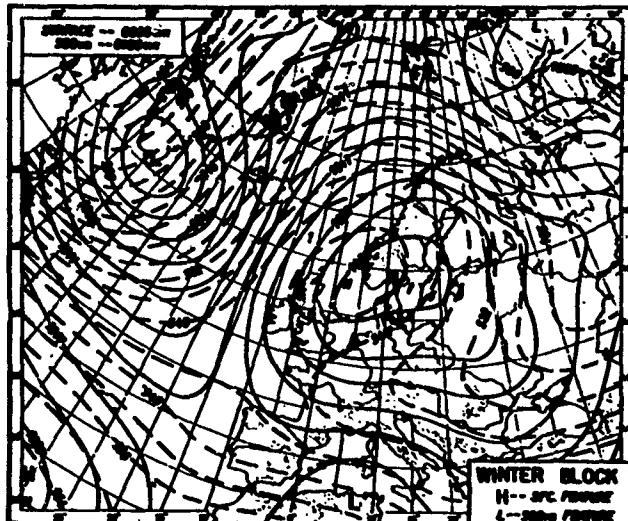
FIG. 3.19: The European winter block (a mean picture). Height of the 500-mb surface (tens of meters) shown by the thin dashed lines. Sea-level pressure distribution (mb) shown by the thin solid lines [67].

a marked decrease of precipitation in western Europe. The summer precipitation pattern is not essentially different from that of winter. A high frequency of blocks can result in large mean temperature and precipitation anomalies during any season or year. However, the details shown by fig. 3.19 also point to the importance of local features in determining the effect of a blocking period on the precipitation at any given station.

Variation in the structure of the westerlies over long periods of time has been offered as a hypothesis for long term climatic changes [109]: If the structure of the westerlies over western Europe varies from periods of essentially zonal flow to other periods in which meridional flow predominates, as during blocking, significant changes in climate should be expected.

INFLUENCE OF JET INCIDENCE ON LOCAL CLIMATE

The climatological element which has been most closely associated with the jet stream is precipitation. Starrett [96] found that precipitation maxima tend to be oriented along or just north of the band of strongest winds at the 300-mb level. This tendency is discussed in relation to synoptic jet streams in chap. IV. Figs. 3.22 and 3.23 show mean precipitation frequency profiles in the case of straight flow and in the vicinity of troughs.
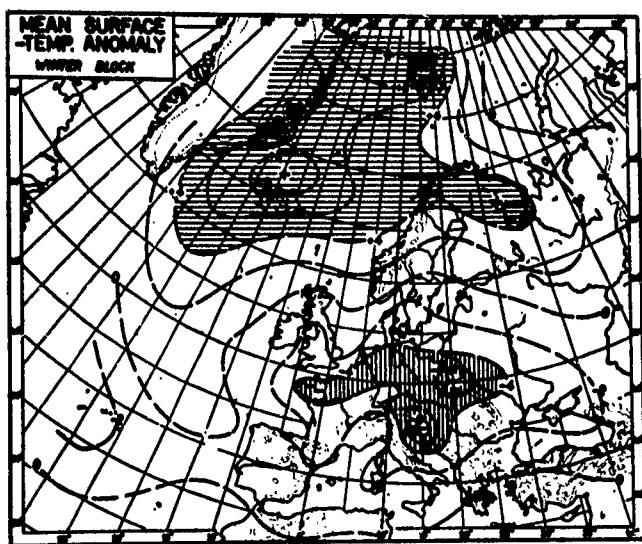
FIG. 3.20: European winter temperature anomalies during blocking. Lines of equal temperature anomaly are given for each 2°C above and below normal and are shown by the thin dashed lines. Areas recording mean temperatures more than 4°C above normal are indicated by the horizontal hatchings and areas recording mean temperatures more than 4°C below normal by the vertical hatchings [67].

Since Starrett's study was made over the United States where the jet position oscillates widely from day to day, averages were taken in respect to the jet position. In East Asia, as discussed previously, the winter jet maintains a nearly constant latitude. Here it is of interest to compare the mean upper-flow pattern with the mean precipitation pattern of winter (fig. 3.24). A maximum of precipitation practically coincides with the center of the upper jet stream. Rainfall decreases northward and southward from there but much more rapidly on the south side. The extreme concentration of this precipitation is evident from the fact that over considerable areas to the north and south of the jet axis the gradient of mean winter precipitation is in excess of 20 cm per 100 miles. Such remarkable agreement between precipitation relative to the jet in the United States as found by Starrett, and the average regional rainfall pattern of China relative to the aver-

age position of the jet over China is possible only if the latitudinal fluctuations of the jet stream over eastern China are restricted to very narrow limits not only from one day to the next but also from one year to the next.

In areas where the jet location is more variable seasonal mean precipitation gradients are much smaller. However, even in these areas the jet may tend to persist for several weeks at times and result in the concentration of the monthly precipitation within narrow zones. Thus, at a given station in middle latitudes the deviation of the seasonal precipitation from the mean can often be linked to above or below average frequency of the jet in the vicinity.

The importance of jet incidence also affects longer term trends. Willett [110] has noted that a correlation exists between sunspot activity and the westerlies which are displaced southward (the circumpolar vortex expands) during periods of weak sunspot activity. Further, Saucier [90] has shown that the frequency of cyclogenesis in the Texas and Gulf region is negatively correlated to sunspots. It would appear that these correlations are physically consistent and that the increase of cyclogenesis during periods of low sunspot activity can be associated with the southward displacement of the westerlies over the central United States.

The seasonal movement of the westerlies is clearly reflected in rainfall curves for stations along the west coast of North America. Fig. 3.25 gives the month of maximum precipitation for selected stations between San Diego, California, and Anchorage, Alaska. At Anchorage, the maximum occurs in August-September when the jet is located near its most poleward position. In more southerly latitudes it occurs at progressively later dates reflecting the southward drift of the jet. At San Diego, the month of maximum precipitation is February. Since most of the west coast precipitation is closely associated with travelling cyclonic disturbances, fig. 3.25 also reflects the seasonal movement of cyclone tracks from summer to winter.

The cyclone tracks have been computed by Petterssen [63] in a novel way by locating the areas where highs and lows alternate most frequently (fig. 3.26). Since the travelling surface disturbances propagate in the main along the jet stream, fig. 3.26 affords a better means than fig. 3.1 to determine the mean jet position in winter. We note that the pattern of fig. 3.26 is much simpler over the oceans than over the continents. In the lee of the Rockies there is no distinct pattern. This suggests a large variability of jet positions and frequent presence of multiple jets. The situation simplifies going eastward, and only one principal belt of alternating highs and lows leads from the North American continent into the Atlantic Ocean. Over Europe-Asia we observe the same condition. The pattern is simple over East Asia where the southern jet is only weakly
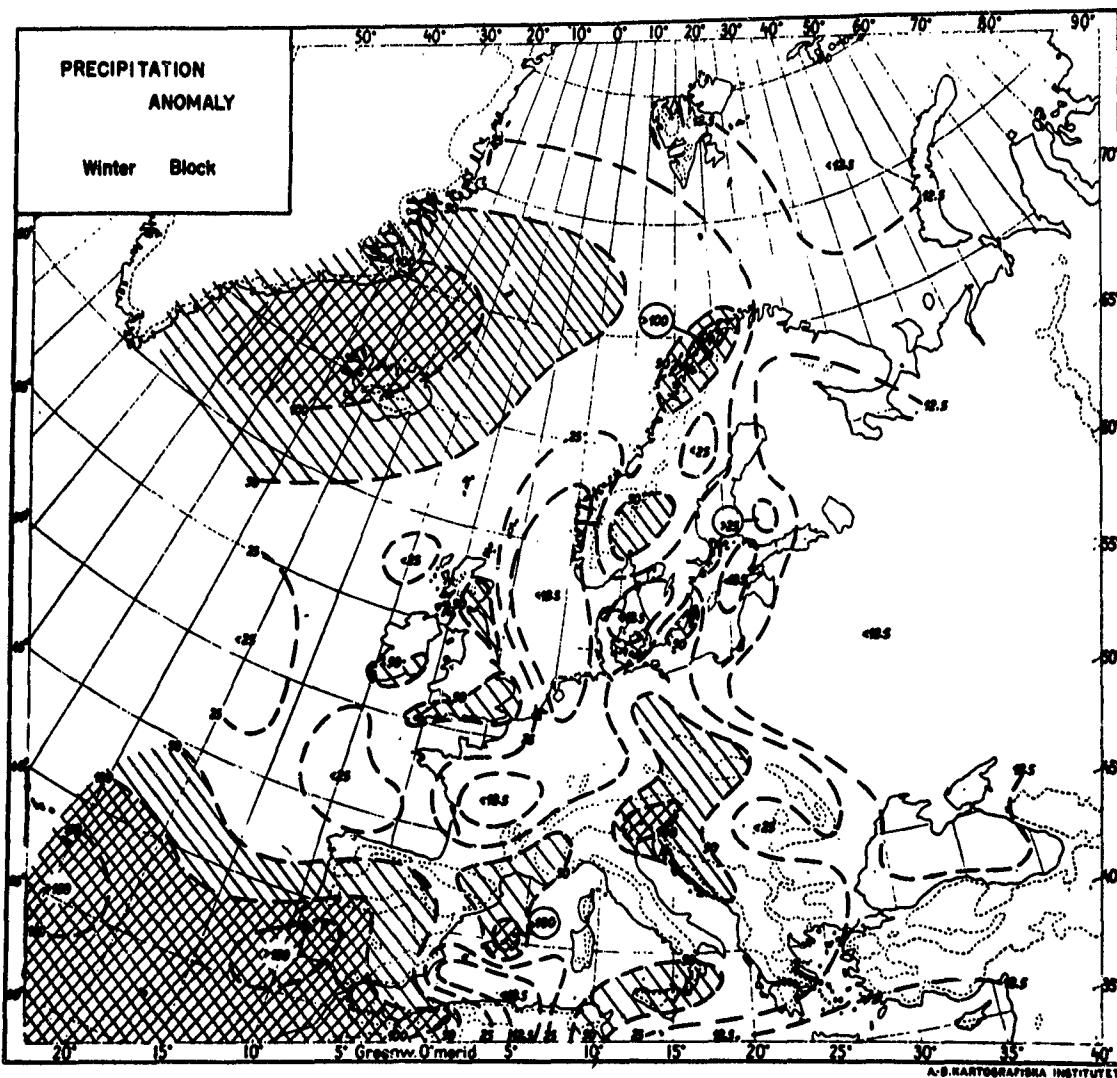
Fıg. 3.21: European winter precipitation anomalies during blocking. Lines of equal precipitation anomaly are given for 12½, 25, 50, 100, 150, and 200 per cent of normal and are shown by the thin dashed lines. Areas recording precipitation amounts in excess of normal are indicated by the double hatching and areas recording precipitations between 50 and 100 per cent, by the single hatching [67].
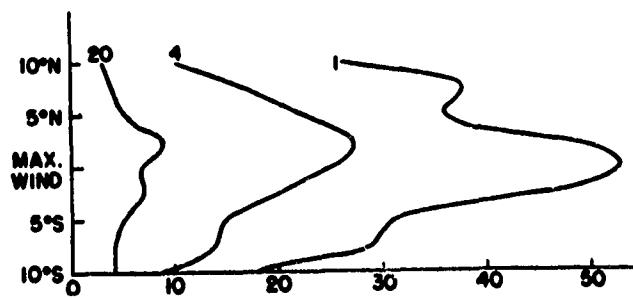
Fıg. 3.22: Profiles of frequency (per cent) of precipitation relative to quasi-uniform (straight) jet streams, obtained by averaging longitudes from 75°W to 123°W. Curve 1 includes all precipitation while curves 4 and 20 include respectively only cases of at least four and 20 per cent of the monthly normal [96].
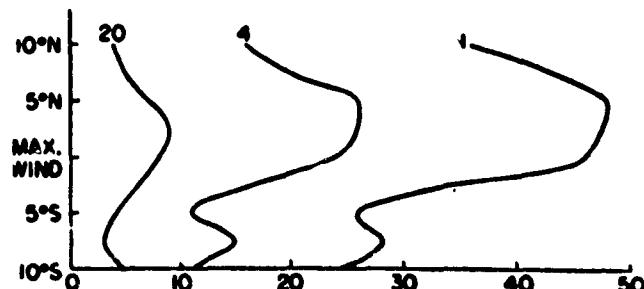
Fıg. 3.23: Profiles of frequency (per cent) of precipitation relative to jet streams with troughs, obtained by averaging longitudinally from 20 degrees east to 20 degrees west of troughs. Curves 1, 4, and 20 have same significance as in fig. 3.22 [96].
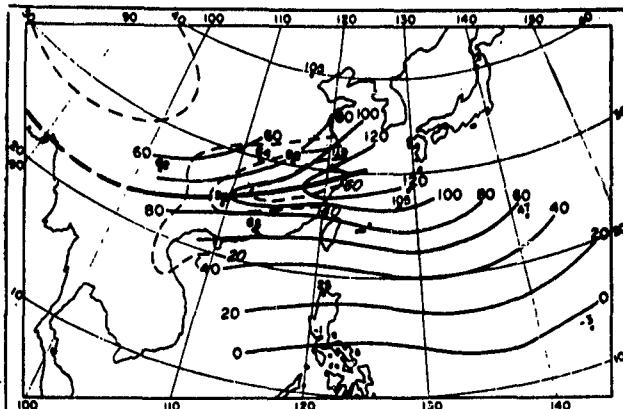
FIG. 3.24: Distribution of mean zonal wind speed in mph (solid lines) of December 1945 and January 1946 at 30,000 ft and mean precipitation pattern in centimeters (dashed lines) in winter over China. The figures are the mean speeds at the various stations and the heavy line shows the position of the jet stream axis [112].

FIG. 3.25: The month of maximum precipitation as a function of latitude along the west coast of North America.

FIG. 3.26: Rate of alternation (per cent) between cyclones and anticyclones during the winter season, indicating the distribution of travelling disturbances. The ratio of alternation is defined as the ratio (F_c/F_A) when $F_c < F_A$, or by (F_A/F_c) when $F_c > F_A$ where F_c and F_A denote the percentage frequencies of occurrences of cyclone and anticyclone centers, respectively, in a given 100,000 km square [63].

reflected at the surface but very complicated over Europe. One belt of frequent cyclonic activity extends from the eastern Atlantic over Britain and Germany and a secondary belt over the Mediterranean. This pattern, which to some extent reflects the frequent blocking activity over the eastern Atlantic, results in a complex rainfall distribution over western Europe. Consequently, stations along the European west coast do not show a simple progression of the month of maximum precipitation as in North America.

The seasonal poleward advance of the jet in spring

and summer does not appear to take place in a continuous manner along the west coast of North America. Instead, one jet tends to die out in the south in late winter and another one develops near the Arctic Circle. Consequently, no definite secondary maximum of rainfall is noted in the Washington-Oregon region, for example, as would be expected if the jet moved slowly northward between late winter and late summer.

Over the central United States, a northward trend of the jet can be noted from the rainfall curves. At most stations in the Arkansas-Tennessee area a March-April maximum is observed; in Iowa-Illinois rainfall is highest in May-June; along the Canadian border we observe a June-July peak. Even far inland from the west coast of North America, however, we observe a definite tendency for a second wind maximum to develop over northern Canada. The "Hudson Bay High," a generally recognized feature of North American weather during spring [15], separates these two streams. Hudson Bay highs are noted for their dryness. Thus, it can happen during spring that the Chicago Forecast Center of the United States Weather Bureau is concerned with floods in the central plains states and at the very same time with forest fire danger near the Canadian border.

CHAPTER IV. THE JET STREAM
IN RELATION TO MIDDLE LATITUDE CYCLONES

1. The Jet Stream as a Factor in the Development of Extratropical Cyclones

Prior to the extensive exploration of the upper air, short-range forecasting was based on the polar-front theory of wave cyclones developed by the Norwegians during World War I. According to this theory, extratropical cyclones are regarded as waves travelling along sloping fronts between cold air masses of polar origin and warm air masses originating in tropical regions. As a result of shearing instability along the fronts, these waves increase in amplitude and eventually develop into closed vortices.

While the polar-front theory had the great merit of crystallizing an amorphous collection of ideas concerning the inception and development of cyclones into a model, it has now become evident that this model does not accurately describe conditions in the upper air. Nor does it provide a complete clue to cyclones observed in middle latitudes. Whereas it is undoubtedly true that extratropical cyclones often do develop as waves on the polar fronts, strong fronts have been known to exist for a number of days without any cyclonic activity developing on them. And conversely, cyclones often develop without the sequence described by the polar-front theory being in evidence. Palmén [56], for instance, has shown with a series of weather maps that the structure characteristic of the occluded frontal cyclone can develop as a result of processes other than the occlusion of frontal waves.

In a recent paper, Berggren, Bolin, and Rossby [9] came to the conclusion that middle latitude cyclones comprise a heterogeneous collection of different types of disturbances including typical frontal waves as well as dynamically quite dissimilar major storms associated with the deepening of planetary wave troughs in the west-wind belt. The development and behavior of these cyclones cannot be adequately studied in terms of a single model such as the polar-front model. They depend on the synchronization of different factors throughout the troposphere. The structure of the jet stream is one of the most important of these factors.

In recent years, several writers [54, 68, 75, 96] have observed that cyclonic activity and precipitation tend to be concentrated along the jet stream. This fact

does not contradict but rather supplements the polar-front theory of cyclone formation. The concentration of a pre-existing meridional temperature gradient into a front and the concentration of the zonal wind speed into a jet are parallel phenomena [56, 102], and the jet stream structure often provides the best single clue to the development of waves along the polar front, the intensification of existing disturbances as well as the distribution of precipitation around them. It also gives an insight into the circumstances in which substantial departures from model conditions are likely to occur. Thus, a good analysis of the jet stream constitutes one of the most useful tools for short-range forecasting.
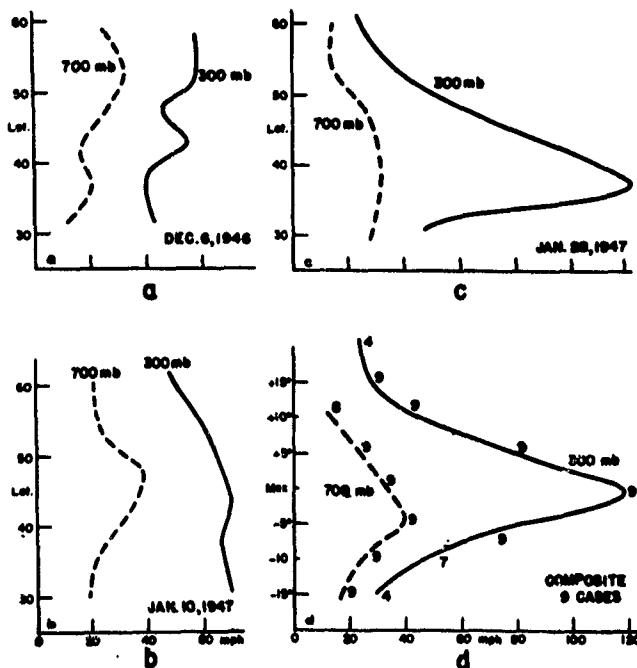

FIG. 4.1: Profile of the westerlies at 700 mb and 300 mb: (a) December 6, 1946, 0300Z; (b) January 10, 1947, 0300Z; (c) January 28, 1947, 0300Z, and (d) for nine cases with pronounced jet stream, averaged with respect to wind maximum at 300 mb. Ordinate gives distance from zone of wind maximum at 300 mb in degrees of latitude, numbers along curves indicate number of observations [68].

EARLY SYNOPTIC EVIDENCE

The formation of extratropical cyclones, for instance over the great plains east of the Rocky Mountains, is known to take place generally in connection with pre-existing upper-air troughs. Such troughs may have great amplitude prior to cyclogenesis. There are numerous cases, however, when they are relatively weak and the upper flow is mainly westerly. When such a weak upper-air disturbance moves eastward from the Rockies, an incipient low pressure center in the lee of the mountains will develop to great proportions in some situations while in others it will remain weak. In an attempt to find possible high-level criteria to separate the deepening and nondeepening situations, the strength of the westerlies over North America was computed on a daily basis for the winter of 1946-47 [68]. The following types of profiles were observed (fig. 4.1):

(1) The lateral shear at 700 mb and 300 mb is small and the vertical shear between the two surfaces also is small (fig. 4.1a). Low pressure centers that formed during this period remained weak.

(2) The lateral shear at 700 mb and 300 mb is small but the vertical shear is considerably larger than in the preceding case (fig. 4.1b). Low pressure centers forming under such conditions moved rapidly eastward without great intensification. They are warm "high index" cyclones. We may relate this type of wind profile to the "fingery" structure of the upper westerlies during high index.

(3) The lateral shear at 700 mb is small but it attains large values in a narrow latitudinal band at 300 mb. Both cyclonic and anticyclonic shears at that surface become very great and between these two shear zones, the wind reaches a well-defined maximum (fig. 4.1c). The vertical shear also attains high values in the region of strong wind. Both horizontal and vertical wind shears are weak outside this narrow central zone. All this accords well with the wind structure of well-developed jets described in chap. II.

When a pronounced jet of this type became superimposed on a strong frontal zone or some perturbation of the low troposphere, intense cyclogenesis ensued. But it is always dangerous to make very broad generalizations. Therefore, it was stressed that the above observations applied only in connection with patterns of very long waves, and that these observations did not imply that the jet stream alone can create cyclones. But there seems to be little doubt that the structure of the jet stream is germane to the problem of formation and deepening of extratropical cyclones. Its coincidence in a favorable sense with other factors like the long-wave pattern and low-tropospheric disturbances largely determines the intensity of cyclones.

LATER DEVELOPMENTS

The above initial investigation considered the jet stream as a more or less homogeneous entity, and the profiles were averaged for the whole United States. Important additions have since been made to our knowledge of the structure of the jet. The alternating regions of maximum and minimum wind speed which travel along its axis, together with the preferred velocity concentrations with respect to the long-wave troughs and ridges during different stages of the index cycle, are now known to play an important role in determining regions along the jet where the formation or intensification of extratropical cyclones is likely to occur.

AN EXAMPLE

The following example illustrates the relation of the jet stream structure to the development of extratropical cyclones.

Fig. 4.2 shows a sequence of surface maps and fig. 4.3 gives the corresponding isotach patterns at 300 mb. In fig. 4.3a a disorganized jet consisting of a number of "fingers" overlies the area between Texas and the Middle West, and a well-organized jet maximum with central speed exceeding 200 knots is approaching from the West Coast.

The corresponding surface map (fig. 4.2a) shows two centers of low pressure. One, with a central pressure of 987 mb and associated with an occluded frontal system is situated outside the region of organized velocity concentration at 300 mb. The other with a central pressure of 990 mb is found at the eastern tip of a cold front running west and southwest to the Pacific Coast. This low is situated to the left of the axis and downstream from the well-organized jet maximum approaching from the northwest.

Fig. 4.3b shows the velocity maximum in a more easterly position and the axis of the organized jet extending over most of the United States in a trough-like configuration. On the corresponding surface map (fig. 4.2b), we see that the deeper of the two lows on the previous map has now started to fill up. On the other hand, the weaker low whose position is indicated by the dot has deepened by some three mb. Notice the region of pressure fall, depicted by the dashed lines, which is centered to the east of the low pressure center.

The next stage is shown by figs. 4.2c and 4.3c. The low which was initially associated with the occluded frontal system, has now disappeared and the other low

dominates the picture. As indicated by the dot on fig. 4.3c, this low is located to the west of a center of strong pressure fall. The jet maximum has advanced further and a new maximum has developed eastward of the trough line. Both the center of pressure fall and the center of the low are located to the left of the axis and forward of the new jet maximum.

During the next 12 hours (fig. 4.2d.), the low center decelerates and intensifies. Its pressure falls to 981 mb, and it now has the appearance of a well-developed wave cyclone.

The following important facts may be gleaned from the example above:

(1) The low which was situated outside the regions of the organized jet filled up and disappeared.

(2) The deepening low was associated with a well-defined jet maximum. Throughout the period of its intensification it was located to the left and forward of this maximum. This region of decreasing velocities downstream is one of diverging upper contours (fig. 4.3d) (delta region).
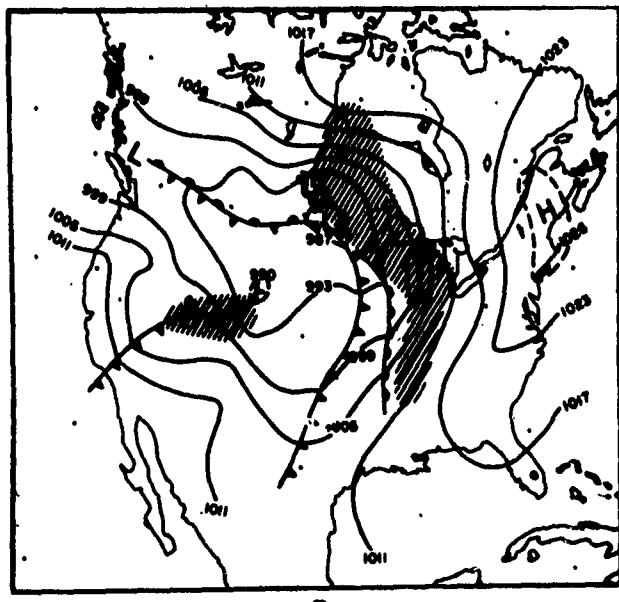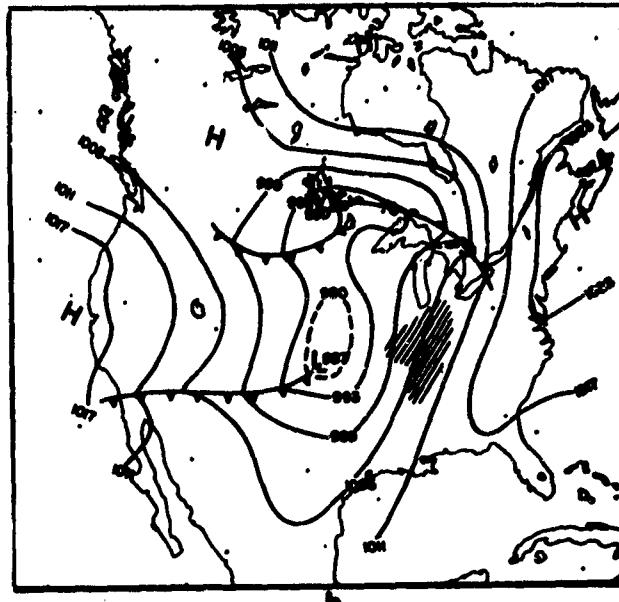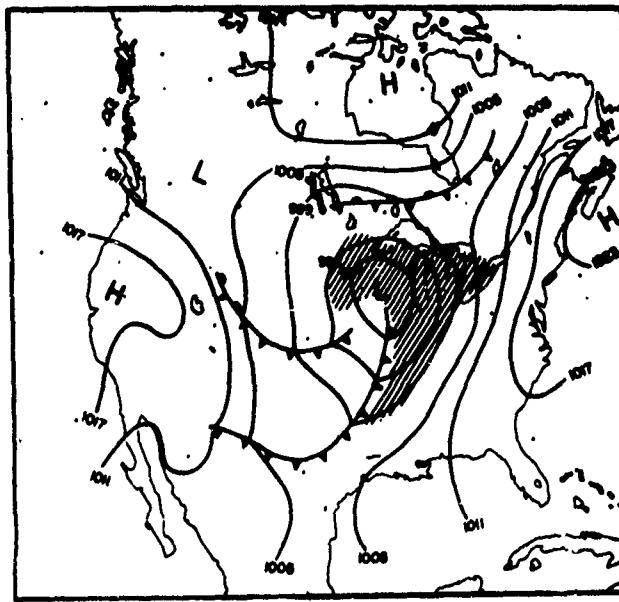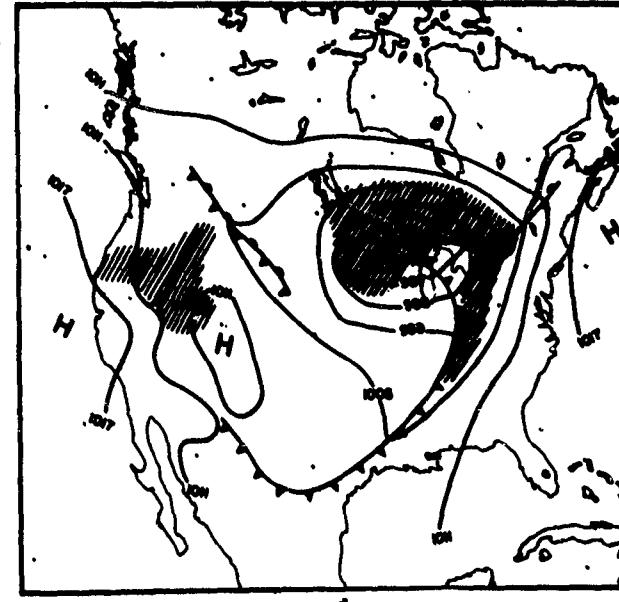
Fig. 4.2: Surface maps drawn at 12-hour intervals: (a) November 12, 1951, 1830Z; (b) November 13, 1951, 0630Z; (c) November 13, 1951, 1830Z and (d) November 14, 1951, 0630Z. Shaded areas denote regions of precipitation [75].
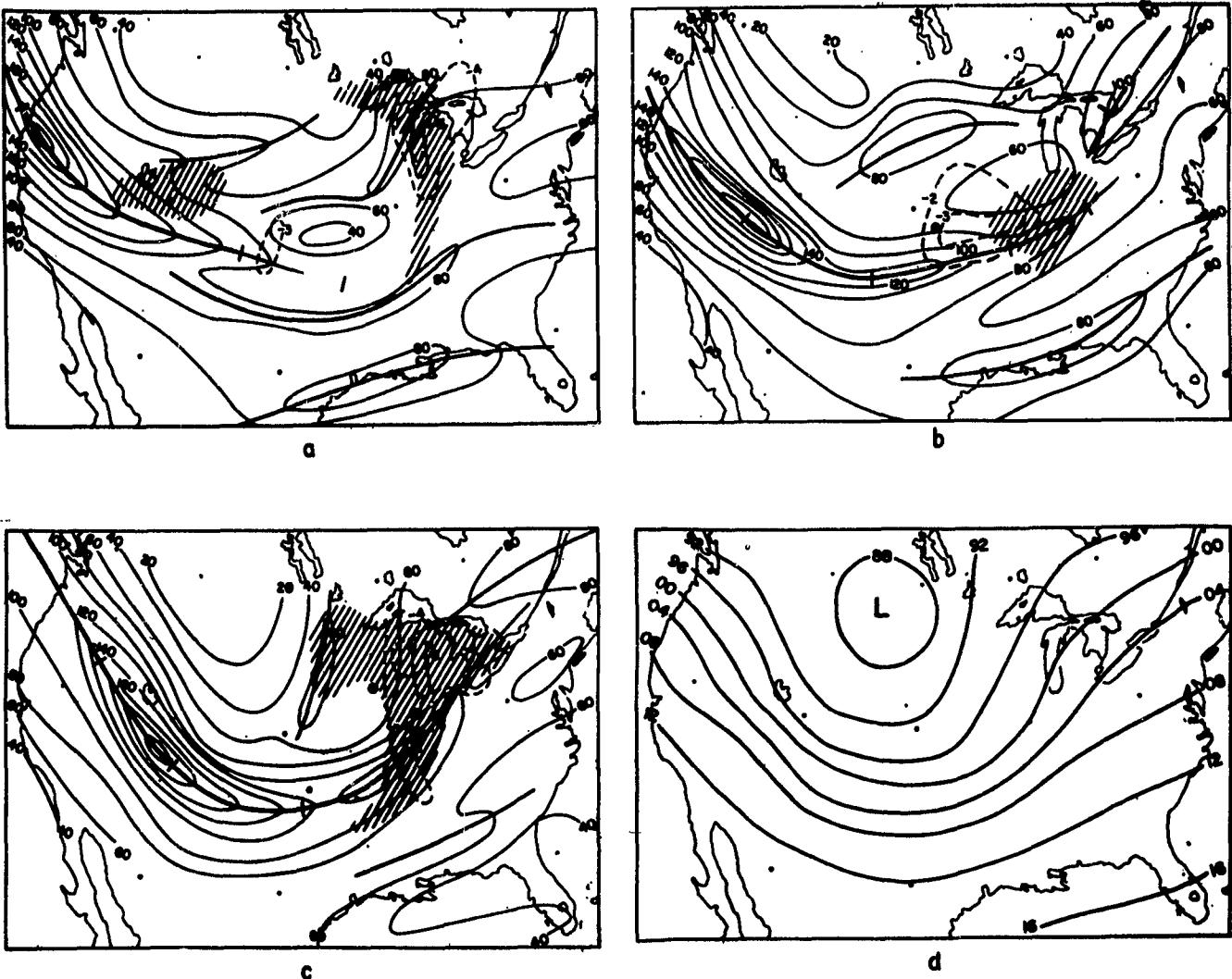
Fic. 4.3: *a, b, c* show the isotach pattern (thin solid lines) at 300 mb for November 12, 1951, 1500Z, and November 13, 1951, 0300Z and 1500Z. Shaded areas denote regions of precipitation; thick, solid lines join points of highest wind speed; broken lines are isolines of three-hour pressure fall at the surface; and heavy dots indicate the location of the lowest surface pressure. Fig. 4.3d represents the 300-mb contour field (100's feet, first digit omitted) at 1500Z November 13, 1951 [75].

(3) The greatest deepening occurred when the low reached a position east of the long-wave trough indicated by the trough in the jet axis.

The above correspondence between the jet stream and deepening of extratropical cyclones has often been observed. In the following we shall try to elucidate some principles governing this correspondence and, at the same time, explain other features of the role of the jet stream in cyclogenesis which were not brought out in this example.

THE PROBLEM OF PRESSURE CHANGES

(a) The jet stream in relation to pressure changes.— The change of pressure at the ground measures the variations of the weight of all the air in a column from the ground to the limit of the atmosphere. Con-

vergence of mass into or divergence of mass from this column produces these variations. We can get a divergence of mass in two ways: (1) The winds advect air that is denser or less dense than the air previously present, and (2) the winds diverge or converge. In the atmosphere, the second effect mentioned predominates, even near strong fronts and, therefore, we shall discuss it exclusively.

If a surface pressure change of three mb/hr were produced by uniform divergence from bottom to top of the atmosphere, this divergence would have an average value of about 10^{-6} sec^{-1}. But direct measurements from wind observations made by Houghton and Austin [33] and Sheppard [93], have revealed values up to 50 times this amount at different levels. This discrepancy indicates that surface pressure change is a relatively small residual between horizontal divergence

of one sign in the lower layers and an approximately equal divergence of opposite sign in the upper layers. Thus, convergence in the lower layers must give way to divergence higher up; conversely, low-level divergence must revert to convergence at some upper "level of nondivergence."

It is our experience that in middle latitudes, cloudiness is in general located at low levels in regions where the surface pressure falls. And when cloudiness is brought about by ascending motion connected with low-level convergence, the surface pressure fall indicates an overcompensating divergence in the higher levels.

Divergence is solely determined by wind structure and in particular by departures from geostrophic conditions since geostrophic winds are nondivergent [39]. *The dependence of surface pressure changes on divergence in the upper troposphere makes the upper wind structure of primary importance in surface development. The jet stream with its strong wind shears and considerable departures from geostrophic conditions is an important seat for higher-level convergence and divergence and must, therefore, play an important role in the formation and intensification of middle latitude cyclones.*

Scherhag [92] was among the first to introduce the idea of diverging upper winds as a basis for surface developments. His rule can be stated as follows:

When cyclones develop, they do so in a "delta" region, i.e., a region where the upper contours diverge. They weaken or fill up in an entrance region where the upper contours come together.

This rule has been the subject of both acclaim [76] and criticism [5, 7]. But in spite of its limitations which are concomitant to the lack of precise definitions of delta and entrance regions, and the implied identification of mass divergence with the divergence of contours, Scherhag's rule served to redirect the attention of meteorologists to the dynamical nature of the processes attending surface pressure changes.

(b) The relation between surface pressure changes and the changes of vorticity aloft.—In view of the difficulty in measuring divergence directly from weather maps, it is more convenient to relate surface pressure changes to some quantity which is related to the divergence and which, moreover, can be measured with some accuracy. Vorticity is such a quantity.

The relation between surface pressure changes and changes of vorticity aloft have been the subject of extensive theoretical investigation by Sutcliffe [97, 98, 99, 100], Charney [16], and others [56, 91]. The following relation evolves from a simplified derivation presented in an appendix at the end of this chapter:

The surface pressure falls where the relative vor-

ticity decreases downstream in the upper troposphere, and conversely.

It should be noted that the sign of the gradient of the vorticity rather than of the vorticity itself is involved in the relation. The same effect obtains if: (1) there is cyclonic relative vorticity upstream and anticyclonic relative vorticity downstream, or, if (2) cyclonic relative vorticity exists everywhere, but its distribution is such that it decreases downstream, or, (3) anticyclonic relative vorticity exists everywhere, provided it increases downstream. Vorticity relative to the earth in any current is produced by sheer within this current and by a curvature effect. The latter is defined as kv where v is the wind speed and k the streamline curvature. Thus, the value of the wind speed enters into the relation and helps to determine the effect of the curvature variation relative to the other terms. But it is important to note that the effect of the wind speed vanishes when the curvature of the streamlines is zero or uniform. This helps to account for the fact that only weak rapidly moving lows are observed to form under some jets of great intensity but having small streamline curvatures and uniform, though intense, wind shears along their axes.

In cases where the relative vorticity gradient is given mainly by the downstream variations of curvature, the principal *surface pressure falls should occur in the region where the curvature of the streamlines changes most rapidly from cyclonic to anticyclonic.* This explains the observed tendency for cyclones to deepen below inflection points downstream from long-wave troughs and upstream from ridges. The fact that the most intense deepening does not always occur exactly below the inflection point but a little distance upstream or downstream from it is a consequence of the appreciable effect of the shear terms.

(c) Some models of upper wind fields and the preferred regions of surface pressure fall associated with them.—The relative contribution toward surface pressure changes of the curvature and the shear terms which compose the relative vorticity varies in different situations. In some cases, they act in the same direction and the sign of their combined effects is easy to determine by inspection of upper-air patterns. In other cases, they act in opposite directions and their respective effects must be determined by computation before their net effect on surface pressure can be ascertained. The following models [72] illustrate different combinations of curvature and shear variations, which are likely to be encountered in the jet stream region, and the preferred localities of surface pressure fall associated with them.

Fig. 4.4a shows a symmetrical sinusoidal streamline pattern with a jet stream in the center. The isotachs are parallel to the streamlines and, therefore, there is no
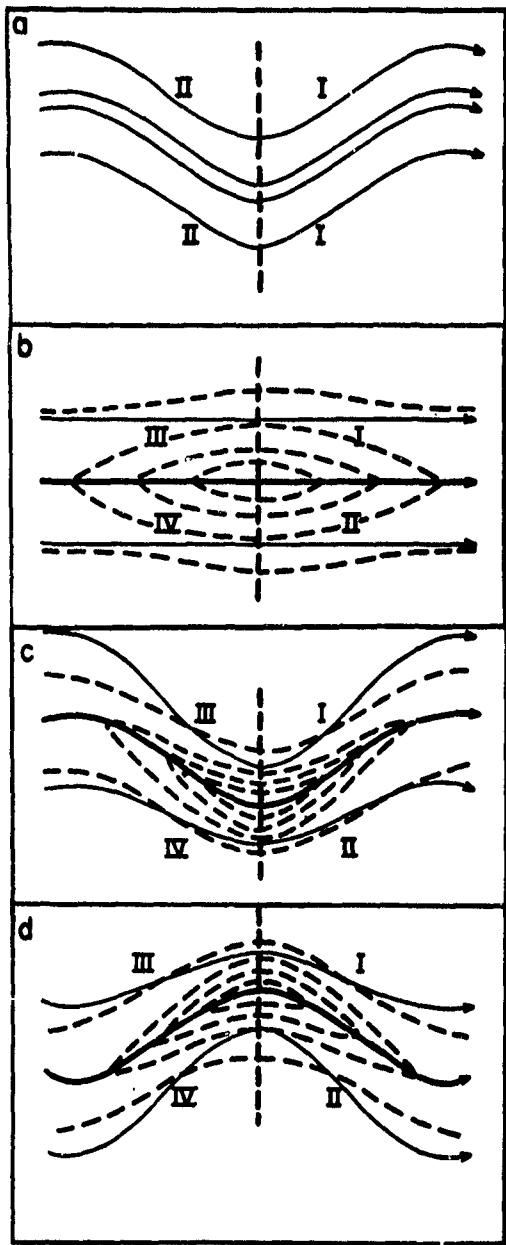
Fig. 4.4: Models of upper flow patterns. Solid lines are stream-lines and broken lines are isotachs [72].

shear along the direction of air flow. Thus, only varia-tions of curvature need to be considered. In region I, east of the trough, the cyclonic curvature and, there-fore, the vorticity decrease downstream. In region II, the vorticity increases downstream. In this case the whole region east of the trough is favorable for deepen-ing of surface systems while the whole region to the west of the trough is unfavorable.

In fig. 4.4b, we see a straight westerly current with no curvature effect. The cyclonic shear which in this case determines the relative vorticity decreases down-stream in regions I and IV. These are consequently favorable for the intensification of surface cyclones.

The reverse is true in regions II and III which are un-favorable for deepening.

In fig. 4.4c, a jet maximum is located in the trough. In region I, both cyclonic shear and curvature decrease downstream. Therefore, this region is highly favorable for deepening. In region III, both quantities increase downstream marking this region as unfavorable for deepening.

In regions II and IV, the situation is not determin-able by inspection since the curvature variation and the shear variation have opposing effects. In the former, the cyclonic curvature decreases and the cyclonic shear increases downstream. Whether or not th:\ region is favorable for surface deepening depends on the pre-ponderance of the variation of the curvature or of the shear.

Similarly, we cannot determine the situation in region IV by inspection. Here, the cyclonic shear decreases downstream while the cyclonic curvature increases in the same direction. Any tendency for deepening or filling depends on whether the effect of the shear variation is greater or smaller than that of the curvature variation.

Fig. 4.4d shows a jet maximum centered on the ridge. For the reasons discussed above, region II is unfavorable and region IV favorable for surface deep-ening. But regions I and III are indeterminate and may not favor deepening, depending on the net effect of the interplay between curvature and shear variations.

The following remarks can be made in the light of the analysis of the above models:

1. A "delta" region is not necessarily favorable for deepening nor is an "entrance" region neces-sarily favorable for filling.

2. The analysis of fig. 4.4 c-d verifies a general rule that deepening of surface systems occurs with preference east of long-wave troughs. It also pro-vides the means to recognize exceptional cases where this rule does not apply.

3. An explanation of the frequent formation of new lows or the occurrence of secondary lows to the southeast of the primary low is obtained by ex-amining figs. 2.7d and 2.8d (chap. II) which correspond to a period when a wind maximum has emerged out of the long-wave trough. Down-stream from the maximum, the analysis of fig. 4.4c still holds and the quadrant to the left of the jet axis remains favorable for deepening. But upstream from the maximum, a new cyclogenetic area is created by the emergence of the wind maximum from the trough. To the right of the jet axis, cyclonic curvature now decreases and anticyclonic shear increases downstream. Both favor deepening and make this region suitable for the formation of new low-pressure centers.

2. The Problem of Precipitation

The problem of the formation of precipitation in middle latitudes, which is intimately connected with that of the development of cyclones, is related to the jet stream in a manner very similar to that existing between the latter and cyclogenesis. Suggestions as to the existence of such a relation appeared soon after the jet stream came into prominence as an important feature of the general atmospheric circulation [68, 102].

tion forms from freezing rain to hail occurred in the Chicago area in heavy amount, as the cyclonic center was advancing rapidly northwestward from the Rockies while deepening strongly.

"The preceding sections show clearly, as has also been observed in connection with many synoptic disturbances of lower latitudes, that the magnitude of rainfall associated with perturbations does not depend on the initial depth of the moist layer that is transported into the disturbed zone.
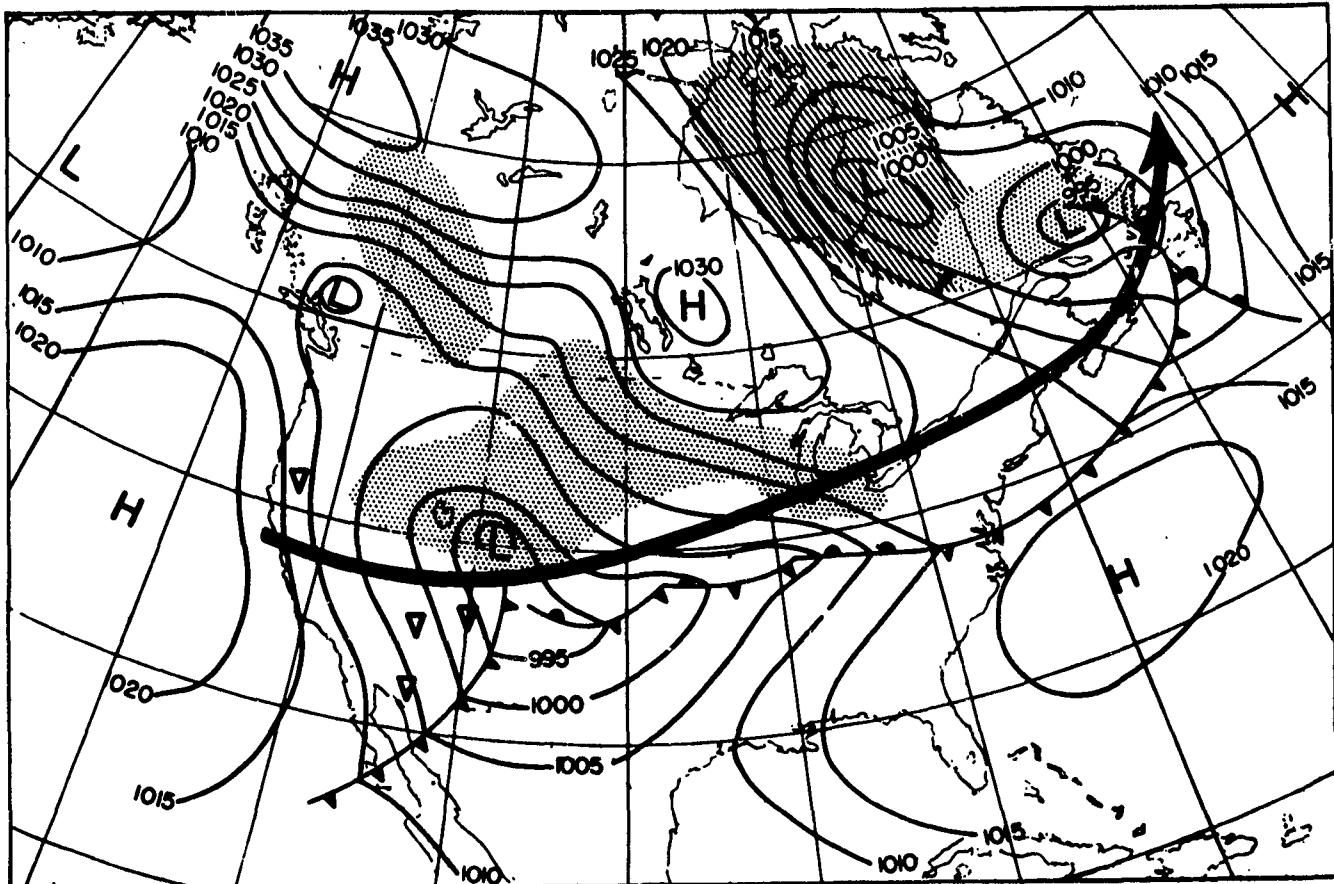
FIG. 4.5: Surface map January 29, 1947, 0630Z: Heavy arrow indicates center of upper jet stream; and shaded areas are regions of steady and intermittent precipitation [68].

In an analysis of the heavy precipitation of January 29, 1947, over the midwestern United States (fig. 4.5) the following was observed [68]:

"The front is of great intensity and extends east-west across the whole United States, roughly parallel to the jet stream. Large-scale frontogenesis has occurred in this front during the preceding day, and a widespread zone of precipitation is developing at map time, with heaviest precipitation oriented along the jet. There is evidence of great instability all along the frontal zone, and there are numerous attempts at wave formations. Such intensification is indicative of strong development. Although the moist layer advancing from the Gulf was restricted to the lowest kilometer, heavy precipitation and widespread thunderstorms developed under the jet. With surface temperatures near freezing, all precipita-

On the contrary, the top of the moist layer lowered appreciably during the period January 27 to 29 in the southern United States and a temperature inversion formed, under influence of subsidence south of the jet below the level of maximum wind. Nevertheless, a deep moist layer was able to form within a few hours in the region of low-level ascent at the northern edge of the jet, demonstrating again that dynamic processes far exceed advective considerations in importance as regards the formation of rain."

Starrett was the first to show that a good statistical correlation exists between the jet stream and precipitation. His results (cf. chap. III) revealed a tendency for the latter to be concentrated, both in frequency and amount, in or slightly to the north of the jet (figs. 3.22-3.23). In China, Yeh [112] suggested, in view

of the steadiness of the upper winds over that country in winter (cf. also chap. II), that a comparison of the mean upper-flow pattern with the mean precipitation pattern during that season should be of interest. He found (fig. 3.24) that "a maximum of precipitation practically coincides with the center of the upper jet stream. Rainfall decreases northward and southward from there, but much more rapidly on the south side." Yeh also noted that charts showing the number of days with rain similarly exhibit a very pronounced maximum that runs east-west along the upper jet.

Finally, Norquest [54] noted in a recent study that almost all major areas of precipitation over the United States and a majority of smaller ones can be linked to the jet stream.

Coincident with the improved understanding of details of the jet structure in relation to cyclone formation, especially the travelling maxima and minima, it has also become possible to develop a closer tie-in between these details and synoptic precipitation patterns. A study of any sequence of maps (cf. figs. 4.2-3) will reveal the following:

(1) Areas of precipitation tend to be localized rather than to extend in long narrow bands reflecting the position of the jet stream over its whole length.

(2) The rainfall pattern as revealed by these areas often departs substantially from the Norwegian models [10] which relate precipitation areas to the surface frontal systems.

The recent strides made in the study of the structure of the jet stream make it possible to arrive at a more precise relation between the jet stream and precipitation and, incidentally, to elucidate the circumstances attending the departure of precipitation areas from those prescribed by the models.

Riehl, Norquest, and Sugg [74] have studied the occurrence of precipitation in terms of a suggested relation between rainfall and changes of vorticity in the upper troposphere [56, 91, 99]. This relation,

derived in the appendix, states that *cloudiness and precipitation should occur in regions where the relative vorticity in the upper troposphere decreases downstream, and fair weather should prevail where the relative vorticity increases downstream.*

The above correlation has proved to be a good one [74] within the following limitations:

(1) The correlation identifies precipitation areas with those where air ascent prevails at the level of nondivergence. It does not take into account the fact that in some cases, due either to low moisture content of the air or insufficient condensation nuclei, ascent does not result in precipitation. Furthermore, precipitation in the upper air as evidenced by virga often evaporates before reaching the ground. In general, areas where the vorticity in the upper troposphere decreases downstream are somewhat larger than the corresponding areas where precipitation reaches the ground.

(2) The correlation does not account for precipitation due to thermodynamic instability, low-level showers, and locally determined precipitation.

It will be noticed that the above relation is identical with that connecting the change of vorticity aloft with cyclogenesis. This is tantamount to stating that precipitation will occur where the surface pressure is falling. This coincidence of areas of precipitation and of surface pressure fall, attested by our experience over many years, is strikingly brought out in figs. 4.2-3.

The present approach to the problem of precipitation provides a clue to the frequent departures of the observed distribution of frontal precipitation from that given by the Bjerknes models for an ideal cyclone. Frontal precipitation is confined to areas where the vorticity decreases downstream in the upper troposphere. The actual distribution of frontal precipitation follows the model distribution only to the extent that this condition is satisfied.

3. Appendix A

The equation of continuity in its complete form is as follows:

$$\frac{\partial \rho}{\partial t} + \text{div}_2\, \rho v + \frac{\partial}{\partial z}(\rho w) = 0, \qquad (1)$$

where ρ is the density, v the horizontal wind velocity, w the vertical wind speed, $\text{div}_2\, \rho v$ the horizontal mass divergence, t the time and z the vertical coordinate. The horizontal mass divergence is composed of two terms:

$$\text{div}_2\, \rho v = \rho \text{div}_2\, v + v.\, \text{grad}\, \rho. \qquad (2)$$

Here $\text{div}_2\, v$ is the horizontal velocity divergence and grad ρ is the horizontal gradient of the density.

In general, $\rho\, \text{div}_2\, v$ is about one order of magnitude larger than $v.\, \text{grad}\, \rho$. We may therefore neglect the last term in Equation (2) and assume that the mass divergence is, to a sufficiently close approximation, accounted for by the velocity divergence.

Integrating Equation (1) from the surface to the upper limit of the atmosphere and applying the hydrostatic equation,

$$-\frac{\partial p_0}{\partial t} = \int_{p_0}^{0} \rho \, \mathrm{div}_2 \, \mathbf{v} \, dp, \qquad (3)$$

where p_0 is the surface pressure.

If h denotes the level of nondivergence at which the divergence along a vertical column reverses sign, and if p_h denotes the pressure at that level,

$$-\frac{\partial p_0}{\partial t} = \int_{p_0}^{p_h} \mathrm{div}_2 \, \mathbf{v} \, dp + \int_{p_h}^{0} \mathrm{div}_2 \, \mathbf{v} \, dp. \qquad (4)$$

Since we are primarily interested in locating preferred regions for surface pressure fall and not in a quantitative investigation of pressure changes, we can avail ourselves of the empirical results, valid in the middle latitudes, that tropospheric convergence or divergence above the level of nondivergence overbalances respectively the divergence and convergence below that level. Thus, for the middle latitudes, the sign of the surface pressure changes is determined by the sign of the second term on the right-hand side of Equation (4). We may write

$$\mathrm{sign \ of} \ \frac{\partial p_0}{\partial t} = \mathrm{sign \ of} \int_{p_h}^{0} \mathrm{div}_2 \, \mathbf{v} \, dp. \qquad (5)$$

Furthermore, for reasons of continuity, convergence in the lower layers is accompanied by ascending motion. The vertical speed increases upward reaching a maximum at the level of nondivergence. Beyond this level, where low-level convergence gives way to divergence, the vertical motion decreases with height but retains its direction. Therefore, above the level of nondivergence, ascending motion is associated with divergence. Thus, if positive w denotes rising tropospheric air,

$$\mathrm{sign \ of} \ w = -\ \mathrm{sign \ of} \int_{p_h}^{0} \mathrm{div}_2 \, \mathbf{v} \, dp. \qquad (6)$$

It will be noticed that Equations (5) and (6) taken together state that there is ascent of air in regions where surface pressure is falling — a result supported by our experience of cloudiness and precipitation in regions of developing low pressure systems.

In view of the difficulty in measuring divergence accurately from the weather map, we replace this quantity with the vorticity by using the vorticity equation for a barotropic atmosphere

$$-\ \mathrm{div}_2 \, \mathbf{v} = \frac{1}{\zeta_a} \frac{d\zeta_a}{dt} = \frac{1}{\zeta_a} \left(\frac{\partial \zeta_a}{\partial t} + v \, \frac{\partial \zeta_a}{\partial s} \right). \qquad (7)$$

Here ζ_a is the absolute vorticity and s the direction of the streamlines. We now integrate from the level of nondivergence to the upper limit of the atmosphere to get

$$\mathrm{sign \ of} \int_{p_h}^{0} \mathrm{div}_2 \, \mathbf{v} \, dp = \mathrm{sign \ of} \int_{0}^{p_h} \frac{1}{\zeta_a} \left(\frac{\partial \zeta_a}{\partial t} + v \, \frac{\partial \zeta_a}{\partial s} \right) dp. \qquad (8)$$

The above equation may be simplified by noting the following:

(1) Although the absolute vorticity may vanish in a narrow strip to the south of the jet stream, this occurs only in a shallow layer near the level of maximum wind. The integral value of ζ_a from the level of nondivergence to the upper limit of the atmosphere is positive, and, therefore, does not affect the sign of the right-hand term of Equation (8).

(2) In most cases the air moves rapidly through the vorticity patterns, and the advective term greatly exceeds the local variation term which we may neglect.

We may thus simplify Equation (8) to

$$\mathrm{sign \ of} \int_{p_h}^{0} \mathrm{div}_2 \, \mathbf{v} \, dp = \mathrm{sign \ of} \int_{0}^{p_h} v \, \frac{\partial \zeta_a}{\partial s} \, dp. \qquad (9)$$

This equation implies that the absolute vorticity advection must be balanced by divergence if the vorticity pattern is to remain stationary.

Advection carries properties downstream, and its sign is solely determined by that of the gradient of the properties along the streamlines. Therefore,

$$\mathrm{sign \ of} \int_{p_h}^{0} \mathrm{div}_2 \, \mathbf{v} \, dp = \mathrm{sign \ of} \int_{0}^{p_h} \frac{\partial \zeta_a}{\partial s} \, dp$$
$$= \mathrm{sign \ of} \int_{0}^{p_h} \frac{\partial}{\partial s} (\zeta + f) \, dp, \qquad (10)$$

where ζ is the relative vorticity and f the Coriolis parameter.

In general, $\dfrac{\partial}{\partial s} f$ is one order of magnitude less than $\dfrac{\partial \zeta}{\partial s}$ and may be neglected. We then have

$$\mathrm{sign \ of} \int_{p_h}^{0} \mathrm{div}_2 \, \mathbf{v} \, dp = \mathrm{sign \ of} \int_{0}^{p_h} \frac{\partial \zeta}{\partial s} \, dp. \qquad (11)$$

Combining Equations (5) and (11), we get

$$\mathrm{sign \ of} \ \frac{\partial p_0}{\partial t} = \mathrm{sign \ of} \int_{0}^{p_h} \frac{\partial \zeta}{\partial s} \, dp. \qquad (12)$$

There are indications that the sign of the divergence and therefore of the vorticity gradient above the level of nondivergence does not reverse a second time in the troposphere. Therefore, the sign of the vorticity

gradient at any level within the troposphere and above the level of nondivergence is identical with the sign of the integral on the right-hand side of Equation (12). If we choose the 300-mb level to represent the whole upper layer, Equation (12) becomes

$$\text{sign of } \frac{\partial p_o}{\partial t} = \text{sign of} \left(-\frac{\partial \zeta}{\partial s} \right)_{300\,mb,} \qquad (13)$$

which states that *the surface pressure falls where the relative vorticity decreases downstream in the upper troposphere.*

We may similarly combine Equations (6) and (11) and assume, as discussed above, that the sign of the vertical integral of the vorticity gradient, above the level of nondivergence, is suitably represented by that at 300 mb. This gives us

$$\text{sign of } w = - \text{ sign of} \left(-\frac{\partial \zeta}{\partial s} \right)_{300\,mb.} \qquad (14)$$

Finally, we assume that some precipitation generally reaches the ground where the vertical velocity at the level of nondivergence is positive,[3] and state that *cloudiness and precipitation should occur in regions where the relative vorticity decreases downstream in the upper troposphere and fair weather should prevail where it increases downstream.*

CHAPTER V. THE JET STREAM
IN RELATION TO EXTENDED FORECASTING

1. The Problem of Extended Forecasting

While the polar front theory served as the only basic model for synoptic meteorology, weather analysis and forecasting concerned itself mainly with the detection of new wave formations and the displacement of fronts and air masses from map to map. And since the time interval between the inception of a new wave and the beginning of its decay can be as short as 24 hours, effective forecasting was necessarily restricted to a correspondingly short range. Moreover, the polar-front theory approaches the problem of forecasting from a purely regional point of view, on the assumption that atmospheric disturbances can be described in terms of interactions between different air masses in a limited area without considering broadscale processes.

There is now ample evidence that the problem of forecasting cannot be isolated from the "profound interdependence in different parts of the atmosphere, above and beyond the interdependence resulting from the displacement of air masses from one part of the globe to another [83]." In their meanderings around the hemisphere, the upper westerlies describe waves with wave lengths ranging between 50° and 120° longitude. These upper long waves determine the position of the frontal zones and the direction of motion of the shorter waves below. Therefore, they are of primary importance in longer-range forecasting. But the individual long waves cannot be treated separately

from adjacent waves. What happens in one reacts on the others. The problem of extended forecasting, therefore, transcends the regional considerations.

Certain broadscale features of the upper-air circulation such as the strength of the upper westerlies and the latitude belt in which they are concentrated figure prominently in determining the changes of amplitudes and displacements of the long waves and are, therefore, important factors in the problem of forecasting. These broadscale features show a tendency to persist for extended periods, often lasting several weeks, and their trends provide a framework into which to fit extended forecasts.

Forecasters have long realized that predicting weather beyond 48 or even 24 hours requires somewhat different techniques than for shorter periods. In the preparation of longer-period forecasts, two main approaches have been followed: (a) Direct statistical correlation between meteorological elements; and (b) extrapolation of trends shown by integrated features of the general circulation of the atmosphere.

As far back as the 1880's, investigators have related the strength of the westerly circulation over the North Atlantic to the Azores-Iceland sea-level pressure difference, which measures the intensity and location of the semi-permanent centers of action (cf. [101]). Since communications were quite slow, these correlations were used primarily in seasonal forecasting.[4]

2. Hemispheric Circulation as a Factor in Extended Forecasting

ZONAL CIRCULATION INDEX

General Concept. — The introduction of the hemispheric zonal circulation index concept by Rossby [2, 87] offered a new quantitative means of determining the strength of the zonal circulation. This index, initially defined as the sea level pressure difference across the mean zone of strongest westerlies (35°-55°N),

averaged around the hemisphere, became a primary tool in describing large-scale flow patterns. In winter, when the concept is most useful, high index is con-

[4]The statistical correlation between temperatures and/or pressures at various North Atlantic stations has been studied by Walker [106]. His "North Atlantic Oscillation," which is essentially a measure of the westerly circulation over the Atlantic, was a result of these studies.

sidered present when the 35°-55°N pressure difference is in excess of eight mb, and low index when the pressure difference is less than three mb.

At the beginning the index was computed only from the sea-level chart but later the three km index became an additional parameter. In subsequent refinements, discussed below, the upper-air circulation is of primary concern.

Synoptic features associated with high and low index. — The usefulness of the introduction of the zonal index in forecasting rested on the premise that distinct weather and flow patterns are associated with high and low indices. To some extent, at least, this proved to be true as discussed in [2, 108]. According to these authors, the following features characterize high index: (a) stronger than average westerly flows in middle latitudes; (b) strong Aleutian and Icelandic lows; (c) strong subtropic highs elongated east-west; (d) strong Siberian anticyclone centered near its mean position; (e) weak continental anticyclones in middle latitudes with few polar outbreaks; (f) fronts generally oriented east-west; and (g) cyclones moving rapidly, usually poleward of the mean seasonal tracks.

Low index, in the main, gives the inverse picture. We observe: (a) weak middle latitude westerly flow; (b) weak Icelandic and Aleutian lows usually split into double centers; (c) subtropical highs elongated north-south and broken by trough extensions to low latitudes; (d) Siberian anticyclone weak or with center displaced far west, sometimes to Europe; (e) well-developed continental highs in middle latitudes with frequent polar outbreaks; (f) large latitudinal extent of frontal systems, and (g) deep cyclones moving on tracks with large meridional components.

Limitations in applying the zonal index concept. — The usefulness of the zonal index is largely a function of its persistence. In the cold season, when it is most persistent, the same sign of the weekly index changes was maintained for at least two weeks in 70 per cent of the cases during the winters of 1935-39 [2]. The investigators also found that during winter the high (or low) index phase tends to recur at average intervals of from six to eight weeks.

The synoptic descriptions given above should be expected to hold mainly when the high or low index phases are well developed. Often, however, the situation cannot be clearly identified as intermediate conditions prevail. During such periods, we may find large longitudinal variations in the type of synoptic systems present. The same map may feature typically high index patterns in one region and low index patterns in another.

Another difficulty limits the value of the zonal index; decreases of the index often do not denote a decrease in the intensity of the westerly circulation but, instead,

a latitudinal displacement of the strongest westerlies to the margin of the 35°-55° zone. In meteorology this type of difficulty is frequent when fixed geographical coordinates are used. It is more realistic to work in a moving coordinate system which is attached to some physical variable. The next technique developed for assaying the strength of the zonal circulation takes into account this movement of the belt of strongest westerlies.

ZONAL PROFILE

Basically the computation of the zonal profile is similar to that for the zonal index except that now the mean geostrophic west wind is computed for a number of 5° lat. belts. The individual values are plotted against latitude to form a profile of the geostrophic west wind against latitude (fig. 5.1). Profiles with strong and weak shears on either side of the maximum are termed peaked and blunt, respectively. High index conditions generally prevail at times when the westerlies have a peaked profile in middle latitudes.
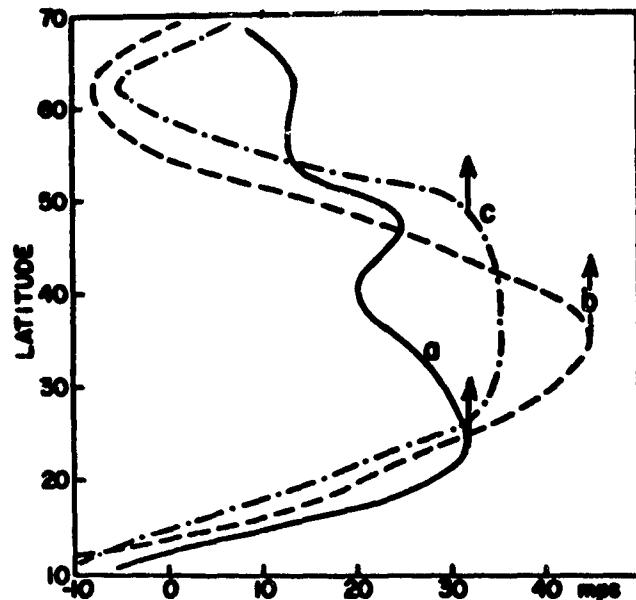
Fig. 5.1: Profile of the westerlies at 300 mb: (a) December 7, 1945; (b) December 19, 1945; (c) December 29, 1945. Arrows mark successive position of the relative maximum [72].

The zonal profile can be computed for any level for which charts are available. At lower elevations, the mean speed is much lower and it varies much less than in the upper troposphere. Thus, low level profiles usually are blunt and often ill-defined. Nevertheless, most computations have been made either at 700 mb or 500 mb. This is due mainly to the fact that (a) there are far fewer upper-air data at 300 mb or 200 mb; (b)

the profile has been used in conjunction with the Rossby long-wave formula [87] which requires the zonal wind at the level of nondivergence. This level, in the mean, lies near 600 mb.

In spite of the shortcomings, 700-mb or 500-mb profiles usually will bring out the major features of the structure of the hemispheric westerlies and their changes with time (cf. [71]). For instance, the wind maximum, if peaked, will appear peaked at all levels, though not to the same degree. At the surface, the profiles are less well defined and interpretation at times is more difficult. However, Namias [50] has followed the index trends for a number of years with sea-level pressure profiles. In recent years the maximum shown on zonal wind profiles has been termed the *hemispheric jet* [102]. Its strength and latitudinal position have been important considerations in the application of long-wave theory [18]. Any integrated picture of the upper wind field taken over a large portion of the earth's surface, however, must necessarily lack the detail of profiles taken normal to the jet stream at one longitude. Also, since only the zonal component of the wind is considered in the hemispheric application, the term "jet" here has a special meaning. For instance, the actual wind speed following the main current in middle latitudes averaged around the hemisphere may often be greater when the profile is blunt than when it is peaked. In such cases the meridional wind component accounts for a large proportion of the total wind speed.

Computational limitations of the zonal profile. — A number of precautions must be taken in the computation of the zonal profile. Otherwise, false oscillations in the strength and position of the maxima may appear. If confidence cannot be placed in the position and intensity of the hemispheric jet, it is of little use in forecasting.

(1) The computation should be made from maps which cover as great a longitude range as possible; profiles computed from data encompassing less than 180° long. are of questionable value. If the maps do not extend through 360°, the movement of troughs and ridges past the end points influence the computation. For example, assume that a progressive wave pattern encircles the earth at a given latitude. If the computation is made in a limited area between two ridges, the westerlies will appear at a higher latitude than at a later time when the pattern has moved a half-wave length so that the calculation is made from trough to trough. On account of this consideration it is also necessary to maintain the same longitude interval from day to day.

(2) The most important factor that can produce spurious oscillations of the profile is lack of accuracy of the charts from which the calculations are made. If the charts are not carefully prepared, other precautions are futile. In analyzing the maps, continuity is an important consideration, particularly in areas of sparse data. Since the analysis depends so much on individual station reports in such areas, time sections of these reports should be kept and systematic checks of heights of standard pressure surfaces should be made. In particular, any height value which appears inconsistent from the viewpoint of continuity should be checked by plotting the sounding and recomputing the height.

As a further precaution, it has also proved of value to plot time sections of overlapping three- or five-day means of the profile. In this manner many of the spurious variations that inevitably enter into series of daily profiles are eliminated.

(3) We have noted that the zonal index often gives an unsatisfactory picture of the state and variation of the structure of the mean westerlies, since fixed geographical coordinates are used for its computation. The zonal profile computation permits us to follow the latitudinal movement of the zone of strongest westerlies. But we are still working in a framework of geographical coordinates as we determine the profile from height gradients of an upper-pressure surface obtained by finding the mean height of the pressure surface on successive latitude circles. At times, particularly during the winter season, the center of the circumpolar westerly circulation departs considerably from the geographical pole. For instance, the strongest westerlies may be located at 30°-40°N over the Pacific but at 50°-60°N over Scandinavia and northern Russia. Then the circulation pole is displaced toward the Pacific and we call the westerlies "eccentric." La Seur has investigated this eccentricity and traced the movements of the circulation pole.[5] He has shown that calculations of the westerlies made from height tabulations taken with respect to this pole often give well-defined maxima when calculations made with respect to the geographical pole feature blunt profiles. Thus, when the westerlies are eccentric, profiles computed from height tabulations made at fixed geographical coordinates will be unrepresentative as to the structure of the hemispheric jet, and a grid centered

---

[5]To be published at the University of Chicago.

on the circulation pole should be used. Methods for finding the circulation pole and the weather patterns associated with eccentricity have been discussed briefly in [72].

(4) As the reader will have noticed, we have throughout this chapter described progressively more complex computations, starting with the surface pressure difference between Iceland and the Azores and winding up with mid- or high-tropospheric profiles of the circumpolar current computed in a coordinate system attached to a variable circulation pole. This increasing complexity results from the fact that the computed circulation indices did not give the information desired by forecasters and research meteorologists alike: the complete picture of the state of the hemispheric circulation. The successive refinements outlined here show the route that has been taken to include an ever increasing amount of the important characteristics of the hemispheric jet. Even at the time of this writing, however, some dissatisfaction with the current methods remains. Various researches are being conducted on the subject, and we should expect the future to bring a continuing evolution of statistical techniques in defining and following the hemispheric jet.

THE INDEX CYCLE

A major difficulty in using the zonal index as a forecasting aid has been the fact that the descriptions of weather patterns associated with different indices apply only when the index is definitely high or low. During the intermediate periods the forecaster obtains but little assistance. It is logical to extend the descriptions to cover all "stages" of an "index cycle." The term "index cycle" describes a complete oscillation of the westerlies from some starting profile to the time when the same profile is observed again. The duration of such a cycle may be several weeks.

The first complete attempt to fit the synoptic systems near the ground and in the upper air into an index cycle was that of Rossby and Willett [88]. Their cycle is based on a model featuring strengthening and expansion of the circumpolar vortex [82]. According to this model, an initial concentration of the westerly circulation starts in high latitudes. While the jet is in the north, typically high index conditions prevail in the high middle latitudes. Then the westerlies expand. The synoptic disturbances become stronger in the lower middle latitudes and the amplitude of the upper-flow patterns begins to increase. This tendency for increasing amplitude persists as the jet continues to propagate southward until eventually the flow pattern aloft loses the open-wave structure and breaks down into

closed cells. Finally, these closed cells, which are mainly of the nature of "cut-off" cyclones and anticyclones, dissipate as formation of a new jet starts in the high latitudes. Thus, Rossby and Willett closely identify the index cycle with the development, movement, and dissipation of the hemispheric jet. Further work, using the same approach, has been carried out by Namias [51, 53], and the description of the index cycle has been carried to further detail in [72]. This description, which is based on the concept of the drift of "relative maxima and minima" across the latitude circles, will now be presented.

TIME VARIATIONS OF THE ZONAL PROFILE

A plot of daily values of the zonal wind for each 5° lat. belt, seen in fig. 5.2, will be referred to as a time section of the zonal wind. Such sections form an important tool in detecting variations in the strength of the westerlies. In fig. 5.2 the values of the zonal wind, averaged over 280° long., have been plotted against latitude for the period November 10-26, 1950. It is apparent from this section that, in general, the westerlies are strongest in the lower middle latitudes. Appreciable changes, however, occur during this 17-day
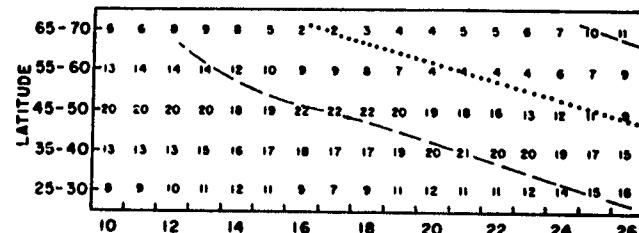
Fig. 5.2: Time section of zonal wind speed (mps) at 500 mb, November 10-26, 1950. Only one quarter of the calculated values is reproduced (every second 5° belt of latitude and every second day). Dashed lines denote relative maxima, and dotted lines relative minima of zonal wind speed [72].

period at any given latitude. For instance, the westerlies in the belt 65°-70°N reach a maximum about November 12-13 and then their strength falls to a low point about November 16-17. Similar tendencies for alteration between high and low speed are apparent in lower latitudes at progressively later times. The dashed and dotted slanting curves of fig. 5.2 show the southward progression of the tendency for increasing and decreasing westerly circulation. These trends will be referred to as relative maxima and minima. They are designated "relative" because they are maxima and minima only for a particular latitude belt. They may progress either poleward or equatorward. The latitude and direction of motion of the relative maxima will be

the basic means of determining the stages of the index cycle and consequently the preferred types of synoptic sequences described below.

Northward or southward drifts of the relative maxima and minima usually are discernible from a series of daily zonal wind profiles. For instance, we see the northward progression of a relative maximum in fig. 5.1. Initially, the zonal circulation is relatively strong in both low and high latitudes and relatively weak in middle latitudes (fig. 5.1, curve a). Then, as the relative maximum moves northward, the high latitude westerlies decrease, and both the middle latitude westerlies and the low latitude easterlies increase. At the time the relative maximum reaches the seasonal position of the mean jet (cf. chap. III), the profile is most peaked with strong easterlies in the tropics and polar easterlies in the subarctic belt (fig. 5.1, curve b). Subsequently, the profile again becomes more blunt (fig. 5.1, curve c).

Two relative maxima and one minimum or the inverse (fig. 5.2) are generally observed on any particular day in the belt 20°-70°N. The separation between individual maxima and minima is of the order of 20°-30° lat. These relative maxima and minima may drift either northward or southward but once a definite trend has been established it usually persists for a month or longer. Northward trends are observed on the average about two-thirds of the time. The latitudinal movement of the relative maxima and minima is of the order of

2°-4° lat. per day and a fairly constant speed is usually maintained throughout a given trend. Thus, extrapolation usually is a satisfactory forecasting technique except in cases of trend reversal. Thus far, the means of predicting the reversal points are not satisfactory.

STAGES OF THE INDEX CYCLE (AFTER [72])

In the following, the letters N and S will distinguish northward and southward trends. The Roman numerals I, II and III will distinguish stages of these trends.

Stage NI. — A relative west wind maximum emerges from the tropics and gradually moves through the lower middle latitudes. Another relative maximum initially located in the upper middle latitudes advances toward the Arctic Circle while weakening.

Stage NII. — The westerlies become stronger than average at the latitude of the seasonal maximum and weaker than average in the subtropics and subarctic. This is the classical "high index" stage.

Stage NIII. — The relative maximum moves to the upper middle latitudes then to the subarctic. It is still the dominant feature. In the subtropics a new belt of westerlies gradually organizes and the cycle is completed.

Stage SI. — A relative west wind maximum emerges from the arctic or forms near the Arctic Circle. It gradually approaches the middle latitudes. Another relative maximum, initially located in the lower middle lati-

TABLE 5.1. — *Northward Trend*

Stage	Cyclones	Anticyclones	Upper air features
NI	Wave cyclones in lower and central middle latitudes, also near Arctic Circle. Moderate displacements with pronounced meridional component.	Cold highs penetrate to fairly low latitudes.	Open, progressive long-wave patterns of pronounced amplitude with configuration shown in fig. 5.3b. Decreases of wave number through "cutting off." Extension of troughs into low latitudes. Well-organized jet stream.
NI-NII	Principal activity shifts to central middle latitudes. Cyclones in subtropics become reflection of upper "cut-off" lows.	Polar outbreaks weaken. Subtropical highs strengthen.	Amplitude in long-wave train decreases. "Cut-off" lows south of westerlies dissipate and/or drop into tropics.
NII	Succession of warm cyclones of weak to moderate intensity. Rapid movement of lows mainly from west to east. Bad weather confined to narrow band along cyclone path. Dryness south of strongest westerlies. Sometimes another belt of weak, rapid moving waves in far south (Mediterranean, Gulf Coast of U. S.).	Few cold air penetrations south of belt of strongest west winds. Lack of cold highs in middle and upper middle latitudes. Intense subtropical highs extend east-west.	Weak long waves of large wave length and small amplitude, slowly progressive or stationary. Rapid weakening of wave amplitude south of belt of strongest westerlies. Few extensions of troughs to low latitudes. Minimum blocking activity. Disorganized, weak jet streams.

TABLE 5.1. — *Northward Trend* (Continued)

Stage	Cyclones	Anticyclones	Upper air features
NII-NIII	Cyclones decelerate and increase in north-south extent. East-west belt of cyclones is broken.	Cold highs reappear in upper middle latitudes.	Often sharp "break" of high index with rapidly increasing amplitudes of flow aloft. Long waves retrograde.
NIII	Complicated surface maps of "irregular" appearance. Cyclones of weak to moderate intensity in middle latitudes. Frequently two trains of disturbances separated by 10°-20° lat. Motion with strong meridional components often is sluggish. Widespread and persistent low cloudiness and fog.	Renewed cold air penetrations of relatively brief duration to lower latitudes. Subtropical highs weaken and assume a more meridional orientation.	Long waves with shape as shown in fig. 5.3a. Increase in wave number. Frequent presence of several "meandering" jet streams with a wave train in each current. Reappearance of trough extensions into the tropics. Some "cutting off" of lows in the south and highs in the north.
NIII-NI	Gradual clarification of surface maps as a more definite succession of wave cyclones and cold highs with "regular" motion develops in middle latitudes. Strong cyclonic activity near the Arctic Circle.		Gradual shift of one-wave train to the arctic and reestablishment of a wave train with shape as shown in fig. 5.3b in lower middle latitude.

TABLE 5.2. — *Southward Trend*

Stage	Cyclones	Anticyclones	Upper air features
SI	One train of strong cyclones near Arctic Circle, and another train of usually weaker cyclones in low middle latitudes.	Cold highs cover upper middle latitudes, build in subarctic.	Two long-wave trains in two westerly currents near arctic and subtropics. Numerous "cut-off" lows and highs in between.
SI transition SII	Southern cyclone train dissipates. Northern train shifts to middle latitudes, assumes a more east-west orientation. Motion of lows becomes more zonal and speeds up. Brief periods of widespread precipitation.	Arctic highs continue building, and there are brief cold air intrusions into middle latitudes following cyclones. Subtropical highs remain weak.	Development of open-wave pattern with shape as in fig. 5.3a. Amplitude diminishes. Waves are slowly progressive or stationary. Dissipation of closed centers aloft.
SIII transition	Cyclones decelerate and increase in north-south extent. East-west belt of cyclones is broken.	Rapid development of cold highs in north and renewed intrusion of cold air into middle latitudes.	Retrogression of long waves.
Climax of SIII	Cyclones of greatest intensity over continents and lower middle latitudes generally.	Major cold outbreaks. Cold highs of great strength move southward. Subtropical ridge is weak and broken in many places.	Long-wave train of extreme amplitude with shape given by fig. 5.3b. Retrograde motion. Cutting off of several dynamic highs in north. Concentrated jet stream with maximum speeds over 200 knots.
SIII-SI	Cyclonic activity shifts toward subtropics as new formations become less frequent and are weaker. New cyclone belt appears near Arctic Circle.	Control of cold highs becomes general in upper and central middle latitudes.	The wave train in the lower latitudes breaks down into closed vortices aloft. No long-wave train is discernible. Many blocks.

tudes, drops into the subtropics and tropics while weakening. As the relative maximum from the north passes through the central middle latitudes, a feeble counterpart to Stage NII, which we may call Stage SII develops. Sometimes, however, this stage does not occur, and we rapidly pass to Stage SIII.

Stage SIII. — This stage best fits the classical "low index" description. The relative maximum, often still continuing to gain intensity, moves to the lower middle latitudes. It is at this time that the peak on the profile, itself, is most apt to be displaced from middle latitudes. In the central and upper middle latitudes, the westerlies are at their weakest. The subtropical ridge is displaced far into the tropics. After several days the extreme situation gradually subsides as the relative maximum moves into the tropics and the westerlies strengthen near the Arctic Circle. Again the cycle is completed.

SYNOPTIC PATTERNS RELATED TO THE INDEX CYCLE

A description of anomalies of surface and upper flow patterns associated with the stages of the N and S trends, and the features of the transition periods are produced in table 5.1. Further details may be found in [72].

The description furnished departs markedly from the simple scheme of an oscillation between periods of high and low index. The synoptic patterns of only one stage, NII, corresponds closely to high index; while four stages correspond to some extent to low index.

PRACTICAL CONSIDERATIONS IN APPLICATION AND INTERPRETATION OF THE INDEX CYCLE

The greatest usefulness of the index cycle as described is perhaps its function as a selection technique. If a forecaster knows the current stage, he is put on guard as to what anomalies in the weather pattern are most likely to occur and which have only an outside chance. Of course, table 5.1 is quite schematic and merely indicates what types of disturbances have a higher or lower than average probability of occurrence. Work on the stages of the index cycle also is continuing, and we can expect that the relation between the stages and the weather patterns gradually will be put on a more objective basis.

The limitations of the descriptions given must always be kept in mind. Most important in this respect

is the realization that cycles seldom are so pronounced or intense that all longitudes around the globe are affected in the same way. For example, strong zonal flow over the Pacific and North America sometimes occurs in winter when blocking patterns dominate the weather of northwestern Europe. There is a tendency for the Pacific, North America, and the western Atlantic to act together while the Eurasian continent may behave differently. In a sense, it is correct to interpret index cycle weather patterns as probability forecasts; certain developments are more likely to occur during some stages than others. For example, during SIII cold outbreaks have a greater than average expectation of occurrence, but clearly these outbreaks will take place in preferred locations and the probability of occurrence is largely a function of longitude.

Further, the transition from one stage of a cycle to another rarely occurs simultaneously around the hemisphere. At times, spectacular changes do occur
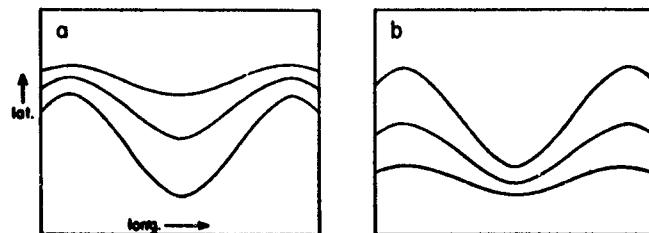
Fic. 5.3: Typical contours of an isobaric surface (*a*) during Stages NIII and SI, and (*b*) during stages NI and SIII [72].

everywhere in association with the cutting-off of low centers at several places around the globe. Ordinarily the changes are much more gradual. A common sequence in the development of the NII stage is for the westerlies to first become strong over the Eurasian continent and then propagate around the hemisphere.

The classification system used for the index cycle is quite flexible. This is desirable since any rigid system continues to add subclassifications and exceptions until it becomes so complicated that it loses its practical utility. For example, the discussion above has dealt primarily with synoptic patterns of the colder season in middle latitudes. Descriptions of the warmer season, however, particularly those of the upper air, would necessitate only minor changes. For mountainous areas and for the lower latitudes, additional modifications would be required.

CHAPTER VI. HIGH LEVEL WIND ANALYSIS

1. Introduction

Given a dense network of accurate wind observations, the wind analysis on any surface (constant level, constant pressure, and isentropic) consists in drawing streamlines and isotachs directly following the data. Streamlines everywhere are parallel to the flow direction. Isotachs are lines that connect points of equal wind speed regardless of direction. They are drawn in accordance with the same rules which apply in the analysis of surface isobars. If great accuracy is desired, drawing of lines of equal wind direction (isogons) [89] may precede that of the streamlines. In constructing the latter, the analyst can avail himself of models of streamline patterns discussed by V. Bjerknes [11] and extensively applied to tropical analysis by Palmer [61].

Over the United States, at levels as high as 500 mb, the data coverage at times is sufficient to permit execution of the routine just described. The analysis then consumes very little time and can be made with an accuracy comparable to that of the surface isobars. Almost the whole of what follows is necessitated by the fact that data coverage and accuracy at high levels usually are far from ideal. The principal reasons for these deficiencies are:

(1) Over the oceans and some extensive land areas, few, if any, observations are available.

(2) Pilot balloons, which still furnish the majority of upper wind reports over land, are quickly lost during bad weather.

(3) Pilot balloons and several types of rawin equipment drift out of range or yield inaccurate wind speeds in the high tropospheric jet stream cores as the elevation angle of the balloons becomes very small. These instrumental defects are gradually being removed and in some areas, notably Great Britain, the standard of upper wind observations is very high.

Although it is often possible to locate a jet stream center merely by noting where wind reports are absent, we wish to emphasize the steady progress made in observational technique and coverage. This is evidenced by the fact that analysis at 300-mb today is on a level of difficulty comparable to that encountered at 700 mb and 500 mb during World War II. Nevertheless, the analyst, faced with the need to turn out a high-level wind prognosis, often must "lift himself by his bootstraps." His problem is comparable to that of a shipbuilder who is requested to deliver a seaworthy vessel but is allocated only a fraction of the needed steel. The only tool available to the meteorologist, to fill in the holes, is analysis of the fields of mass and temperature, and use of relations between these fields and the winds given by simplified equations of motion.

Throughout the following, we shall be concerned only with analysis at standard isobaric surfaces in the high troposphere, such as 300 mb, which is situated near the level of strongest wind in middle latitudes in winter (chap. II). Before entering into details of the many steps that lead to a wind analysis at high levels when only a few wind reports are available, it is worth while to begin with several general points of practical importance.

AREA OF ANALYSIS AND CHOICE OF BASE MAP

As the complete analysis routine described below is fairly extensive, an individual analyst usually should not be concerned with a longitudinal interval of more than 90°, if the latitudinal distance covered is at least 40° and if the analysis is to be of value for operational forecasts.

Since the calculations suggested later involve the measurement of streamline or contour curvature, the base map chosen should be such as to permit a fairly reliable measurement of curvature without auxiliary correction tables. Yet, the areal distortion of the projection should also be a minimum. For these objectives the Lambert conformal conic projection, with standard parallels at lats. 30° and 60°, is well suited. If a hemi-

spheric analysis in high latitudes is desired, a polar projection should be used. At the University of Chicago, a polar stereographic projection, true at lat. 60°, has done good service for this purpose. In lower latitudes, however, the curvature of the latitude circles on this base map departs sufficiently from the true curvature to necessitate corrections, especially when the winds are high and the flow curvature anticyclonic. Thus, even if a hemispheric isotach picture is wanted, we feel it is preferable to work with the Lambert projection.

At the University of Chicago, the scale of the hemispheric base map used is 1:22,500,000. This scale is convenient to depict gross features of the hemispheric circulations without employing maps of unwieldy size. Near the jet stream core, however, the crowding of isotachs often becomes so great that the analysis will not be sufficiently reliable for operational purposes. If a sectional Lambert conic is used, one can employ a larger-scale map and still retain a convenient map size. In large measure, the ultimate choice of scale also depends on the station density. For analysis from the eastern Pacific to Europe, we believe that a scale of 1:15,000,000 or 1:17,500,000 is most suitable.

PLOTTING MODEL

When complete observations are available at a station, the items to be entered on the high-level chart are: wind speed and direction, contour height (first and last digits omitted), temperature (whole degrees centigrade), and 12- or 24-hour height and temperature change (fig. 6.1). In addition to the traditional practice of plotting the wind vector, we recommend that speed and direction also be written out below the station circle as shown in fig. 6.1. This aids plotters in detecting errors. For the analyst, it greatly reduces the time spent in the checking of data required on account of the frequent inaccuracy of the pictorial wind representation. Besides, the isotach analysis is simplified. We do not wish to imply, however, that the conventional plotting of wind data should be abandoned. On the contrary, the pictorial representation is well suited as an aid in the contour analysis, when the analyst concentrates on the height data.

In making isotach analyses at the 300-mb level, it has been found that the 200-mb temperature field serves as a useful aid in locating the axis of the jet. It is, therefore, recommended that the 200-mb temperature be included in the plotting model on the 300-mb chart.

Neat plotting facilitates the rapidity and accuracy of an analyst's work to a greater extent than is thought at times. In particular, use of heavy pens, wide spacing of numbers, and drawing of excessively long wind vectors blacken the map in a way that renders analysis

slow and difficult. Plotting of data close to the station circle and usage of other Weather Bureau standards [103] are recommended.

CONTINUITY

Because of the irregular receipt of wind observations, complete charts containing all observed winds should be plotted and analyzed every six hours as an aid to the complete analysis made at 12-hour intervals. The anaylst then has at his disposal: (a) a map of the current winds, (b) a map of the winds 12 hours before, and (c) an intermediate map which often has observations in areas which are blank on the other two maps.[6]

In addition, any available aircraft reports should be plotted by marking the time of observation and denoting the aircraft position with a square rather than a circle to differentiate these reports from those of ground stations. Careful use of aircraft reports is of particular importance over the oceans where data always are at a premium. We also suggest that complete time sections be kept of the reports of stationary weather ships, moving aircraft carriers, and any other vessels taking upper-air observations.

We wish to emphasize that high-level analysis should not be attempted except in conjunction with a carefully prepared 500-mb chart and, when available, a temperature analysis above the level of strongest winds (usually 200 mb in middle latitudes, as discussed in chap. II). Over the oceans, a great deal must be inferred regarding the upper winds by using methods of indirect aerology and models. Here, accurate surface analysis with good continuity, sketching of areas with cloudiness, and tracks of highs, lows, and fronts can prove of inestimable value. The relation of these parameters to the jet stream and, therefore, their value in

Fig. 6.1: Model for plotting upper-air data on constant pressure charts: —55° is temperature in °C; 985 is height in feet of 300-mb surface, first and last numbers omitted; +31 is height change in tens of feet; —2 is temperature change in °C; and 0160 is wind direction in tens of degrees and speed in knots, i.e., direction 10° and speed 60 knots. The direction is graphically represented by shaft. One barb is 10 knots, one triangle 50 knots.

[6]This is especially true in the United States at 2100Z.

placing jet stream axes and/or maximum centers has been pointed out in the earlier chapters.

For operations requiring knowledge of the level of strongest winds, we recommend plotting a separate chart containing height and wind direction and speed at this level as obtained from the upper winds transmission. As an auxiliary tool, analysis of the temperature field at 300 mb, 200 mb, and possibly 250 mb is helpful as will be discussed later.

PROCESSING OF THE DATA

Transmission. — At the time of this writing, the transmission of radiosonde data is accomplished in two sections. The data above 400 mb follow the low-level observations by a considerable margin in time. There can be little doubt that administrative revision of the transmission schedules and elimination of the "second transmission" would increase the number and accuracy of high-tropospheric observations, and, also, the regularity with which existing data are transmitted. Too often, a post-mortem on data reveals that a much needed observation was taken but not transmitted at the proper time.

Accuracy of observations. — The accuracy of wind data at high levels is still uncertain. According to recent tests [104], wind observations taken by double theodolite, rawin, and radar usually agree within five knots of speed and 20° of direction at 300 mb. Presumably, the discrepancy with pilot balloons would be greater, due to use of assumed balloon ascension rates.

The accuracy of contour heights is also discussed in [104]. Evaluation of *all* radiosondes in use in the United States on June 14, 1951, has shown a maximum possible height error of 459 feet at 300 mb. This performance error is a cumulative effect of total maximum variations of temperature and pressure upon the computed 300-mb height, assuming that the variations were all of the same sign and occurred throughout the whole layer. The report points out that "while errors of the above magnitude seldom, if ever, occur, these figures are helpful in explaining occasional large apparent discrepancies." Experienced analysts will agree that such large errors among reported heights seldom occur over North America. In support of this impression, it has been found [104] that the largest 300-mb height difference between two U.S. Weather Bureau instruments, alike in all respects, was 95 feet at 0300Z and 154 feet at 1500Z.

The main reason for discrepancies of observations at 300 mb lies in the employment of different types of radiosondes by the several agencies now engaged in the radiosonde program [111]. This is a serious shortcoming which can be avoided.

In addition to the general suggestions on plotting

made initially, the following will discuss details of the plotting routine that will permit maximum utilization of the sparse data for the construction of 300-mb charts:

Plotting of winds. — While wind reports at 300 mb or 30,000 feet evidently are plotted first, lower winds should not be ignored when an ascent fails to reach this standard level. Such lower winds, in nearly all cases, will give the wind direction quite accurately since, as is well known, the wind direction changes only slightly with height through the high troposphere. The speed also is helpful since, with certain exceptions in the subpolar and arctic latitudes, the wind speed increases upward at least to the vicinity of the 300-mb surface. Wind speeds at lower altitudes, therefore, indicate a minimum value for the 300-mb wind speed to which, in general, an upward correction is to be added.

We recommend that lower winds be entered down to 23,000 feet (400 mb) over areas with good data coverage, usually over land, and down to 20,000 feet where data is scarce, usually over the oceans and in some regions of the high latitudes. Inclusion of these lower winds may increase the total number of reports by as much as 50 per cent, especially at 0300Z. The lower level winds should be distinguished from the 300-mb reports. This is best done by plotting them dashed and adding the height of the level used. For example 0150 (23′) denotes a wind of 50 knots blowing from a direction 10°E of North at 23,000 feet.

Gustafson [28] suggests use of an expanded plotting model that includes more extensive temperature and wind data at lower levels for extrapolation to 300 mb. This, however, is a delicate task. As seen in chap. II, the vertical wind shear varies rapidly through the jet stream zone, and often is largest above 500 mb. An estimate of the vertical shear, thus, is a function of the proximity of the report to be extrapolated to the jet stream axis and the particular jet stream structure which, as also shown in chap. II (fig. 2.3) is variable along the jet axis. No report on the practical applicability of Gustafson's method has come to our attention, possibly because much time is consumed in plotting the additional low-level data and extrapolating to 300 mb.

Extrapolation of contour height. — When a radiosonde observation fails to reach the 300-mb level, we can employ several techniques in securing an extrapolation. Two of these techniques are statistical. The first method is based on the fact that a very high correlation exists between the temperature at 500 mb and the thickness of the layer 500-300 mb [49]. If the sounding reaches 500 mb, this correlation can be utilized to compute the 300-mb contour height.

A second approach has been proposed by Riehl and

La Seur [69] who have suggested a model based on a statistical investigation. This model permits an estimate of the temperature lapse rate between 700 mb and 300 mb, given 700-mb data and a general idea of the type of flow pattern (troughs, ridges) present in the area of the station to be extrapolated. Further discussion of the detailed techniques in extending low-level soundings to the vicinity of the tropopause is beyond the scope of this summary.

As an alternative, it may be preferable to employ synoptic techniques of extrapolation since the statistical correlations, though high, are not perfect. Such extrapolation, of course, is easiest when the top of the sounding is not far from 300 mb. In such cases, it is quickest to extend the upper portion of the sounding linearly to 300 mb or determine from surrounding stations what the 300-mb temperature should be and extrapolate with use of this temperature. The 300-mb height then is obtained with any of the devices for quick height computations now in use in many weather services.

Since the observed range of 300-mb temperatures is quite small, the above procedure will yield very good results in most cases. In the layer 400-300 mb, an error in estimating the mean temperature by 1°C produces an error of 28 feet at 300 mb. In the layer 500-300 mb, the corresponding error is 49 feet. An experienced analyst seldom will make errors much in excess of 2°C at 300 mb when extrapolating a sounding surrounded by other reports, and this, of course, only leads to a 1°C mean temperature error. If the sounding is isolated in space and time, the result may be much poorer. It is better, however, to attempt an extrapolation than to draw contours with a constant gradient through the area surrounding the station in question.

Extrapolation of soundings which do not reach 500 mb is much more difficult, and is likely to result in poor 300-mb heights except when the low-level flow and temperature field is undergoing little change. In such cases, the change of temperature at 500 mb and 300 mb from the preceding soundings can be estimated with fair accuracy. This statement does not hold in low latitudes nor in the middle latitudes in summer. When the flow pattern at the surface and 700 mb is changing rapidly, extrapolation should be attempted only at stations which are quite isolated, such as weather ships. Such extrapolation can be performed with methods of differential analysis by gradually building a pressure-temperature curve by layers. Here, a time section of past data may prove highly valuable.

The analysis of 300-mb charts could be further facilitated if soundings made with different types of instruments would be reduced to some common base. The value of such corrections would be greatest in the jet stream zone where otherwise a portion of the reports would have to be omitted entirely, thereby de-

creasing an already inadequate network. The analyst who makes corrections must, of course, keep track of instrumental developments and changes in the types of instruments employed which occur from time to time. He should also become thoroughly acquainted with all reporting stations and their peculiarities. At least, one station in the southern United States transmitted 300-mb heights during the autumn of 1951 that were too high compared to all surrounding stations. As an auxiliary means, a temperature analysis at 500 mb often helps detect soundings that are consistently too cold or too warm.

300-MB CONTOUR ANALYSIS

Analysis of the high-level contour field is the step subsequent to the plotting and extrapolation routine described. The previous 300-mb chart and a current 500-mb analysis should be available for constant reference.

At 300 mb, the basic principle of analysis is non-uniform spacing of contours. In order to achieve this, the analyst must draw precisely for all reliable stations and as closely as possible for all corrected and extrapolated reports. A moment's consideration will show that "smoothing" of the analysis eradicates the very features that one desires to find, i.e. variations in the strength of the winds.

The following contour analysis procedure is suggested:

(1) Begin the analysis where data are most dense.

(2) At first, sketch a contour passing through the center of the zone of dense data coverage.

(3) Sketch adjoining contours at 400-foot intervals. The analyst may carry these contours immediately to the limits of the data or he may prefer to analyze the map by sections. The latter procedure usually yields better results.

(4) Returning to the center of the map, enter the adjoining 200-foot contours and at the same time correct the previously drawn contours where necessary. Continue the procedure over the whole field. This step yields the final contour configuration.

(5) Make a finished product from the sketched map and enter trough lines with solid orange lines and ridge lines with dashed orange lines. The analyst should compare these lines with those at lower levels to make sure that a reasonable vertical slope is indicated. It is extremely rare that a 300-mb trough line is situated downstream from the 500-mb or 700-mb trough line.

Throughout the contour analysis the question occurs as to what extent the wind data should be used as an analysis aid by assuming simple dynamical relations

between the fields of mass and motion. These relations, as given by the geostrophic and gradient wind equations, generally will give good results except near the jet stream center where the nongeostrophic wind components may be very large. This will be discussed later in the chapter. Normally, especially over the oceans, the analyst has no choice but to draw the contours parallel to the observed winds and space them in accordance with the geostrophic or gradient wind scales. Wherever the 300-mb height data suffice for a unique analysis, contours should be drawn without reference to the observed wind vectors. As yet, this is possible only on some days and in limited areas.

The additional comments listed below may prove helpful:

(1) As stated earlier, corrections should be applied to reconcile Weather Bureau and military radiosonde data over the United States. If this is not done, the analyst should use the Weather Bureau data exclusively. If all reports are drawn for without any corrections, a very complicated wind pattern containing entirely fictitious jet streams invariably results.

(2) As noted above, analysis by regions tends to improve the result. For instance, in case of an analysis extending from lat. 20° to the pole and from the eastern Pacific to the central Atlantic, we recommend the following division: (a) United States and southern Canada; (b) Atlantic Ocean; (c) Pacific Ocean; (d) arctic zone; and (e) subtropical zone.

(3) Continuity in placing troughs, ridges, closed centers, and axes of maximum contour concentration increases in importance as data becomes more scarce. The same is true for the use of lower charts as an aid in the 300-mb analysis.

(4) Especially over the oceans, reference to surface charts can prove very helpful. As seen in the earlier chapters, cyclones tend to develop under jet streams and move in the direction of the upper current. Where the surface chart reveals a cyclone family, the analyst should concentrate his 300-mb contours at least qualitatively. The storm tracks indicate the direction of the contours.

(5) In areas of sparse data, one should take care not to draw with the geostrophic approximation in mind when the contour curvature is large. This will result in excessive contour packing in ridges, and gradients that are too weak in troughs. It is well to remember that for a given gradient wind speed the contour spacing is much wider in ridges than in troughs.

ANALYSIS OF THE FIELD OF WIND DIRECTION

As just stated, in areas of deficient data, the analyst must draw the contours parallel to the observed wind directions. Herewith, the problems of contour and streamline analysis become identical.

In areas of plentiful data, separate construction of contour and streamline fields reveals that appreciable departures of the streamline from the contour direction do occur in and near jet stream cores [73]. These departures mainly depend on the rate with which the wind speed varies along the jet stream axis. As is well known, air flows toward lower pressure while accelerating and toward higher pressure while decelerating. Thus, the streamline amplitude may be less or more than the contour amplitude in the area of a jet maximum or minimum which is displaced downstream at a speed less than that of the winds, which is the usual situation. Relative to the trough-ridge patterns, we can state that:

(1) When velocity maxima are situated in ridges and velocity minima in troughs, the streamline amplitude exceeds the contour amplitude.

(2) When velocity minima are situated in ridges and velocity maxima in troughs, the streamline amplitude is less than the contour amplitude.

(3) When the wind speed is quasi-uniform over an extended portion of the jet stream axis passing through the trough-ridge pattern, contours and streamlines will be nearly parallel.

The analyst may allow qualitatively for these rules after the isotach analysis is completed, remembering, however, that the angle between streamlines and contours is not likely to exceed 20° over a large portion of the jet axis.

Large differences between streamline and contour direction also will be found along the axis in sharp troughs and ridges where it is difficult for the air to make the sharp bends prescribed by the contour field for balanced flow.

ANALYSIS OF THE FIELD OF WIND SPEED

Prior to computing the wind speeds and performing the 300-mb isotach analysis, some preliminary steps are necessary to ensure maximum accuracy:

(1) The analyst should prepare a sketch of the 30,000-ft isotach pattern for the intermediate wind reporting period (0900Z or 2100Z) to the extent that the data permit. This will help to provide continuity in the analysis. It is not considered advisable, however, to enter winds which are six hours old on the current chart.

(2) As already stated, a 500-mb analysis should pre-

cede the 300-mb analysis. Because of the larger number of station wind reports, flight, and radiosonde data at this level compared to those in the high troposphere, this analysis can be made with considerable accuracy. It furnishes useful indications concerning the location of jet axes and speed maxima along these axes. In regions without wind reports, the same computational procedure should be followed as outlined below for 300 mb.

(3) Another tool, valuable for locating jet axes and maxima along the axes, is the temperature analysis at 200 mb. Following chap. II, a jet axis with strongest winds below 200 mb usually will be situated parallel to the 200-mb isotherms and located below the zone of isotherm concentration, with cold air to the right and warm air to the left of the axis looking downstream. Exceptions occur occasionally, indicating a basic rearrangement of the upper flow. In most situations, however, again especially over the oceans, a combination of 500-mb wind analysis and 200-mb isotherm analysis will locate the position of the 300-mb jet axis with sufficient precision.

(4) The isotach analysis should be performed on a transparent overlay, preferably with the latitude-longitude grid printed thereon. At first, the current jet axes at 500 mb are entered on this overlay as light ink lines and the past positions of jet maxima at 300 mb are denoted with crosses. Light dashed lines indicate the past positions of 300-mb jet axes which are not reflected at 500 mb. Such high-level jets generally are found, as described earlier, in summer and in the lower latitudes.

(5) Copy the reported wind speeds *in ink* on the overlay over the station circles. Given a wind speed of 50 knots, write 50 for the 300-mb wind, 50 for the 30,000-ft. wind, and 50, in red, for lower winds, adding the reporting level for winds at 25,000 feet and lower, such as 50(23′). Also mark the centers of highs and lows. Here the wind speed is zero.

(6) To the extent possible, mark the lower winds +, or —, or ±, depending on whether the 300-mb wind should be higher, lower, or the same as the reported wind. This step, entirely qualitative, is based on considerations of the temperature field and can only be executed if a temperature analysis at the level of the reported wind and a 300-mb temperature analysis are available. Although there are notable exceptions [34] good verification will, in general, be ob-

tained for the assumption that the wind increases with height when the reported temperatures on an isobaric surface drop from the right to left side of the current looking downstream; that the wind decreases upward if the temperature gradient is reversed; and, that the vertical wind shear is small when the reported temperatures are quasi-uniform. This statement implies that the sense of geostrophic and actual vertical wind shear have the same sign though not necessarily the same magnitude. In regions where the gradient wind equation is a good approximation, the foregoing suggestion can be put on a quantitative basis by utilizing diagrams giving the vertical shear of the gradient wind.

(7) Enter the past rate of motion of trough and ridge lines along the orange lines marking their axes. This step is optional in view of the suggestion in Appendix A.

Computation of wind speeds. — The most critical task in preparing the isotach analysis is the calculation of wind speeds from the contour field. According to present knowledge this can be done only with the geostrophic or gradient wind approximation. It is well, therefore, to recall briefly in what situations these approximations are most likely to be valid.

(1) The air flow should approach geostrophic balance where the contours are straight and equidistant over considerable areas. At inflection points, the geostropic wind is likely to be a poor approximation if contour curvature and direction change rapidly through the point.

(2) The air flow should approach gradient balance in regions of equidistant, curved contours where the contour curvature is uniform over a long distance or changes only slowly.

Gradient balance also should be approximated in areas of strongest and weakest wind along the jet axis.

It should be mentioned that doubt has been expressed at times whether the gradient wind actually is a better approximation to the observed flow than the geostrophic wind in regions with curvature. Research on this subject has not yet been concluded.

(3) Either approximation is apt to yield entirely incorrect results in the vicinity of sharp trough and ridge lines, in regions where the contour curvature changes rapidly downstream, and where the contours converge or diverge sharply. In all of these areas a balanced wind computation should never be attempted.

With this in mind, a suitable procedure for computing winds is as follows:

(1) Draw a number of lines *normal* to the 300-mb contours in all areas suitable for computation and not covered with actual wind reports. Since the height *gradient* is used in calculations, care is necessary to draw the lines *strictly normal* to the contours. The lines themselves may have arbitrary shapes. Whenever possible, they should be spaced with sufficient density so that along any contour either a reported or computed wind is available at least every 500 miles in open wavy-flow patterns.

(2) Compute geostrophic winds along each line for overlapping 400-ft. intervals. Place the computed wind values on the right side of the lines in the center of the 400-ft. intervals.

(3) With a transparent overlay such as shown in fig. 6.2, measure the radius of contour curvature and with the aid of nomograms obtain the gradient wind from the geostrophic wind and the radius of contour curvature at the appropriate latitude. Write the computed gradient winds on the left side of the lines in ink and now mark, also in ink, all geostrophic winds which are not subject to adjustment.

While any accustomed procedure in computing gradient winds may be followed, Appendix A contains diagrams (fig. 6.3) believed suitable for rapid calculation. These diagrams also permit inclusion of the rate of motion of upper troughs and ridges to obtain trajectory rather than contour (streamline) curvature.

(4) In general, it will be evident which winds are computed since these will be plotted along lines.
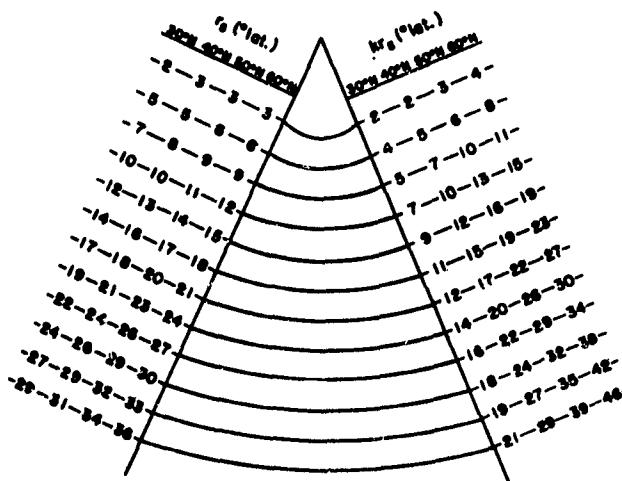

Fig. 6.2: Overlay for measuring radius of streamline curvature on polar stereographic projection, true at lat. 60°. Numbers on left give radius of curvature, r_s, in °lat. at indicated latitudes; numbers on right give r_s multiplied by latitude factor, k.

In cases where the distinction between reported and computed winds is not obvious, place a circle around the computed wind.

Isotach analysis. — The following procedure is recommended:

(1) As in the case of the contour analysis, it is advisable to treat each region of the map separately.

(2) A suitable isotach interval at 300 mb is 20 knots.

(3) Begin the analysis in an area with dense reports. Drawing of the 60-knot isotach at the start has proved advantageous as this wind speed is sufficiently low so that numerous reported winds will exist on most days.

(4) Draw the 40 and 20 knot isotachs and place the letter S (slow) in regions with wind speeds less than 20 knots.

(5) Analyze the high-speed band contained within the 60-knot isotach. In placing the centers of maximum wind note that these usually propagate downstream at moderate rates but occasionally remain nearly stationary for 24 hours. We have not encountered centers that retrograded. Erratic displacement of these centers should be checked for analysis errors. Place the letter J in the high-speed centers.

(6) Sketch the jet axis which in nearly all cases should be located above or slightly to the left of the 500-mb axis when the jet extends down to 500 mb. See also earlier comments.

(7) The isotach analysis must be interpolated through regions unsuitable for balanced wind computations and without reported winds. Only one other approach for computing winds in such areas is open. As noted in chaps. II and VII, a zone of zero absolute vorticity several hundred kilometers wide frequently, if not regularly, is situated on the right-hand margin of intense jets. Given the position of, say, the 60-knot isotach and the position of the jet axis from the completed part of the analysis, we can compute what the wind on the axis would be if the absolute vorticity is zero between the 60-knot isotach and the jet axis. A graphical solution of this problem and various instructions for computation are given in Appendix B.

The main problem at this time is to estimate correctly when the absolute vorticity will be zero. From past work, it is plausible to suggest that the vorticity implied by the isotach analysis should not be less than zero. Thus, the analyst should check the wind speed with aid of Appendix B whenever the isotachs are so

crowded on the right margin of the current that it is
suspected an absolute anti-cyclonic vortex has been
drawn. If the check bears this out, the central wind
value and the isotach spacing should be adjusted down-
ward to the case of zero vorticity.

It is more difficult to suggest precise rules as to
when the analyst should increase a central wind speed,
derived by other methods, to some high value obtained
with the zero vorticity method. In this case, the lower
wind speed computed by other methods automatically
prescribes that $\zeta_a > 0$ and as such is entirely possible,
but it is fairly certain that the vorticity is zero at least
over some distance to the right of intense jets and
maxima along the jet axis. The analyst should take
this into account. At this time, however, it must be left
to his judgment as to what constitutes a sufficiently
"intense" jet.

At this point, it is of advantage to take up several
qualitative considerations helpful in constructing iso-
tach patterns.

(1) High-speed isotachs are nearly parallel to the
     contours. Their shape generally is elliptical. At
     lower wind speeds, contours and isotachs may
     cross at large angles.

(2) As noted earlier, statement (a) should be modi-
     fied somewhat just upstream and downstream
     from jet centers. The jet axis and the isotachs

tend to cross toward lower contours upstream,
and toward high contours downstream from a
maximum.

(3) Frequently, it is necessary to reconcile com-
     puted and observed winds. In areas of low
     speeds, the observed winds should be accepted.
     In areas of high speeds, the observed winds also
     should be accepted if they are higher than the
     computed winds. In the reverse case, reliance
     should be placed on the reported wind only if
     taken with high-grade radio wind equipment.
     Otherwise, the reported wind speed is likely to
     be too low, and more weight should be given to
     the computed wind. A glance at the 500-mb
     chart and an estimate of the vertical shear from
     500 mb to 300 mb also may prove helpful. In
     general, this shear should not exceed 10 mps/km
   or about 80 knots between 500 mb and 300 mb.

Fig. 6.3: Gradient wind nomograms: (a) anticyclonic, (b) cyclonic [35]. See text for details of computing the gradient wind.

(4) Over the oceans, where the use of models is a necessity, the isotachs should be drawn to conform to the dynamical models of the upper wind structure (figs. 2.7, 2.8, 4.4) in regions of falling and rising surface pressure. Together with our earlier suggestion on the placing of jet axes relative to the surface map features, the analyst has a considerable body of models at his disposal that does not suffice to yield a precise analysis everywhere over the oceans but does permit the drawing of logical and orderly oceanic wind patterns aloft.

(5) The analyst may be requested to indicate the level of strongest wind. This information partly is given in the rawin transmissions. An additional aid is the temperature distribution, which can be used as described earlier for estimating the sense of the vertical wind shear. As long as the temperature decreases from right to left across the jet axis, the level of strongest wind lies above the level analyzed. In the reverse case, it lies at a lower elevation Thus, by inspection, the analyst can quickly decide whether the strongest wind is above or below 300 mb, above or below 200 mb, etc. He can also judge, from variations of temperature gradient along the jet axis (cf. chap. II) whether the core of the current is ascending or descending in space.

If very detailed information on the height of the jet core is desired, numerous cross-sections can be constructed. In general this is impractical from the operational point of view as much time is consumed when five or 10 sections are needed. We would suggest that it is much quicker to draw intermediate constant pressure charts, such as 250 mb. Then, the location of the core becomes restricted to a 50-mb interval, with good qualitative indications as to whether it is situated near the upper or lower end of this interval. This should suffice for most purposes.

We also believe that drawing of intermediate constant pressure charts, in general, is more satisfactory than to attempt tropopause charts. However, for a large weather center with ample personnel, the methods suggested by [1] may be helpful, especially, in view of the good relation found between the "predominant tropopause" and the level of maximum wind. However, the relation is not exact, though statistically good (most frequent height of jet axis is just below "predominant tropopause").

After completion of the isotach analysis, the map should be polished. Isotach patterns can be very pictorial and used to much greater advantage than contours in many operational tasks, as for instance in flight briefing.

(1) At first, draw the principal jet axis as a heavy purple line with arrows indicating the flow direction. Indicate secondary jets and jet "fingers" with dashed purple lines.

(2) Shade regions with wind speed less than 20 knots purple and regions with wind speed greater than 80 knots (at 500 mb, 60 knots) green. Intense jet centers may be emphasized by increasingly heavy shading toward the centers.

FORECASTING THE WIND FIELD

The prediction of the high-tropospheric wind field is a subject with a history of research and experience so brief that it is in a constant state of rapid development. As apparent from chaps. II-V, the jet stream is intimately connected with all physical variables operative in the atmosphere and, in the future, progress will depend greatly on the discovery and solidification of the dynamical laws that govern the formation and life cycle of individual and average jet streams. As seen in chap. VII, it is C.-G. Rossby, in particular, who has attempted to find such laws.

We believe it fallacious to say that "the jet stream appears to be no more than a local intensification of the thermal gradient in the upper air and there is no reason to expect that its forecasting should present any greater difficulty to the upper-air forecaster than that of forecasting the thermal gradients at levels below that of the jet stream."[7] As will be stressed throughout chap. VII, dynamical means are requisite to make and destroy temperature gradients through lateral concentration and dispersion by upward and downward motion. The forecaster's main consideration regarding the temperature field is whether an initial temperature gradient exists that can be concentrated. We would suggest that motion in a rotating fluid has a basic tendency to break down into narrow jets but that attempts to form such jets are successful only in the areas where, and to the extent that, a simultaneous concentration of temperature gradients can be accomplished, so that in the end quasi-geostrophic balance is attained.

At the time of this writing, kinematical jet stream prognosis may be made with or without reference to the other factors. For periods in excess of 24 hours, detailed reference to all large-scale developments is necessary. For 24-hour periods and less, several semi-quantitative techniques have been offered. Predictions over 24 hours or more are discussed in [72] and the reader is referred to this publication.

The forecaster should be aware of the limit: of accuracy of his prognosis. If a mean de ation of 20°

---

[7] *Quart. J. Roy. Meteor. Soc.*, 1952, **78**, p. 451.

in wind direction and of 20 per cent in wind speed is achieved, we would regard that as good, considering the data situation and the prognostic tools available. Certainly the isotach analysis, itself, is not likely to be more than 90 per cent correct in regions with good observations and substantially less where good data are scarce. In view of this, the accuracy of wind speed

predictions even for only a few hours is not likely to exceed the limits of accuracy cited above. It may be less as the effect of jet microstructure, not determinable from ordinary synoptic networks, becomes important. The users of jet stream prognoses should at all times be kept fully aware of the limitations of the forecast so that excessive expectations will not be encouraged.

2. Appendix A. — Gradient Wind Nomograms

The gradient wind nomograms shown in fig. 6.3 are not an integral part of the jet stream survey. They are included because they are considered compact and convenient graphs for rapid wind calculation. It is suggested that the graphs be mounted on a stiff cardboard to facilitate use. Details of their construction will be found in [35]. Here we take up only the mechanical routine of wind calculation.

Gradient winds are more difficult to compute than geostrophic winds because the former involve more variables. These variables are: (a) The geostrophic wind, (b) the latitude, and (c) the radius of curvature of the trajectory of the air particles.

The first two items are readily measured on charts, but not the trajectory curvature. Moreover, this curvature may be cyclonic or anticyclonic, necessitating separate graphs. The trajectory curvature is identical with the streamline (contour) curvature if the atmospheric flow patterns remain stationary. Otherwise, the two curvatures differ. This difference can be accounted for in practical computation work by determining the movement of troughs and ridges. The short-wave troughs and ridges aloft usually propagate downstream and at a mean rate not far from 20 knots. This rate has been incorporated in the nomograms. It will be our procedure to compute at first the gradient wind assuming that the synoptic systems aloft propagate downstream at 20 knots. Then we shall adjust the result obtained for other rates of trough and ridge movements.

COMPUTATION OF GRADIENT WIND

Rate of downstream propagation of systems. — It is possible to combine graphically two of the variables: latitude and radius of curvature. The combined variable, called kr_s, (k is a dimensionless function of latitude) [35] appears as the abscissa in fig. 6.3 and its value in degrees of latitude can be read directly by superimposing fig. 6.2 on the contours. The ordinate of fig. 6.3 is the geostrophic wind (v_g). Note that in the anticyclonic case, a limit exists beyond which the gradient wind cannot be computed.

Procedure. — Enter fig. 6.3 with the value of kr_s and v_g as measured from the analysis, and read the gradient wind as given by solid curved lines at intersection of kr_s and v_g lines.

Example. — Given $kr_s=20°$ lat., and $v_g=100$ knots. If the curvature is cyclonic, use fig. 6.3b and obtain a gradient wind of 87 knots. If the curvature is anticyclonic, use fig. 6.3a and obtain a gradient wind of 140 knots.

In general, no corrections for other rates of motion of the upper-air systems are necessary, since such corrections amount to less than 10 per cent of the values obtained by the above method. The shaded area of fig. 6.3a and the area to the left of the short-dashed curve in fig. 6.3b indicate where the correction is likely to be important. We note that in our example the gradient wind value for cyclonic curvature lies outside this area but that it lies inside for anticyclonic curvature.

Adjustment for rate of motion of systems other than 20 knots. — The rate of motion of troughs and ridges aloft can have a marked influence on the radius of trajectory of air particles. Consider, for instance, a particle on the ridge line moving from the west at 40 knots. If the ridge travels eastward at 40 knots, the particle will stay on the ridge line. The direction of motion of the particle continues to be westerly and it moves eastward with zero trajectory curvature, i.e., as a geostrophic wind if the flow is balanced. If the ridge travels at 20 knots, the particle will move through it from west to east on a clockwise curved path, and the gradient wind will exceed the geostrophic. If the ridge moves at 60 knots, it will overtake the particle which travels through the ridge actually on a path with counter-clockwise curvature. In this case, the gradient wind in the ridge is less than the geostrophic. Similar reasoning holds for trough lines.

Here we shall consider the rate of motion of the systems (c_s, + in direction of streamline flow, — in opposite direction) as given by the 12- or 24-hour past displacement of trough and ridge lines, irrespective of direction of motion. This is not an exact pro-

cedure and requires theoretical and computational justification. The latter may be found in [35].

Procedure. — Read Δv value at intersection of kr_s and v_g lines as given by slanting dashed lines in fig. 6.3. In insert table read value of α opposite appropriate value of c_s. Multiply Δv by a and add to or subtract from value obtained from uncorrected gradient wind (i.e. where system movement is 20 knots), depending on sign of a.

Examples. — (a) To correct gradient winds of previous examples if $c_s=60$ knots. Cyclonic case: $\Delta v=3$, $a = +2$, $a\Delta v = 6$ knots. Gradient wind $= 87 + 6 = 93$ knots. Anticyclonic case: $\Delta v = 20$, $a = -2$, $a\Delta v = -40$ knots. Gradient wind $= 140 - 40 = 100$ knots. (b) To correct gradient winds of previous example if $c_s = -20$ knots. Cyclonic case: $\Delta v = 3$, a

$= -2$, $a\Delta v = -6$ knots. Gradient wind $= 87 - 6 = 81$ knots. Anticyclonic case: $\Delta v = 20$, $a = +2$, $a\Delta v = + 40$ knots. Gradient wind $= 140 + 40 = 180$ knots.

It is well to keep in mind that the use of Δv to aid in calculating gradient speeds, when $c_s \neq 20$ knots, results in a small error in the gradient speed, which does not exceed 10 per cent, as long as the computation is carried out in the nonshaded area of fig. 6.3 and $-20 \leq c_s \leq 60$ knots. The only exception is that the gradient wind solution is exact for system speeds of 0 and 20 knots.

It is also to be noted that the anticyclonic gradient wind especially is very sensitive to trough and ridge speeds if kr_s is small. Much care in analy. is and computation is needed to avoid large errors.

3. Appendix B. — Estimating Wind Speeds in the Jet Stream

As shown by physical and statistical studies (cf. chaps. II, VII), the absolute vorticity is zero or close to zero on isentropic surfaces within a few hundred kilometers to the right of pronounced jet stream centers. Near the level of strongest wind (e.g., 300 mb in middle latitudes in winter) isobaric and isentropic surfaces coincide closely, and we can make the following computation on constant pressure surfaces.

In a region of zero absolute vorticity:

$$- \frac{\Delta v}{\Delta n} + \frac{v}{r_s} + f = 0. \qquad (1)$$

Here v is the wind speed, n the axis normal to the streamlines taken positive to the left of the flow (fig. 6.4), f the Coriolis parameter, and r_s the radius of streamline curvature. The above equation can be solved formally as an exponential function, but graphical representation of the exact solution is complicated, and calculation requires more time than is available in forecast offices or warranted by the approximate character of the whole computation. Instead, the following route of evaluation is suggested.

The interval Δn over which zero absolute vorticity exists rarely exceeds 5° lat. as far as is known. Thus, we may treat the values of f and r_s in the center of the interval Δn as mean values over the whole interval.

Then:

$$\Delta v = \left(\frac{v}{r_s} + f \right) \Delta n, \qquad (2)$$

Further we can say that:

$$\Delta v = \Delta v_1 + \Delta v_2, \text{ where } \begin{cases} \Delta v_1 = f \Delta n, \\ \Delta v_2 = \frac{v}{r_s} \Delta n. \end{cases} \qquad (3)$$

If there is a definite jet core, Δv_1 will always be present, but the existence of Δv_2 depends on the presence of streamline curvature. It will be our procedure to compute at first Δv_1 and consider Δv_2 as a correction factor to be applied to the wind value attained on the basis of shear alone.

On this basis, figs. 6.5-6 solve the problem of computing the wind at the jet center, given the position of the jet stream axis and an observed or computed wind some distance to the right of this axis looking downstream.

Fig. 6.5 is an overlay for the polar stereographic projection. This figure should be transparent and should, of course, be constructed on the same scale as that of the base map used. Values of Δv_1 are entered in knots at 20 knot intervals between $\Delta n = 1°$ lat. and $5°$ lat. (slanting curves). Tick marks indicate the intermediate Δn values at intervals of 1° lat.

Set the base line (bottom edge) on the point at which wind report exists at appropriate latitude, orient latitude line normal to upper flow (contours), and read Δv_1 at intersection of latitude line and jet axis.

Example. — Given $\Delta n = 3°$ lat., then at lat. 40°, $\Delta v_1 = 60$ knots. If, as in fig. 6.5 the wind speed at the starting point is 50 knots, then the speed at the jet center is 110 knots and the isotachs are spaced as on the 40° lat. line of fig. 6.5.

In the case of straight flow, the computation is complete. If curvature is present, we now adjust for it utilizing fig. 6.6. For construction of the diagram, we note that the definition $\Delta v_2 = \frac{v\Delta n}{r_s}$ may also be written $\frac{\Delta v_2}{v} = \frac{\Delta n}{r_s}$ so that the ratio $(\Delta n/r_s)$ can
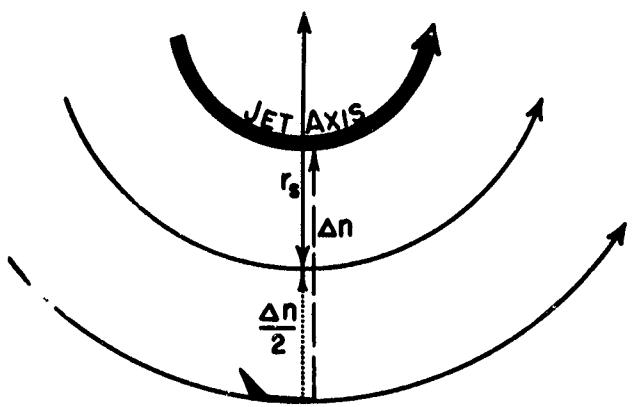
FIG. 6.4: Schematic illustration of situation allowing use of the vorticity equation for purpose of computing speed of jet axis. Δn is the interval, not greater than 5° lat., between the reported speed and the jet axis.
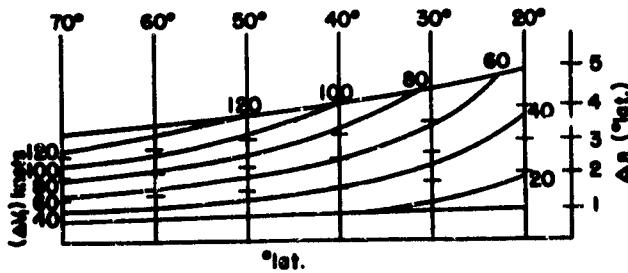

FIG. 6.5: Overlay for obtaining isotach gradient in the case of straight flow, assuming $\varsigma_a = 0$. (Polar stereographic projection, true at lat. 60°. Scale to be adjusted to base map.

be considered as a percentage correction to be applied to v, positive for cyclonic and negative for anticyclonic curvature. v is the mean speed over the distance Δn, actually an unknown quantity, since so far we have only computed the speed distribution for straight flow. For anticyclonic flow, the method of successive

approximations is recommended for evaluation. For cyclonic flow, it suffices to apply fig. 6.6 only once; namely, to the wind value at the center obtained with fig. 6.6.

Example for cyclonic flow. — Continuing our previous example, if $r_s = 1000$ km, $(\Delta n/r_s)$ is 33 per cent and Δv_2 is 35 knots for the 110 knot wind computed before. The central wind value is 145 knots.
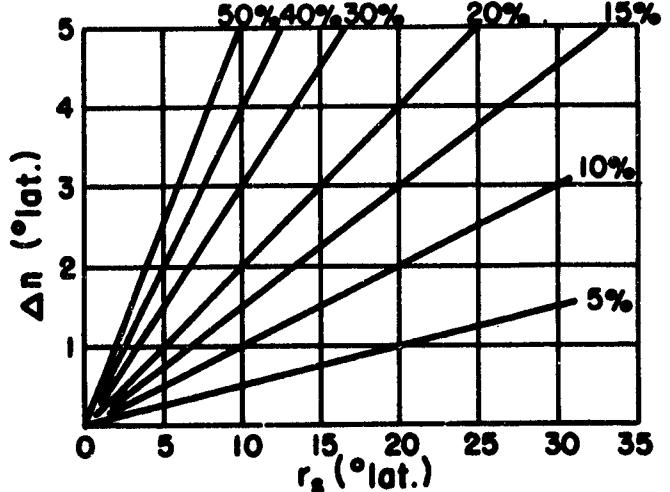
FIG. 6.6: Overlay for obtaining percentage correction to jet axis speed due to curvature of flow pattern, assuming $\varsigma_a = 0$.

Example for anticyclonic flow. — $(\Delta n/r_s)$ is the same as for cyclonic flow, namely, 33 per cent. The mean wind speed over Δn, excluding curvature, is $(110 + 50)/2 = 80$ knots. For a first approximation, Δv_2 is 33 per cent of 80 knots or 26 knots. The central wind is $110 - 26 = 84$ knots.

We now repeat the above procedure, but using 84 knots instead of 110 knots for the central wind. The mean wind speed over Δn now is $(50 + 84)/2 = 67$ knots. For the second approximation, Δv_2 is 33 per cent of 67 knots or 22 knots. The central wind is $110 - 22 = 88$ knots.

In rare cases when the curvature changes greatly through the interval Δn, it is necessary to compute the central wind in two steps.

CHAPTER VII. DYNAMIC PRINCIPLES RELATING TO JET STREAM FORMATION AND MAINTENANCE

1. Formulation of the Problem

The circulation in the middle lat   s is an integral part of the general atmospheric c. .lation, and the factors which are operative in driving it cannot be isolated from those which are responsible for the planetary circulation. Therefore, a solution to the problem of the formation of the jet stream must be sought within the framework of the laws governing the general circulation.

The traditional model of the general circulation, the cornerstone of which was placed by Hadley [29], does not provide such a framework. This model proposes steady meridional circulations to redistribute the different amounts of insolation reaching the earth's surface at different latitudes. Thermally induced ascent of air in the equatorial region leads to removal of air poleward at higher levels and a compensating flow toward the equator in the lower layers. Hadley was aware that his scheme would have to be confined to the regions between the equator and latitudes 30°N and 30°S, since both direct and indirect evidence existed for strong descending air motion within the lower half of the troposphere in the region of the horse latitudes. Later, as observations became more abundant, Hadley's picture was extended to include three meridional circulation cells. The "tradewind" and the "polar front" cells were assumed to be "direct," driven by the heat and cold sources of the atmosphere, while the middle latitude cell was visualized as "reverse," driven by frictional interaction with the adjoining direct cells [8, 80]. Two typical representations of this model are given in fig. 7.1. The difficulty in reconciling it with upper air observations at all latitudes has been discussed in detail by Rossby [84]. Here it suffices to say that the model is based on the principle of conservation of absolute angular momentum which requires, among other things, that the low-level westerlies of the middle latitudes decrease with height and ultimately revert to easterly winds aloft. The occurrence of the jet stream is, therefore, at variance with the re-

quirements of the momentum principle as applied in the three-cell theory. Its discovery was one of the important factors which pointed to the necessity of abandoning conservation of absolute angular momentum of individual air particles as the leading dynamic principle underlying the general circulation. A satisfactory dynamical treatment of the general circulation must


a

b
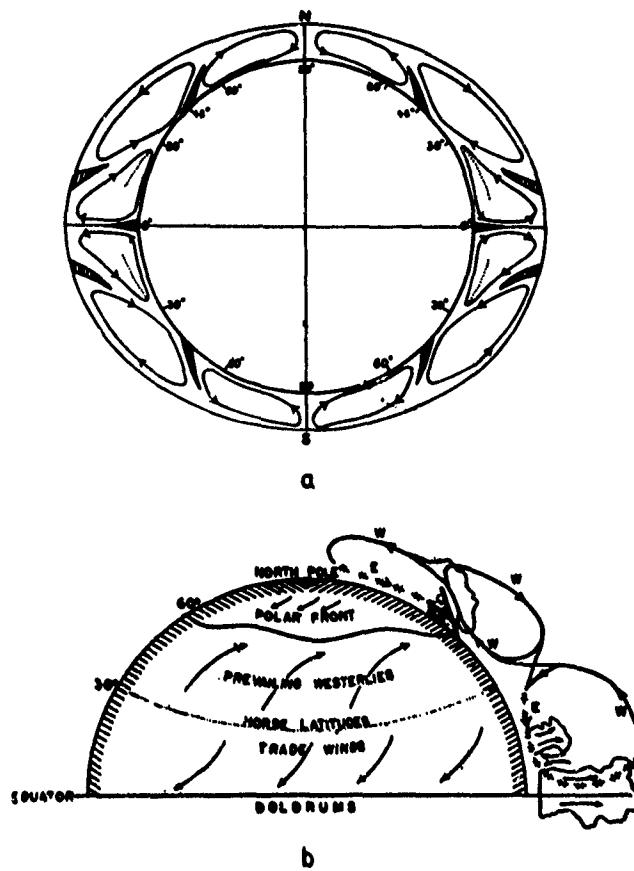
FIG. 7.1: Schematic representations of the meridional circulation: (a) according to Bergeron [8]; (b) according to Rossby [80].

6

account for the following important features:

(1) The maintenance of the upper west winds and the concentration of a large fraction of the total kinetic energy of the atmosphere in the jet stream belt.

(2) The concentration of the bulk of the latitudinal temperature gradient in a narrow zone approximately coincident with the west wind belt, in

spite of the relatively continuous distribution of radiative heat and cold sources in the atmosphere.

(3) The occurrence of a frontal zone below the jet stream.

A clue in the search for appropriate dynamical laws could be found in studies of the Gulf Stream system made during the 1930's.

2. The Similarity Between the Jet Stream and Ocean Currents

Prior to the large-scale exploration of the upper air (after 1945), a duality existed in the approach of investigators to the problems of air and ocean currents, since no marked similarity between the structure of low-level atmospheric currents and major ocean currents could be detected. The discovery of the jet stream, however, soon brought about the realization that there were significant similarities.

It has long been recognized that in the oceans the concentration of the horizontal density gradient in a narrow zone is a dynamic consequence of the motion and must, therefore, coincide with the current [77, 102]. This is illustrated by fig. 7.2 [102] which shows the relationship between temperature distribution and current speed in the Gulf Stream. We see that the measurable current is confined to a narrow zone, and its highest speeds coincide with the strongest slope of the thermocline. Comparison with fig. 2.1 clearly reveals the analogous correspondence between the horizontal potential temperature gradient and wind speed in the jet stream.

Spurred by this analogy, studies were initiated with a view to discovering how far it could be extended. Soon other similarities emerged of which the following are considered of utmost significance [22, 23, 37]:

(1) Neither the Gulf Stream nor the jet stream shows any appreciable spread along the direction of flow for considerable distances.

(2) The Gulf Stream meanders and sometimes develops "cut-off" centers in a manner very similar to the jet stream.

(3) Exceedingly large shear values, comparable with those observed in the jet stream regions, also occur in a narrow zone on either side of the current maximum in the Gulf Stream.

(4) The multiple structure of the jet stream has a counterpart in the Gulf Stream which, at least at times, is composed of narrow currents of great intensity separated by weak countercurrents.

The establishment of such remarkable similarity between these apparently unrelated current systems is significant in that it offers important directives toward a satisfactory solution of the problems of atmospheric and oceanic circulation. It provides, through comparison of these systems, indications concerning the nature of the essential processes underlying their development and behavior, and thus helps guide investigators toward pertinent and fruitful channels.

The similarity also eliminates from consideration factors which otherwise may be thought to have a fun-
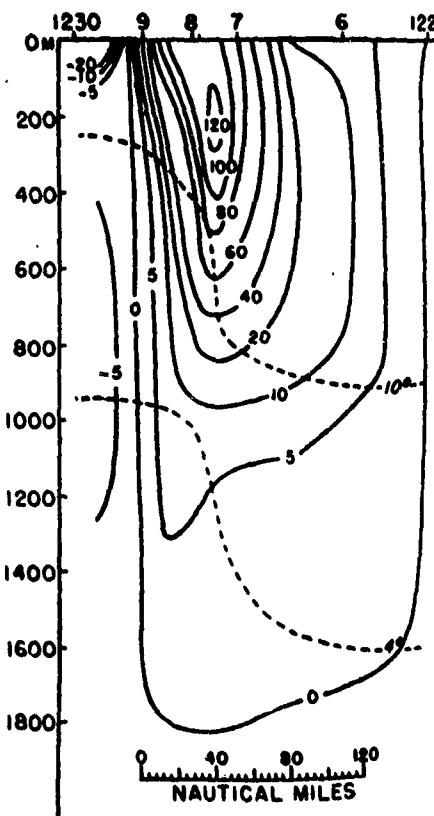

Fig. 7.2: Relationship between the distribution of temperature and current in Gulf Stream off Chesapeake Bay. Isotherms are given by broken curves, current speed (cm/sec) by full lines [102].

damental bearing on the jet stream problem. Among these, we list the following as being of particular importance:

(1) The linear dimensions of the currents of ocean and atmosphere differ by one order of magnitude. This indicates that the scale of motion is of limited importance only and that a degree of "dynamic similarity" exists between these current systems of different linear scale.

(2) The atmosphere is compressible whereas the ocean is nearly incompressible. This eliminates compressibility as a major variable. It also casts added doubts on explanations of atmospheric currents based on considerations of differential heating, since compressibility enters vitally into these explanations.

(3) The mechanisms by which the energy necessary for the development and maintenance of currents is introduced into ocean and atmosphere are very different. For instance, the oceans do not receive latent heat of condensation. This renders untenable hypotheses about the formation of atmospheric currents which depend entirely on the mode of energy infusion. It is, therefore, permissible to attempt to explain the existence of currents from dynamical principles alone and relegate energy consideration to a secondary role.

The following sections will reveal the extent to which the *structural similarities* of atmospheric and oceanic currents have proved useful in the treatment of the general atmospheric circulation.

3. Lateral Mixing

THE MEAN ZONAL WIND DISTRIBUTION

Rossby [82] was among the first to attempt to find a solution of the problem of the general circulation in the light of the upper-air observations which became available during and after World War II. He proposed that since the ratio of the horizontal to the vertical extent of the troposphere is 1000:1, it might, to a first approximation, be compared to a thin spherical shell. The distribution of the mean zonal motion may be a consequence of horizontal mixing processes effected by large-scale eddies.

Types of atmospheric eddies. — In the higher latitudes, air particles accelerated in the direction of the pressure gradient are not likely to proceed in this direction over long distances. The Coriolis force, strong in these latitudes, quickly deflects the path of these particles to the right so that soon they merely execute an inertia oscillation about a mean latitude. This expresses the tendency of the air to approach geostrophic balance. It follows that air is not likely to move on closed trajectories in broadscale meridional cells outside the tropics, but is more apt to meander as an alternating north and south current around a latitude circle and to appear on maps in the form of highs, lows, troughs, and ridges. These systems are predominantly horizontal eddies which rotate about axes normal to the earth's surface. In an analysis of the circulation of the middle latitude cell, Rossby [78] found that the mean free path of the lateral mixing process required to drive the upper westerlies had the dimen-

sion of the migratory cyclones and anticyclones of middle latitudes. This agrees with a suggestion by A. Defant [20] that these disturbances may be considered as the large-scale turbulence elements of the atmosphere. Any important exchange of mass and physical properties of the atmosphere outside the tropics is, therefore, most readily accomplished through their agency. We refer to such exchange as lateral mixing. Its effect should be most fully developed well above the layer of friction near the ground.

If it is our objective to find principles governing the establishment of the observed average west wind profiles aloft as described in chap. III, we can utilize the mixing mechanism just outlined, provided we can specify conservative properties which the atmosphere exchanges over distances corresponding to the dimension of synoptic disturbances. We can then take the position that mixing is a basic physical characteristic of our medium and we wish to explore its behavior, given arbitrary initial conditions of the variables that are to be exchanged. This approach has the merit of not endowing the assumptions with the result, a procedure at times found in the literature.

As stated earlier, we wish to discuss the concentration of the upper westerlies into a narrow current which coincides with a similarly narrow zone in which the meridional temperature gradient is concentrated. If we say, for reasons outlined above, that in the mean the geostrophic wind equation represents a good approximation of actual conditions, as for instance demonstrated empirically for the Far East by Yeh

[112] (cf. chap. III), then the two parts of our problem become related through the thermal wind equation. By this, we do not wish to imply that "the thermal. wind equation explains the high winds aloft," — a quotation sometimes heard. Such an interpretation assumes the temperature concentration *a priori* — a viewpoint with which it is difficult to concur after comparing charts showing climatic and synoptic temperature gradients. Unless we wish to sidestep the issue, we must find means that will tend to concentrate the high winds and the temperature gradient *simultaneously* in a narrow zone. The mixing process may, provide such a means.

Heat Exchange. — We know that over the time interval for the mixing here in question (approximately 24 hours), the potential temperature is nearly conserved in the middle and upper troposphere in high latitudes in winter. *We shall, therefore, state as our first proposition the conservation of potential temperature.*

If, initially, there is present a poleward temperature gradient, produced by radiation, regions within the zone of the mixing elements which have southerly winds will, in the mean, be a little warmer than those with northerly winds. As a result, the south winds import more heat across any latitude circle toward the pole than the north winds export. If this mixing extends all the way from pole to equator, the temperature must of necessity increase at the pole, and the meridional temperature gradient diminish. If the mixing ceases more or less abruptly south of a given latitude, the whole temperature gradient will become concentrated near the equatorward boundary of the mixing zone. For the present, we shall assume the existence of such a limit and later offer suggestions as to why it should exist and where.

We have seen qualitatively that if, initially, a poleward directed temperature gradient exists, mixing by horizontal eddies in an atmosphere in which the potential temperature is conserved will produce the observed mean latitudinal temperature profiles. Over a wide latitudinal belt, the potential temperature becomes nearly uniform and its gradient becomes concentrated in a narrow zone at the equatorward limit of the mixing elements. We now turn to the field of motion.

Conservation of absolute vorticity. — In several fundamental papers Rossby [78, 79, 81] has proposed
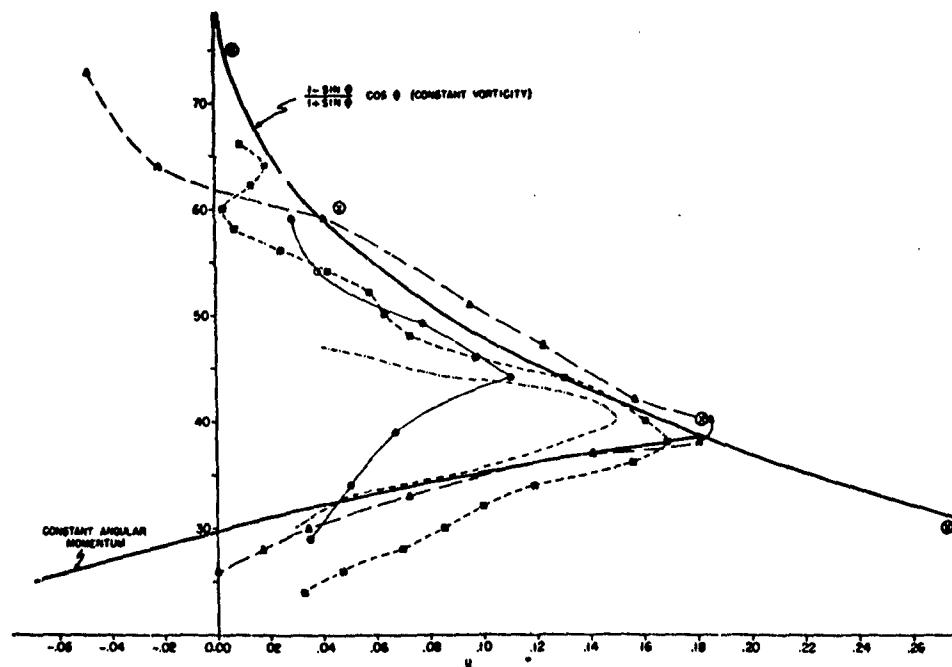

FIG. 7.3: Comparison between theoretical wind profiles obtained from vorticity and momentum considerations (heavy lines) and some observed geostrophic wind profiles at the tropopause level (thin lines). Large circles represent solar rotation data. All velocities are expressed in percent of the linear equatorial velocity of the planet [102].

that the potential vorticity or, in case of horizontal motion, the absolute vorticity is a basic property that columns of air tend to conserve for some time. Indeed, his theory of the long waves in the atmosphere originated from this concept. If we plot the wind speed distribution against latitude near the level of highest west wind, we find that the curves north of the jet stream center (fig. 7.3) closely follow the theoretical wind profile which we would observe if the absolute vorticity was constant. It is true that in individual synoptic cases a large vorticity maximum exists just to the left of the jet axis (fig. 2.13) and that the vorticity of the moving air changes rapidly in this zone (chap. IV). In the mean, however, fig. 7.3 holds and we have therewith the suggestion that the absolute vorticity can be the property of the motion that is conserved during the mixing process leading to jet stream formation [104]. The hypothesis of the conservation of absolute vorticity receives added credence from the fact that the observed zonal circulation on the sun follows a constant vorticity profile to about 30° heliographic latitude.

In discussing the equalization of vorticity as well as that of heat, we must remember that mixing can redistribute vorticity but cannot change the total amount present. Following Stokes' theorem, the circulation around any curve is equal to the vorticity in the area enclosed by the curve. Therefore, in our case, the wind speed must remain constant at the latitude which marks the equatorial limit of the mixing zone. Further, in the absence of sources and sinks, the total absolute angular momentum of the air must remain constant in accordance with basic principles of physics. With these two points in mind, let us turn to fig. 7.4 which illustrates how a jet stream may be developed as a result of lateral mixing, subject to the constraints of the above dynamical principles. We see that the total absolute angular momentum is conserved. North of the jet stream center the absolute vorticity is constant and in this case has the value of the Coriolis parameter at lat. 70°, since at this latitude the lateral shear of the wind is zero. The limiting latitude of the mixing zone is near lat. 33°. Here the wind remains constant and therewith the total vorticity north of 33° also remains constant.

One quantity that does not remain constant during the transition from the initial to the final wind profile of fig. 7.4 is the total kinetic energy. This quantity increases, specifying the need for an energy source. Criticism levelled at times against the whole approach discussed here has stressed that if the mixing theory holds, then, contrary to classical turbulence theory, energy must flow from the disturbances to the basic current. This objection has become obsolete since according to modern turbulence concepts, energy can be

transferred in the required sense, especially as this energy is not mechanical but is gained mainly through release of latent heat of condensation and sinking of cold domes in the disturbances. As stressed at the outset of this chapter, we need not be concerned with the precise cycle through which the transformation of energy forms is accomplished.
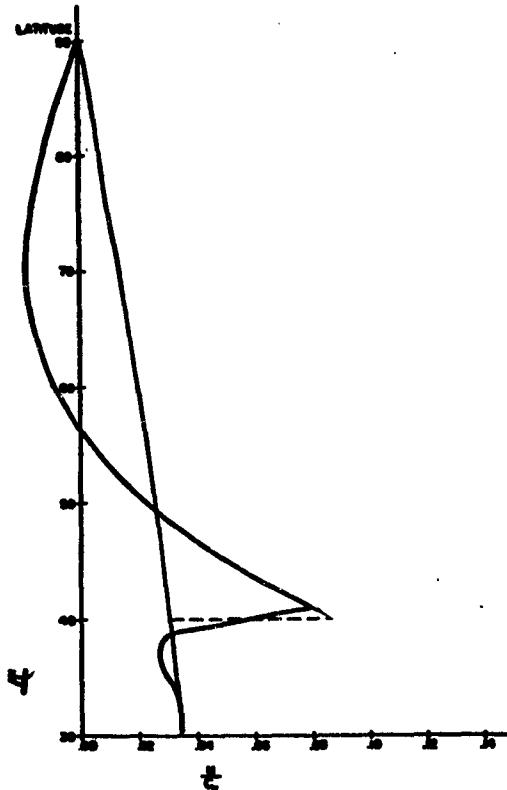

Fig. 7.4: Theoretical diagram illustrating the effect of lateral mixing within a polar cap, extending to lat. 33°, in producing jets. The initial wind distribution is given by the thin straight line and is assumed to correspond to a constant angular velocity. The final wind distribution is given by the heavy line. The total angular momentum is the same for both profiles. Mixing equalizes the vertical vorticity poleward of lat. 40° where the wind speed reaches a maximum. All speeds are expressed in per cent of the linear equatorial velocity of the earth [102].

The major problem still to be resolved is the fact that the absolute vorticity is not constant throughout the entire mixing zone of fig. 7.4 but only north of the jet center. On its south side, to the limit of the mixing zone, the vorticity is very small — often zero. The value of the vorticity north of the jet center does not equal the mean for the whole mixing zone but is substantially higher. In fig. 7.4, as already noted, it has the value of the Coriolis parameter at 70°. Thus, if lateral mixing is to be accepted as the process that accounts for the observed wind distribution, it must not only be capable of equalizing the vorticity over a wide belt of latitude but also of effecting a vorticity flux from low to high latitudes against the mean vorticity gradient.

Such a flux, while not envisioned in classical turbulence theory is nevertheless possible as has been shown with special clarity by Priestley and Swinbank [65] for the vertical heat flux.

Much theoretical work has been done in recent years on the flow of vorticity as accomplished by large-scale eddies. Here, we merely refer to two papers by Kuo [41, 42]. From a descriptive standpoint, we may note that a northward transfer of vorticity across a latitude circle is possible, provided that on this circle the relative vorticity of the southerly winds is more cyclonic than that of the northerly winds. If this picture holds in the mean, it becomes requisite that there is a vorticity source in low latitudes and a sink in high latitudes, the opposite of what one might assume *a priori*. Yeh [113], however, has demonstrated that this is indeed the case. At the surface, the ground friction perpetually seeks to reduce all wind motion. Since we have quasi-permanent anticyclones in the subtropics and quasi-permanent cyclones in the subpolar belt, friction tends to destroy anticyclonic vorticity in low and cyclonic vorticity in high latitudes. We can put this in another form by saying that cyclonic vorticity is transferred from earth to atmosphere in low latitudes and absorbed by the earth from the atmosphere in high latitudes. Herewith, we obtain the needed distribution of sources and sinks to permit a mean vorticity flux from the subtropics to the polar belt at high levels. It is thus seen that lateral mixing accomplished by the agency of the migratory cyclones and anticyclones of middle latitudes can provide the link between the observed fields of motion and temperature described in chaps. II and III.

Limit of the constant vorticity profile. — According to Rossby's concept, the equatorward extension of the constant vorticity profile is restricted by the development of "dynamic instability." When this occurs, an air particle which is displaced north or south from its position of equilibrium continues to move in the direction of this displacement with no tendency to return to its initial latitude. In order to illustrate how this may happen, consider a uniform westerly geostrophic current. At every point the pressure force acting northward is balanced by the Coriolis force which acts southward. So long as this balance is maintained, the wind remains steady. Now suppose that an air particle is given an impulse to the south (i.e., in the direction of greater pressure). The westerly component of the motion suffers a deceleration, and the Coriolis force which is proportional to it also decreases. As a consequence, the northward directed pressure gradient overbalances the Coriolis force and the particle tends to return to its initial position.

Now suppose that the pressure gradient decreases rapidly southward. When the particle is now given an

impulse to the south, both the Coriolis force and the pressure force acting on it decrease. If the pressure force decreases more rapidly than the Coriolis force, the particle will tend to continue in the direction of the impulse. When this happens, the air particle is said to be dynamically unstable.

Dynamic instability is said to develop in a zonal current under certain assumptions when the anticyclonic shear measured along an isentropic surface exceeds the Coriolis parameter [94], i.e., when the absolute vorticity is anticyclonic. At a given latitude, this can occur as a result of increasing anticyclonic shear or a change of slope of the isentropic surface.

The gradual production of a wind profile as shown in fig. 7.4 with its attendant removal of absolute vorticity from low to high latitudes continually will lead to values of the anticyclonic shear south of the jet center that attain the critical value for dynamic instability. Then, a free exchange of air particles north and south begins in the zone of instability preventing further strengthening of the jet. Rossby [82] has found on theoretical ground based on turbulence theory that the breakdown of the constant vorticity profile due to development of dynamic instability should occur at lat. 34°. This is in fairly good agreement with observations. He also has estimated that near lat. 30° the width of the zone of zero vorticity would be about 5½° lat. This again is in fair agreement with observations.

THE MERIDIONAL CIRCULATION PATTERN IN THE JET STREAM REGION

We have so far shown that lateral mixing results in two parallel manifestations at the equatorward boundary of the mixing zone: (a) production of fast westerlies in a narrow zone; and (b) concentration of the meridional temperature gradient in the region of the jet.

Now, we have seen in chap. III that local temperature contrasts such as those created through differential heating at a coastline cannot serve as a starting mechanism for jet formation. Nor can we make use of condensation heat, since currents like the jet stream develop in the ocean and in rotating dishpans where it does not rain. Pre-existing winds in the form of the horizontal eddies discussed above must be responsible for initiating the concentration of the equator-pole temperature gradient. The fact that the winds are capable of moving the isotherms provides us with good grounds for assigning the leading role to the windfield, and suggesting that the thermal adjustment necessary to provide geostrophic balance lags the strengthening of the windfield. If this is true, the winds in the jet

stream are somewhat supergradient, while the current builds, and tend to move to the right of the contours of constant pressure surfaces. As a result, some mass is evacuated equatorward across the current axis.

When the state of dynamic instability is reached, ·this transverse circulation can intensify greatly since, as discussed above, the restraint against lateral displacement of air particles is removed. At least part of the air in the maximum wind belt is flung southward [102]. This leads to surface pressure falls under the jet and to pressure rises farther south. A compensatory northward mass flow starts at the surface. When mass continuity is taken into account, the complete meridional circulation cell in the troposphere looks as shown in the lower half of fig. 7.5. Air sinks equatorward from the strongest westerlies and ascends below the jet stream maximum.

Meridional circulation below level of strongest winds. — A meridional cell of the type just outlined is called a "reverse" cell, since it acts to raise cold air and lower warm air. Except in isolated instances (cf. [75]), it has proved a difficult task to demonstrate the existence of such cells with direct evidence. This is much easier in the ocean than in the atmosphere. For instance, it is quite evident in fig. 7.2 that cold water has been lifted and warm water lowered. In the atmosphere we mainly have indirect indications. Apart from exceptional situations mentioned in chap. IV, dryness prevails south of the jet axes and the precipitation is concentrated underneath and to the left of portions of the axes. Statistically, this has been demonstrated in chap. III (fig. 3.22-24). We see that the observed distribution of precipitation favors the model for the meridional circulation represented in fig. 7.5.

The concentration of the meridional temperature gradient is affected by the reverse circulation cell. As a jet stream becomes fully developed, our initial picture of purely horizontal motion no longer holds. In a stable atmosphere, downward motion of air through the pressure surfaces will produce warming on those surfaces while ascent produces cooling. If, then, we have a "direct" meridional circulation, i.e., the cold air sinks and the warm air rises, this circulation will tend to destroy the meridional temperature gradient. It counteracts the concentration of isotherms due to lateral mixing and acts to impede the formation of jet streams if the wind is approximately geostrophic. We see here one of the major paradoxes of meteorology — a kinetic energy producing circulation acts to reduce the strength of the winds. This is one of the reasons why, in contrast to other branches of physics, the precise relation between motion and the sources of energy for the motion has remained untractable up to now. Without wishing to enter into a prolonged discussion of this subject, we again refer to one of our initial state-
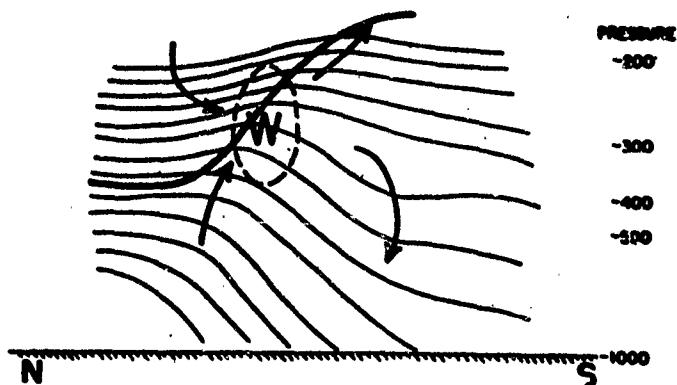

Fig. 7.5: Schematic representation of the probable meridional circulation pattern during intensification of jet stream (W). Tropopause is represented by heavy line, isentropes by thin lines [102].

ments that the development of jet streams apparently is independent of the exact mechanism of infusion of energy. We should point out, however, that according to Van Mieghem [105], the classical terminology of "direct" and "indirect" circulation is an oversimplification.

A reverse circulation will strengthen the temperature gradient in the jet stream zone, and, therefore, will not oppose the development of strong winds. Thus, assuming fig. 7.5 to be essentially correct, the cross-stream circulation is such as to permit a maximum jet development. It is of interest to estimate whether the contribution of this circulation in concentrating the temperature gradient, therefore in producing frontogenesis, can be appreciable. In the absence of advection, the temperature change at any point in adiabatically moving dry air is

$$\frac{\Delta T}{\Delta t} = -\left(\gamma_d - \gamma\right)w,$$

where γ_d is the dry adiabatic lapse rate, γ the observed lapse rate and w the vertical component of motion. If $w = 1$ cm/sec, $\gamma = -0.6°C/100$ m, and if the time interval over which γ and w remain essentially constant is one day, then $\Delta T = 4°C$. Further, if we have ascent of 1 cm/sec lasting one day north of the jet center, and a descent of the same amount to its south, the temperature gradient across the jet will increase by 8°C during this day, or by 25 per cent of the whole meridional temperature gradient in the middle troposphere. We see that the effect discussed is by no means negligible. We also note that its importance will decline and eventually vanish as, with full jet development, the lapse rates in the upper troposphere tend toward the adiabatic.

Meridional circulation above level of strongest winds. — If the jet stream is to have a definite core along the

vertical, as is observed, and if the atmosphere tries to
act as nearly as possible as a *perpetuum mobile*, i.e.,
move geostrophically, then the slope of the isobaric
surfaces must decrease with height above the jet stream
core. Statically, this requires cold air to the south
and warm air to the north of the jet axis. As demon-
strated by figs. 2.21-22, such a distribution is indeed
observed. Moreover, as stressed in chap. II, it is im-
possible to account for the high-level bands of cold
and warm air in middle latitudes by horizontal advec-
tion. Ascent south of the jet core produces the cold
air, and descent on the north side produces the warm
air. The resulting meridional circulation at high levels,
sketched in the upper half of fig. 7.5, is also of the
reverse kind. In this case, however, owing to the very
nonlinear character of the temperature field, it has
been possible to prove the sense of the circulation di-
rectly from the data, as in the case of the ocean cur-
rents.

Variation with Longitude. — The foregoing general
description of vertical circulations in the plane normal
to the jet stream must be amplified when we consider
the variations of jet stream structure with longitude,
such as the travelling maxima and minima, and the
passage of the jet through the ridges and troughs of
the long-wave pattern. Often the temperature is colder
in stratospheric ridges than in stratospheric troughs.
As the air rapidly moves through these systems which
remain quasi-stationary, ascent must take place from
trough to ridge and descent from ridge to trough. The
reality of this vertical circulation pattern along the
current has been demonstrated empirically by Fleagle
[21] (fig. 7.6). Rainfall, therefore ascending motion,
is not evenly distributed along the whole length of a
jet stream (cf. chap. IV), but shows a bias for locali-
zation to the left of the axis downstream from jet
maxima and to the right of the axis upstream from
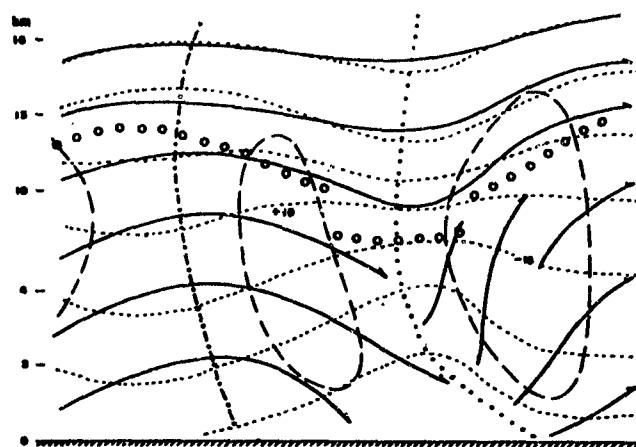
Fig. 7.6: Vertical cross-section showing idealized composite
fields of potential temperature, pressure change, and wind field
in the vicinity of trough and ridge lines. The thin dotted lines
are isentropes and the dashed lines are isallobars 'or ± 6 mb/12
hrs. The pressure trough is represented by dots, the ridge line
by alternate dots and dashes, and the tropopause by open circles.
Full lines are streamlines projected on the vertical cross-section.
Notice the ascent of air from trough to ridge and descent from
ridge to trough [21].

them. These observations point to the complexity of
the vertical circulation pattern, both normal and paral-
lel to the jets. On any given map, we obtain the com-
plete field of vertical motion only through superposition
of the three effects discussed. Since, however, we have
been able to put down general features of wind and
temperature distribution of the jet stream region in
cross-section form in chap. II, it follows that both the
trough-ridge circulation and that associated with travel-
ling maxima and minima must very nearly add up to
zero when we integrate over the whole length of many
jets. Only the planetary reverse cell is retained as
residual.

4. Balance of Momentum

So far we have surveyed those papers in the litera-
ture which try to suggest dynamical mechanisms for
formation and maintenance of the mean jet stream
aloft. The same problem can be approached over an
entirely different route, namely, by considering the
continuity or balance of absolute angular momentum.
When this is done at any point, it amounts to treating
the continuity of relative angular momentum, in other
words, the maintenance of the zonal winds. A continu-
ity equation may be applied to momentum just as to
other properties of the atmosphere. It states that the
change of momentum in any volume is composed of

the difference between inflow into and outflow from
this volume, plus the difference between momentum
sinks and sources within the volume. Inflow and out-
flow are accomplished by horizontal and vertical ad-
vection. Pressure forces and friction are the sources
and sinks. Such an approach to the jet stream prob-
lem, of course, is much more limited in scope than the
dynamical route chosen earlier since continuity equa-
tions do not furnish explanations. But it has the ad-
vantage of being more quantitative and, therefore, can
shed some light on the validity of our preceding sec-
tions.

It is a fundamental law of physics that the total momentum of a rotating system like earth plus atmosphere cannot change except by addition to or subtraction from this quantity through some external agency. The interaction between the atmosphere and the earth's surface is the most significant mechanism which can bring about changes in the absolute angular momentum of the atmosphere. In the regions between 30°N and 30°S, easterly winds prevail. Frictional interaction with the ground produces a large eastward torque on the atmosphere, necessitating a continuous flow of angular momentum from earth to atmosphere. Continued accumulation of this quantity would eventually destroy the wind system. Therefore, in order to maintain the surface easterlies, a removal of the absolute angular momentum gained from the ground must take place. This can be accomplished only by the exertion of an opposite torque by the earth on the atmosphere at some other latitude where surface westerlies prevail. Consequently, a horizontal flow of absolute angular momentum from the tropics to higher latitudes must exist.

Mechanism of transport of absolute angular momentum. — According to rough estimates which can be made from the surface frictional forces on the easterlies, the normal flow of angular momentum across the latitude of the subtropical ridge is equivalent to a tangential stress of 50-100 dynes/cm², [95].

The flow of angular momentum across a given latitude may be accomplished as a result of one or both of the following:

(1) An exchange of equal masses having unequal angular momentum. This involves the existence of large horizontal eddies as discussed earlier.

(2) A net equatorward flow of mass across the given latitude. Such net flow at a given level, if continuing as a permanent feature, must for reasons of mass continuity be compensated by a return flow at some other level. This implies the existence of a mean meridional circulation.

Rossby's lateral mixing theory is based on the view that the strong upper westerlies of middle latitudes are maintained primarily as a result of quasi-horizontal mixing processes. In recent years many investigators [47, 57, 95, 107] have attempted to test his reasoning numerically by computing the momentum exchange accomplished by the synoptic disturbances. This is done in a manner quite similar to that described earlier for heat exchange. Suppose we have alternating north and south winds around a latitude circle as is the case on all synoptic charts. Then, if the southerly winds are associated with a little higher west wind speed than the north winds, we have a net poleward momentum transfer across this latitude. If this transfer decreases as

we go to successively higher latitudes, we have a region of momentum flux convergence; if it increases, we have flux divergence. It is beyond the scope of this book to discuss the details of making these computations. We merely wish to point out that under some assumptions they can be carried out from a contour analysis on any constant pressure surface, such as the 500-mb surface.
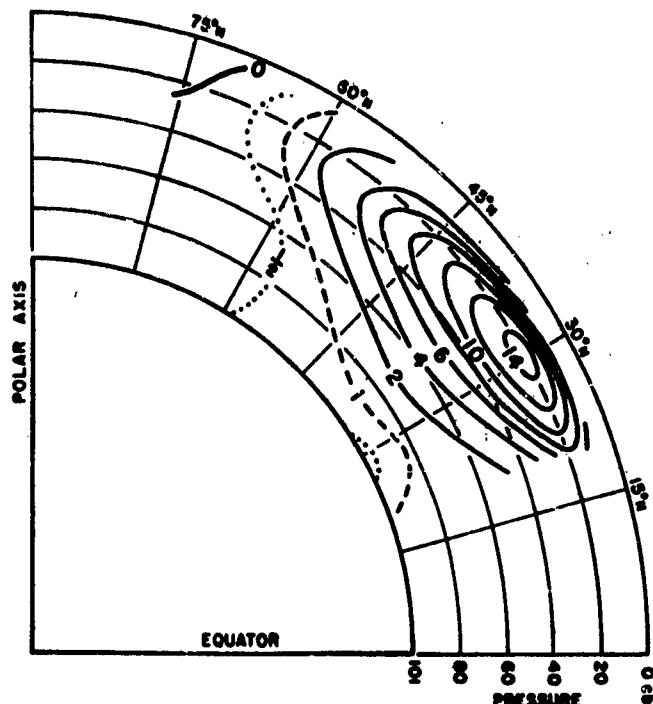

FIG. 7.7: The mean geostrophic poleward flux of angular momentum in 10^{14} t m^2 sec^{-2} per layer of 10 mb thickness in January 1949 [47].

Fig. 7.7 gives the results of computations as just described for January 1949 [47]. It is the first result of this figure that the computed momentum flux is in the right direction, namely poleward. Four-fifths of this flux took place at high levels, between 500 and 100 mb, with a marked center near 200 mb. The latitude of maximum transport was about 32°N. To its north, there was momentum flux convergence. As the strength of the westerlies changed little during January 1949, this convergence had to be balanced by vertical removal of momentum. Since the convergence zone was situated in the belt of westerlies, this removal had to be downward. Ground friction plus the retarding action of mountain barriers constituted the momentum sink.

Equatorward from lat. 32½°, January 1949 was characterized by momentum flux divergence. In this month, the center of the mean jet was situated as shown in fig. 3.2a precisely within this region of divergence. Thus, it is not possible to explain the presence and maintenance of the maximum wind in the belt

25°-30°N by the transfer of angular momentum accomplished by synoptic disturbances alone. We can try and see whether inclusion of the meridional circulation in the subtropics [70] leads to a more satisfactory result.[8] This is done in fig. 7.8 which shows a momentum budget between lats. 20°-30°N, the belt where the mean jet of winter is centered.

Precise inclusion of the meridional circulation of winter requires an exact knowledge of its intensity at all heights. As yet, upper-air data are much too scant to permit such a determination. We merely know the meridional circulation at the surface and must make a reasonable assumption about its vertical gradient. Here we shall make the conservative assumption that the circulation decreases linearly with height to become zero 200-mb above the surface, i.e., at 810 mb since the surface pressure is about 1010 mb. For reasons of mass continuity a corresponding return flow must take place above 810 mb. We assume that this return flow ends near the tropopause at about 100 mb. Fig. 7.8, thus, is divided into two parts: a shallow lower layer with equatorward meridional mass flow and a deep upper layer with return flow.
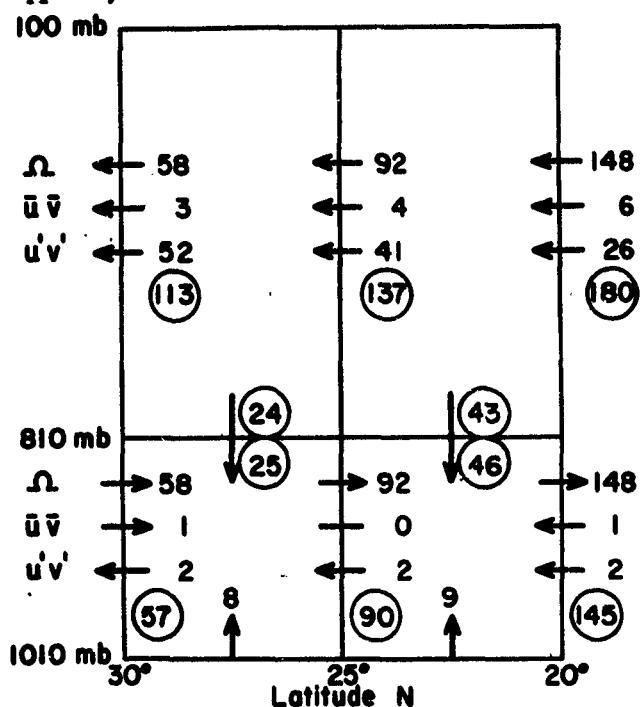
Fig. 7.8: Balance of absolute angular momentum (10^{25} g cm² sec⁻¹) between lats. 20° and 30°N in January. Ω indicates transfer of angular momentum of the rotating earth, $\bar{u}\ \bar{v}$ transfer of relative or u-angular momentum, and $u'v'$ eddy transfer of momentum. Circled letters underneath above quantities indicate total flow across latitude circles in each layer. Flow from surface is indicated by upward arrows at bottom. Vertical arrows through 810-mb level show direction of flow through this level. Momentum flow available for transport through this level is given by circled numbers above 810-mb line, momentum flow required for balance by circled numbers below the line.

[8]See also Palmén and Alaka [58].

Given a meridional circulation as just defined, the flow of momentum across any latitude circle stems from three components:

(1) The lateral eddy stresses, denoted $u'v'$ in fig. 7.8, discussed above.

(2) The tendency of the meridional circulation to move the mean monthly isotach pattern aloft in the direction of the meridional circulation. At 200 mb, for instance, the southerly winds of the meridional cell try to move the whole jet center poleward. This contribution, denoted $\bar{u}\ \bar{v}$ in fig. 7.8, is quite small.

(3) The transport of momentum of the rotating earth. At any latitude, the air possesses a component of momentum which is equal to the linear speed with which the earth revolves about its axis multiplied by the distance from the axis. This momentum necessarily is zero at the pole and has its maximum value at the equator. The meridional circulation also will move this component. Its flow is marked Ω in fig. 7.8 and its value is very large. Owing, however, to the fact that this momentum is almost identical at all heights in the troposphere on any latitude circle, its flow, as fig. 7.8 indicates, will be equal and opposite in the lower and upper layers.

In addition to the foregoing mechanisms which accomplish a meridional flow of momentum, we have a momentum source at the ground since we are in the belt of easterlies. The strength of this source, indicated by the vertical arrows at the bottom of fig. 7.8, has been taken from computations by Widger [107] for January 1946. Although this is a different year, it is to be presumed that the year-to-year variations in the total intensity of the frictional stress are small and that serious errors are not made by combining mean data obtained from different periods and, in case of the meridional circulation, from long-term means.

We are now in a position to make the balance of fig. 7.8. In the belt 25°-30° the source is eight units measured in 10^{25} gm cm² sec⁻² and the outflow across lat. 25° is 90 units. This leaves a deficit of 25 units which must be imported from above through the 810-mb surface. The crucial question now is whether we obtain a corresponding excess in the upper layer that can be used for the downward transport. In fig. 7.8, the circled numbers alongside the vertical arrows through the 810-mb surface below the 810-mb line indicate what is required for continuity; the circled arrows above the 810-mb line indicate what is available. We see that a balance is very nearly obtained. The residuals certainly are within the limits of error of all calculations that have been made to construct fig. 7.8.

It is plausible from the foregoing that the mean seasonal jet of winter is maintained by a combination of

eddy stresses and meridional circulation, rather than by one of these mechanisms alone.

It should be pointed out again (cf. also chap. III) that the mean upper jet computed from mean meridional cross-sections is not identical with the "meandering" jet stream described in chap. II, [57]. It seems likely that we are dealing with two distinct phenomena: (a) The fluctuating jet stream, the salient features of which are explainable by lateral mixing, and (b) a low latitude jet stream with less latitudinal fluctuation maintained by the mean meridional circulations of the trades. Statistical combination of these two current systems on a monthly or seasonal basis accounts for the low latitude of the mean jet (chap. III). Fig. 7.9 represents an attempt by Palmén [57] to describe the essential features of the tropospheric circulation in winter. Two meridional cells are in evidence: (a) The tropical cell which is the principal source of angular momentum, and (b) the "reverse" cell associated with the middle latitude jet.
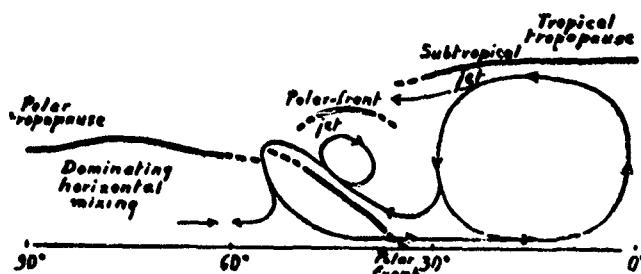
Fic. 7.9: Schematic representation of the meridional circulation in winter according to Palmén [57].

The flow of angular momentum as a predictor of the zonal index. — The possibility of predicting changes in the intensity of zonal flow on the basis of meridional transport of angular momentum has suggested itself to several investigators [45, 46, 48, 62, 107]. The results so far should be considered preliminary, but they contain the seed for some promising future developments. Basically, the same technique is used as just described. A continuity equation is written that contains the momentum flow across two latitude circles, say, 5° apart, plus the momentum sources and sinks. The sum of all these terms, averaged over a short time interval as one day, should be equal to the momentum change in the latitude belt during the day.

Computations of this kind so far have been made only in middle latitudes where, as seen in chap. V, a good prediction of the change of the profile of the westerlies can materially aid the forecaster. Within the westerlies, the source term is negative. Ground friction and the obstacle effect of the large mountain barriers combine to diminish the west winds. Momentum convergence due to lateral eddy stresses counteracts the frictional drag. If this convergence is stronger than the frictional

retardation, the westerlies should speed up. If, on some days, the eddies aloft produce a momentum divergence, the west wind speed should drop rapidly since in such situations ground friction and eddy stresses act in the same sense. The mean meridional circulation is not included here, partly because it is considered to be unimportant in the higher latitudes and partly because it cannot be measured on a daily basis. Further, since vertical flow of momentum cannot be computed as yet, all statistical work done so far refers to the changes of mean geostrophic wind averaged through the troposphere.

Table 7.1 shows the results of calculations made on the basis of the foregoing considerations by Mintz and Kao [48], for January 1949. A correlation between computed and observed tendencies is indeed present. But the correlation coefficient falls far short of the value of 1.0 which it must have if a complete continuity equation containing all terms can be evaluated. At this time, it is not possible to tell whether the coefficient of 0.66 is due to the imperfections in measurement of the quantities used for the correlation (cf. chap. V), or whether it is due to omission of other mechanisms, especially nongeostrophic winds, that can produce momentum changes. It is clear, however, that the mechanism investigated by Mintz and Kao is an important one.

TABLE 7.1

Correlation coefficients between computed and observed quantities, January 1949

Quantities	Correlation coefficient
Computed index tendency vs. observed tendency	0.66
Forecast 24-hr index change vs. observed 24-hr change	0.28
Persistence forecast of 24-hr index change vs. observed 24-hr change	0.17

Unfortunately, the persistence of momentum convergence resulting from eddy stresses is very low from day to day [45]. Therefore, forecasts based on the instantaneous momentum convergence have a much smaller success than contemporary correlations as seen from a comparison of the first and second rows of table 7.1. Still, the second coefficient is positive, and the forecasts verify better than those based on linear extrapolation of the preceding tendency of the profile of the westerlies shown in third row of table 7.1. It is evidently worth while to continue developing this approach in the future and perhaps to go over to longer time increments. This would be desirable because it would eliminate the erroneous day-to-day fluctuations, mentioned in chap. V. Moreover, as brought out in that chapter, a knowledge of extended trends of the profile is much more useful than a knowledge of 24-hour trends.

5. On the Formation of Regional Jets

While lateral mixing seems to account for the general features of the observed average zonal wind profile and the average distribution of the horizontal shear poleward from the west wind maximum at the tropopause level, it does not take care of all the details which characterize any given situation. In particular, the theory does not provide for the extremely sharp regional jets of limited geographical extent and life span which occur along two or more narrow bands extending in the general direction of flow and separated by regions of weaker winds.

In an attempt to study the processes responsible for these "streaks" of high velocities, Rossby [85, 86] again had recourse to the remarkable similarity in the structure of atmospheric jets and of the Gulf Stream. His approach was influenced by the following considerations:

(1) He noted that these local jets appear to be always associated with a strong solenoidal concentration as required by the thermal wind equation, and also with intense vertical shears. This suggested that the distribution of vertical stability may be a determining factor in the observed concentration of momentum.

(2) He compared the Gulf Stream with its streaks of velocity concentrations with the broader and more diffuse California current which is considered as driven by local wind systems. He inferred that the velocity concentrations in the Gulf Stream are not a result of local momentum additions by the prevailing winds, but that the concentrating mechanism must be inherent in stratified air and ocean currents.

(3) Finally, he observed that on many occasions, and especially during the summer months, the westerly currents entering the United States from the Pacific Ocean are characterized by fairly flat speed maxima at the 200-mb level. After crossing the Rockies, the vertical structure of these currents undergoes a marked change. Above 300 mb, a sharp jet of limited vertical and horizontal extent appears, while the layers below this level are characterized by very weak winds. This led to the conclusion that the velocity concentration must be associated with momentum losses sustained by the currents during their passage over the mountains.

In view of the above considerations, Rossby reasoned that stratified currents subject to momentum losses to the environment and prevented from escaping sideways, but required to transport within each material sheet a prescribed amount of fluid per unit time, would gradually assume a wind distribution with height corresponding to a minimum value of momentum transfer per unit time across a vertical section normal to the current.

He showed that when such currents reach their limiting state of minimum momentum transfer, they normally shrink in depth and show an increase of velocity in the center. This wind increase requires a pressure drop in the direction of motion thus limiting both the geographic extent and presumably the life span of jets formed by this process.

Further research on this important problem of meteorology can be expected in the future.

6. Experimental Analogues to Atmospheric Motions

From the foregoing sections it is apparent that, in most cases, application of dynamic equations to the diverse and complex motions of the atmosphere can be made only by introducing certain simplifying assumptions. Often it is very difficult to evaluate the magnitude of the effects which must be neglected. An alternative means of studying motion which avoids this limitation is through the use of models and analogues. Models of atmospheric phenomena have been attempted for a long time[9] but only within the past few years has extensive quantitative evaluation of such experiments been made [24, 27, 44].

Complete similarity between motions in the atmos-

phere and those developed in the laboratory can never be expected. Paramount is the impossibility of utilizing the effect of gravity in its correct geometric distribution. For atmospheric motions, gravity is a central force, i.e., acting toward the center of the earth, but, in the models, it is a force which always acts in the same direction. Despite such difficulties much progress is being made with models.

Laboratory experiments offer a means whereby some effects can be made to predominate over others. The correspondence between the resulting motions and those found in the atmosphere serves as an index of the importance of the particular factor as a determinant of atmospheric flow patterns. For example, since Fultz [25] has been able to obtain flow patterns in an in-

[9]A summary of these experiments has been prepared by Fultz [24].
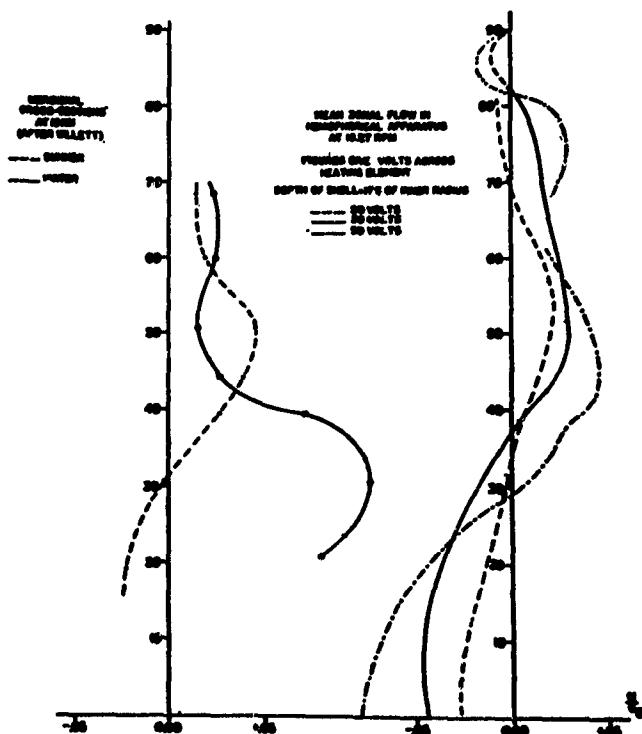
Fic. 7.10: Left hand side represents wind distribution with latitude at the tropopause level after Willett [106]. Right hand side is a graphical representation of zonal relative motion produced in a rotating hemispherical fluid sheet for different rates of heating. Atmospheric velocities are expressed in terms of the linear equatorial velocity of the earth. Velocities relative to the rotating shell are expressed in terms of their ratio to the linear equatorial velocity of the shell [102].

compressible fluid which resemble those of the atmosphere, both in character and scale, it has been concluded that the compressibility of the atmosphere is not a primary factor in determining the gross features of the atmospheric circulation.

Much of the research of the University of Chicago Hydrodynamics Laboratory has been aimed toward the investigation of factors which may be of importance in concentrating the zonal flow. The results of these jet stream experiments have shown at least four means whereby strong relative motions can be established in the laboratory setups.

The first of these sets of experiments was designed to test the influence of lateral mixing on the circulation of a thin sheet of fluid contained between two rotating bowls [24]. Convective interchange of mass between pole and equator in a hemisphere heated at the pole resulted in the establishment of zonal motions whose speeds were of the same relative magnitude as those of atmospheric jet streams. Even the profile of these zonal motions has some resemblance to that of the upper troposphere (fig. 7.10).

A cyclindrical obstacle introduced between the two

bowls and rotated at a lower angular velocity [27, 44] resulted in the establishment of a definite wave pattern resembling the long waves of the upper westerlies, and in concentration of the zonal motion (fig. 7.11). To some extent these results can be considered as verification of the effect attributed by Yeh [112] to large orographic barriers in concentrating a portion of the middle latitude westerlies.

Fultz [25] also has shown that narrow zonal currents may be established in a rotating dishpan by heating the outer rim. "Westerlies" near the rim reach values which correspond to atmospheric speeds of 50-150 mph and definite cyclonic and anticyclonic eddies are in evidence (fig. 7.12).

Very concentrated jets with associated waves and cyclones on an inclined density discontinuity surface can be produced in dishpans containing two liquids of densities differing by around 0.5 per cent or more. The initial field of motion is produced mechanically. When suitable rotation rates are established, jet concentrations develop in association with the discontinuity surface [26].

The results of these experiments are significant not only because the motions resemble those of the atmos-
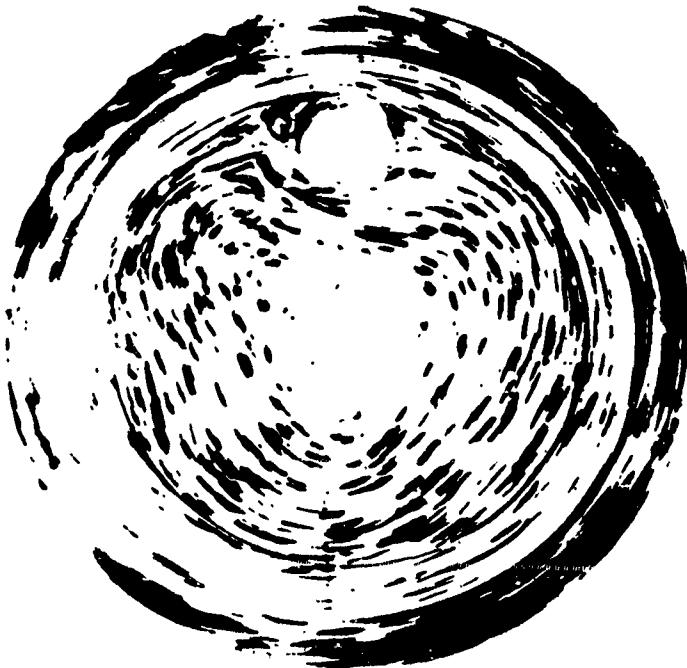
FIG. 7.11: Flow in a hemispheric shell relative to an obstacle, showing a well-defined wave pattern with a wave number of three. The obstacle is centered at lat. 45°. Its rate of rotation is approximately one-tenth of that of the shell. The North Pole is located at the center of the picture. The relative circulation (counter-clockwise) and its speed are indicated by the length of the streaks made by tracer particles. Notice the concentration of higher velocities downstream from obstacle (from records of Hydrodynamics Laboratory, University of Chicago).

phere but also because it has been possible, to some extent, to interpret them dynamically through the use of the vorticity equation. At least those experiments performed with the spherical bowls have strengthened Rossby's contention that the atmosphere outside the tropics can be treated as a thin shell in which horizontal processes predominate, and in which the broadscale circulation patterns can be interpreted in terms of the conservation of the vertical component of the absolute vorticity.

A   B

031150 - 1 - 2
DPII Rim Heat
7.2 rpm
6 cm. depth
3m 20s after heating begins
concrete bottom
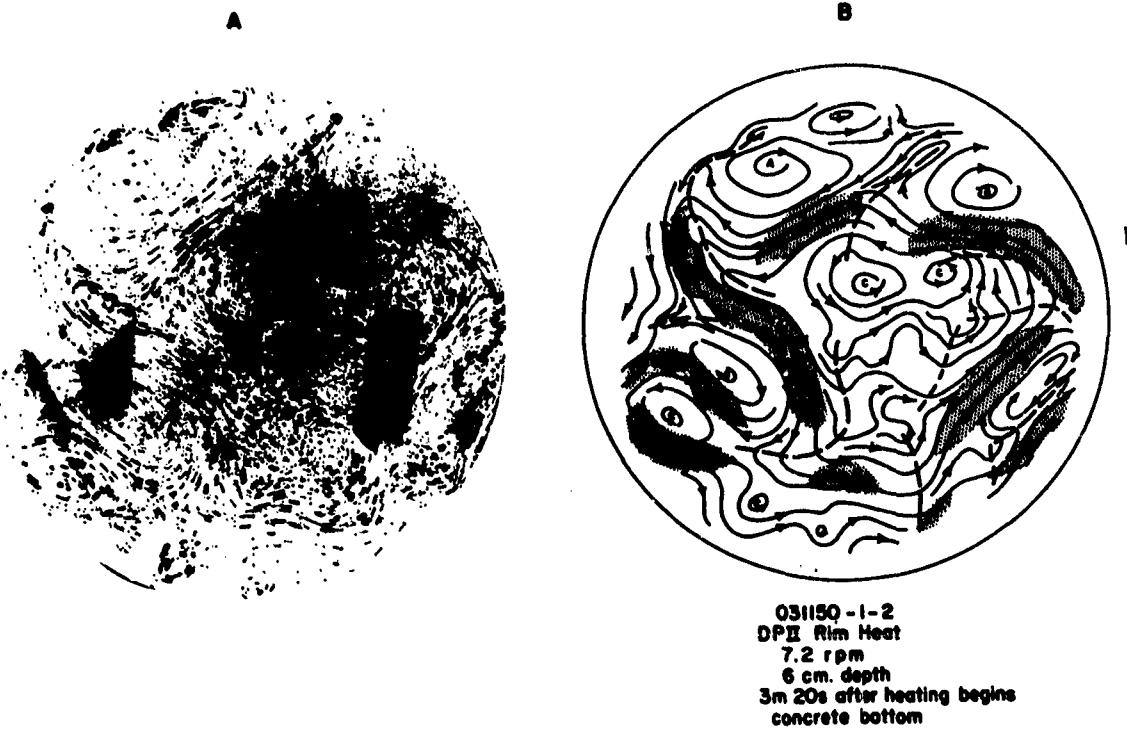
FIG. 7.12: (a) Photograph of the relative circulation at the surface of water in a pan rotating clockwise (7.2 r.p.m.), which is being heated at the bottom near the rim. Relative circulation is indicated by streaks made by tracer particles (aluminum tristea- rate) floating on surface of water; (b) A streamline analysis of the relative circulation, showing a well-defined wave pattern with cyclonic and anticyclonic centers. Regions of high relative velocity are indicated by shaded areas. The ratio of the maximum observed relative speed to the linear equatorial speed of the pan is .21, which is equivalent to a westerly wind of about 80 mps. (From records of Hydrodynamics Laboratory, University of Chicago.)

REFERENCES

1. Air Weather Service, 1952: *Trng. Rpt.* 105-86.
2. Allen, R. A., and Collab., 1940: *Pap. Phys. Ocean, Meteor.*, Mass. Inst. of Tech. and Woods Hole Ocean. Inst., **8**, No. 3.
3. Bannon, J. K., 1951: *Prof. Notes Meteor. Off.*, **7**, No. 104.
4. ———— 1952: *Meteor. Mag.*, London, **81**, p. 97.
5. Baum, W. A., 1944: *Bull. Amer. Meteor. Soc.*, **25**, p. 319.
6. ———— 1948: *Aspects of the jet stream over North America in the mean monthly pattern, July 1947-June 1948* (unpublished report to the Office of Naval Research).
7. Baur, F., and H. Phillips, 1936: *Beitr. Phys. Frei. Atmos.*, Leipzig, **24**, p. 1.
8. Bergeron, T., 1928: *Geof. Publ.*, Oslo, **5**, No. 6.
9. Berggren, R., B. Bolin and C. -G. Rossby, 1949: *Tellus*, Stockholm, **1**, p. 14.
10. Bjerknes, J., and H. Solberg, 1921: *Geof. Publ.*, Oslo, **2**, No. 3.
11. Bjerknes, V., and Collab., 1911: *Dynamic Meteorology and Hydrography, Part II-Kinematics.* Washington, D.C.: Carnegie Inst., 59 plates.
12. ————, ————, 1933: *Physikalische Hydrodynamik.* Berlin: J. Springer, 797 pp.
13. Boffi, J. A., 1949: *Bull. Amer. Meteor. Soc.*, **30**, p. 242.
14. Bolin, B., 1950: *Tellus*, Stockholm, **2**, p. 184.
15. Bowie, E. H., and R. H. Weightman, 1914: *Mo. Wea. Rev.*, Suppl. 1, 37 pp.
16. Charney, J. G., 1941: *J. Meteor.*, **6**, p. 371.
17. Chaudhury, A. M., 1950: *Tellus*, Stockholm, **2**, p. 56.
18. Cressman, G. P., 1948: *J. Meteor.*, **5**, p. 44.
19. ————, 1950: *Ibid*, **7**, p. 39.
20. Defant, A., 1921: *Geograf. Annal.*, Stockholm, **3**, p. 209.
21. Fleagle, R. G., 1947: *J. Meteor.*, **4**, p. 165.
22. Fuglister, F. C., 1951: *Tellus*, Stockholm, **3**, p. 230.
23. ————, and L. V. Worthington, 1951: *Tellus*, Stockholm, **3**, p. 1.
24. Fultz, D., 1949: *J. Meteor.*, **6**, p. 17.
25. ————, 1951: *Tellus*, Stockholm, **3**, p. 137.
26. ————, 1952: *J. Meteor*, **9**, p. 379.
27. ————, and R. R. Long, 1951: *Tellus*, Stockholm, **3**, p. 61.
28. Gustafson, A. F., 1951: *Air Weather Service Manual*, 105-26.
29. Hadley, G., 1735: *Concerning the cause of the general trade winds.* London. Reprinted in *Neudrucke von Schriften und Karten über Meteor. und Erdmag.* G. Hellman, ed. Berlin: A. Asker & Co., 1896.
30. Harrison, H. T., 1950: *Some characteristics of the upper-level low and the jet stream.* United Air Lines Circular No. 34 (typescript).
31. Hess, S. L., 1948: *J. Meteor.*, **5**, p. 293.
32. Holmboe, J., G. E. Forsythe, and W. Gustin, 1945: *Dynamic Meterology.* New York: Wiley and Sons, 378 pp.
33. Houghton, H. G., and J. M. Austin, 1947: *J. Meteor*, **4**, p. 16.
34. Hovmöller, E., 1952: *Tellus*, Stockholm, **4**, p. 126.
35. Hughes, L. A., E. S. Jordan, and R. J. Renard, 1952: *On the computation of upper-level winds from constant pressure charts* (unpublished report to the Office of Naval Research, University of Chicago).
36. Hutchings, J. W., 1950: *J. Meteor.*, **7**, p. 294.
37. Iselin, C. O. D., and F. C. Fuglister, 1948: *J. Mar. Res.*, **7**, p. 317.
38. James, R. W., 1951: *Meteor. Mag.*, London, **80**, p. 341.
39. Jeffreys, H., 1919: *Phil. Mag.*, London, **37**, p. 1.
40. Jones, R. F., 1949: *Meteor. Res. Pap.*, London, No. 484.
41. Kuo, H., 1950: *J. Meteor.*, **7**, p. 247.
42. ————, 1951: *Ibid*, **8**, p. 307.
43. Loewe, F., and U. Radok, 1950: *Ibid*, **7**, p. 58.
44. Long, R. R., 1951: *Ibid*, **8**, p. 207.
45. Lorenz, E. N., 1951: *Ibid*, p. 52.
46. Mintz, Y., 1949: *The maintenance of the mean zonal motion of the atmosphere* (unpublished Ph.D. dissertation at UCLA).
47. ————, 1951: *Tellus*, Stockholm, **3**, p. 195.
48. ————, and S. K. Kao: *J. Meteor.*, **9**, p. 87.
49. Murray, R., 1949: *Meteor. Mag.*, London, **78**, p. 263.

50. Namias, J., 1947: *Extended forecasting by mean circulation patterns*. Washington, D. C.: Dept. of Commerce, 89 pp.

51. ————, 1950: *J. Meteor.*, **7**, p. 130.

52. ————, and P. F. Clapp, 1949: *Ibid*, **7**, p. 330.

53. ————, ————, 1951: *Compendium of Meteorology*. Boston, Mass.: Amer. Meteor. Soc., p. 551.

54. Norquest, K. S., 1952: Contribution to *experiments in quantitative prediction with the aid of upper air charts* (to be published).

55. Palmén, E., 1948: *J. Meteor.*, **5**, p. 20.

56. ————, 1951: *Compendium of Meteorology*. Boston, Mass.: Amer. Meteor. Soc., p. 599.

57. ————, 1951: *Quart. J. Roy. Meteor. Soc.*, London, **77**, p. 337.

58. ————, and M. A. Alaka, 1952: *Tellus*, Stockholm, **4**, p. 324.

59. ————, and K. M. Nagler, 1948: *J. Meteor.*, **5**, p. 58.

60. ————, and C. W. Newton, 1948: *Ibid*, **5**, p. 220.

61. Palmer, C. E., 1949: 1: *Quarterly reports of tropical project*, to Air Material Command, Base Directorate for Geophysical Research, UCLA.

62. Panofsky, H., and Collab., 1950: *Progress Report on study of day to day changes of angular momentum of atmospheric zonal rings*, Rep. No. 5, Contract No. AF 19(122)-48 between Geophys. Res. Direct. and UCLA.

63. Petterssen, S., 1950: *Centenary Proceedings*. London: Roy. Meteor. Soc., p. 120.

64. Phillips, N. A., 1950: *Tellus*, Stockholm, **2**, p. 116.

65. Priestley, C. H. B., and W. C. Swinbank, 1950: *Proc. Roy. Soc.*, London, **189**, p. 543.

66. Rex, D. F., 1950: *Tellus*, Stockholm, **2**, p. 196.

67. ————, 1951: *Ibid*, **3**, p. 100.

68. Riehl, H., 1948: *Trans. Amer. Geophys. Union*, **29**, p. 175.

69. ————, and N. E. La Seur, 1949: *J. Meteor.*, **6**, p. 420.

70. ————, T. C. Yeh, 1950: *Quart. J. Roy. Meteor. Soc.*, London, **76**, p. 182.

71. ————, ————, and N. E. La Seur, 1950: *J. Meteor.*, **7**, p. 181.

72. ————, and Collab., 1952: *Meteorological Monographs*. Boston, Mass.: Amer. Meteor. Soc., **1**, No. 5, 80 pp.

73. ————, and C. O., Jenista, 1952: *J. Meteor.*, **9**, p. 159.

74. ————, K. S. Norquest, and A. L. Sugg, 1952: *Ibid*, **9**, p. 291.

75. ————, and S. Teweles, 1952: *Cyclogenesis of November 12-13, 1951* (to be published).

76. Rodewald, M., 1938: *Ann. Hydr.*, Berlin, **66**, p. 42.

77. Rossby, C. -G., 1938: *Pap. Phys. Ocean, Meteor.*, Mass. Inst. of Tech. and Woods Hole Ocean. Inst., **7**, No. 1.

78. ————, 1939: *J. Mar. Res.*, **2**, No. 1.

79. ————, 1940: *Quart. J. Roy. Meteor Soc.*, London, **66**, Suppl., p. 68.

80. ————, 1941: *Yearbook Agriculture, Climate and Man*. Washington, D. C.: U. S. Govt. Printing Office, p. 599.

81. ————, 1942: *Misc. Rep. No. 5*, Inst. of Meteor., Univ. of Chicago.

82. ————, 1947: *Bull. Amer. Meteor. Soc.*, **28**, p. 53.

83. ————, 1947: *Proc. of the Third Hydraulics Conf.*, Studies in Engineering, Univ. of Iowa, p. 103.

84. ————, 1949: *The Atmosphere of the Earth and Planets*. Chicago: University of Chicago Press, G. P. Kuiper, ed., p. 16.

85. ————, 1951: *Tellus*, Stockholm, **3**, p. 15.

86. ————, 1951: *Archiv fur Met., Geophysik und Bioklimat.*, Ser. A, Vienna, **4**, p. 3.

87. ————, and Collab., 1939: *J. Mar. Res.*, **2**, p. 38.

88. ————, and H. C. Willett, 1948: *Science*, **108**, p. 643.

89. Sandstrom, J. W., 1909: *Ann. Hydr. Mar. Meteor.*, Berlin, **37**, p. 242.

90. Saucier, W. J., 1949: *Mo. Wea. Rev.*, **77**, p. 219.

91. Sawyer, J. S., 1949: *Quart. J. Roy. Meteor. Soc.*, London, **77**, p. 185.

92. Scherhag, R., 1948: *Wetteranalyse und Wetterprognose*. Berlin: Springer Verlag, 424 pp.

93. Sheppard, L. A., 1949: *Quart. J. Roy. Meteor. Soc.*, London, **75**, p. 188.

94. Solberg, H., 1936: *P. V. Met. Un. Geod. Geophys. Int. Mem.*, Edinbourg, **2**, p. 66.

95. Starr, V. P., 1949: *A physical characterization of the general circulation*, Rep. No. 1, Contract No. AF 19(122)-152 between Geophys. Res. Direct. and M.I.T.

96. Starrett, J. G., 1949: *J. Meteor.*, **6**, p. 347.

97. Sutcliffe, R. C., 1939: *Quart. J. Roy. Meteor. Soc.*, London, **65**, p. 518.

98. ————, 1947: *Ibid*, **73**, p. 370.

99. ————, and A. G. Forsdyke, 1950: *Ibid*, **76**, p. 189.

100. ————, and Collab., 1951: *Ibid*, **77**, p. 457.

101. Teisserenc de Bort, L., 1881: *Annales*, Bureau Central de France, Paris, Part 4, p. 17.

102. University of Chicago, Dept. of Meteor., 1947: *Bull. Amer. Meteor. Soc.*, **28**, p. 255.

50. Namias, J., 1947: *Extended forecasting by mean circulation patterns.* Washington, D. C.: Dept. of Commerce, 89 pp.

51. ――――, 1950: *J. Meteor.,* 7, p. 130.

52. ――――, and P. F. Clapp, 1949: *Ibid,* 7, p. 330.

53. ――――, ――――, 1951: *Compendium of Meteorology.* Boston, Mass.: Amer. Meteor. Soc., p. 551.

54. Norquest, K. S., 1952: Contribution to *experiments in quantitative prediction with the aid of upper air charts* (to be published).

55. Palmén, E., 1948: *J. Meteor.,* 5, p. 20.

56. ――――, 1951: *Compendium of Meteorology.* Boston, Mass.: Amer. Meteor. Soc., p. 599.

57. ――――, 1951: *Quart. J. Roy. Meteor. Soc.,* London, 77, p. 337.

58. ――――, and M. A. Alaka, 1952: *Tellus,* Stockholm, 4, p. 324.

59. ――――, and K. M. Nagler, 1948: *J. Meteor.,* 5, p. 58.

60. ――――, and C. W. Newton, 1948: *Ibid,* 5, p. 220.

61. Palmer, C. E., 1949-51: *Quarterly reports of tropical project,* to Air Material Command, Base Directorate for Geophysical Research, UCLA.

62. Panofsky, H., and Collab., 1950: *Progress Report on study of day to day changes of angular momentum of atmospheric zonal rings,* Rep. No. 5, Contract No. AF 19(122)-48 between Geophys. Res. Direct. and UCLA.

63. Petterssen, S., 1950: *Centenary Proceedings.* London: Roy. Meteor. Soc., p. 120.

64. Phillips, N. A., 1950: *Tellus,* Stockholm, 2, p. 116.

65. Priestley, C. H. B., and W. C. Swinbank, 1950: *Proc. Roy. Soc.,* London, 189, p. 543.

66. Rex, D. F., 1950: *Tellus,* Stockholm, 2, p. 196.

67. ――――, 1951: *Ibid,* 3, p. 100.

68. Riehl, H., 1948: *Trans. Amer. Geophys. Union,* 29, p. 175.

69. ――――, and N. E. La Seur, 1949: *J. Meteor.,* 6, p. 420.

70. ――――, T. C. Yeh, 1950: *Quart. J. Roy. Meteor. Soc.,* London, 76, p. 182.

71. ――――, ――――, and N. E. La Seur, 1950: *J. Meteor.,* 7, p. 181.

72. ――――, and Collab., 1952: *Meteorological Monographs.* Boston, Mass.: Amer. Meteor. Soc., 1, No. 5, 80 pp.

73. ――――, and C. O., Jenista, 1952: *J. Meteor.,* 9, p. 159.

74. ――――, K. S. Norquest, and A. L. Sugg, 1952: *Ibid,* 9, p. 291.

75. ――――, and S. Teweles, 1952: *Cyclogenesis of November 12-13, 1951* (to be published).

76. Rodewald, M., 1938: *Ann. Hydr.,* Berlin, 66, p. 42.

77. Rossby, C. -G., 1938: *Pap. Phys. Ocean, Meteor.,* Mass. Inst. of Tech. and Woods Hole Ocean. Inst., 7, No. 1.

78. ――――, 1939: *J. Mar. Res.,* 2, No. 1.

79. ――――, 1940: *Quart. J. Roy. Meteor Soc.,* London, 66, Suppl., p. 68.

80. ――――, 1941: *Yearbook Agriculture, Climate and Man.* Washington, D. C.: U. S. Govt. Printing Office, p. 599.

81. ――――, 1942: *Misc. Rep. No. 5,* Inst. of Meteor., Univ. of Chicago.

82. ――――, 1947: *Bull. Amer. Meteor. Soc.,* 28, p. 53.

83. ――――, 1947: *Proc. of the Third Hydraulics Conf.,* Studies in Engineering, Univ. of Iowa, p. 103.

84. ――――, 1949: *The Atmosphere of the Earth and Planets.* Chicago: University of Chicago Press, G. P. Kuiper, ed., p. 16.

85. ――――, 1951: *Tellus,* Stockholm, 3, p. 15.

86. ――――, 1951: *Archiv fur Met., Geophysik und Bioklimat.,* Ser. A, Vienna, 4, p. 3.

87. ――――, and Collab., 1939: *J. Mar. Res.,* 2, p. 38.

88. ――――, and H. C. Willett, 1948: *Science,* 108, p. 643.

89. Sandstrom, J. W., 1909: *Ann. Hydr. Mar. Meteor.,* Berlin, 37, p. 242.

90. Saucier, W. J., 1949: *Mo. Wea. Rev.,* 77, p. 219.

91. Sawyer, J. S., 1949: *Quart. J. Roy. Meteor. Soc.,* London, 77, p. 185.

92. Scherhag, R., 1948: *Wetteranalyse und Wetterprognose.* Berlin: Springer Verlag, 424 pp.

93. Sheppard, L. A., 1949: *Quart. J. Roy. Meteor. Soc.,* London, 75, p. 188.

94. Solberg, H., 1936: *P. V. Met. Un. Geod. Geophys. Int. Mem.,* Edinbourg, 2, p. 66.

95. Starr, V. P., 1949: *A physical characterization of the general circulation,* Rep. No. 1, Contract No. AF 19(122)-152 between Geophys. Res. Direct. and M.I.T.

96. Starrett, J. G., 1949: *J. Meteor.,* 6, p. 347.

97. Sutcliffe, R. C., 1939: *Quart. J. Roy. Meteor. Soc.,* London, 65, p. 518.

98. ――――, 1947: *Ibid,* 73, p. 370.

99. ――――, and A. G. Forsdyke, 1950: *Ibid,* 76, p. 189.

100. ――――, and Collab., 1951: *Ibid,* 77, p. 457.

101. Teisserenc de Bort, L., 1881: *Annales,* Bureau Central de France, Paris, Part 4, p. 17.

102. University of Chicago, Dept. of Meteor., 1947: *Bull. Amer. Meteor. Soc.,* 28, p. 255.

103. U. S. Weather Bureau, 1942: *Preparation of* *Weather Maps.* Washington, D. C.: U. S. Govt. Printing Office, 45 pp.

104. _____, 1952: *Radiosonde Compatability Tests.* Washington, D.C.: U.S. Govt. Printing Office.

105. Van Mieghem, J., 1950: *Tellus,* Stockholm, **2,** p. 52.

106. Walker, G. T., 1924: *Mem. India Meteor. Dept.,* Delhi, No. 24.

107. Widger, W. K., 1949: *J. Meteor.,* **6,** p. 291.

108. Willett, H. C., 1944: *Descriptive Meteorology.* New York: Academic Press, 305 pp.

109. _____, 1949: *J. Meteor.,* **6,** p. 340.

110. _____, 1951: *Trans. N. Y. Acad. of Sci.,* Set II, **13,** p. 277.,

111. World Meteorological Organization, 1950: *Comparaison Mondiale des Radiosondes,* Payerne, Switzerland.

112. Yeh, T. C., 1950: *Tellus,* Stockholm, **2,** p. 173.

113. _____, 1951: *J. Meteor.,* **8,** p. 146.

114. _____, J. E. Carson, and J. J. Marciano, 1951: *Meteorological Monographs.* Boston, Mass.: Amer. Meteor. Soc., **1,** No. 3, p. 47.

115. Yin, M. T., 1949: *J. Meteor.,* **6,** p. 393.

INDEX